Development of Drug Loaded Nanoparticles for Treatment of *Mycobacterium avium* Infection

Eva Marie Restis

Dissertation submitted to the faculty of the Virginia Polytechnic Institute and State University in partial fulfillment of the requirements for the degree of

Doctor of Philosophy
In
Biomedical and Veterinary Sciences

Nammalwar Sriranganathan, Chair
Joseph O. Falkinham III
Elankumaran Subbiah
Judy S. Riffle

September 20th 2013
Blacksburg, VA

Keywords: *Mycobacterium tuberculosis, Mycobacterium avium*, infection, nanoparticle, antimicrobials

Development of Drug Loaded Nanoparticles for Treatment of *Mycobacterium avium* Infection

Eva Marie Restis

ABSTRACT

Currently, about one third of the world's population is latently infected with *Mycobacterium tuberculosis* and about 4 million people die from the disease annually worldwide. Although treatment with antimicrobials can be curative, many people fail to complete the prescribed therapeutic regimen which can increase the risk of disease re-emergence, spread of infection to others and development of drug resistance. An improved approach is urgently needed for patient compliance. Development of safe and effective colloidal drug delivery systems may reduce the amount and frequency of antimicrobial therapy needed. The major goal of this research effort is to explore the safety and efficacy of antimicrobial loaded nanoparticles against *M. avium*. Various *in vitro* efficacy studies were done with a) amikacin-loaded nanoparticles, b) clarithromycin-loaded nanoparticles, and c) with aerogel nanoparticles loaded with rifampicin, clarithromycin and ethambutol.

Clarithromycin (CLA) and amikacin (AMK) loaded nanoparticles showed a significant reduction in viable *M. avium* compared to free antibiotics and untreated controls. Cytotoxicity assays revealed that all types of drug-laden nanoparticles were non-toxic to J774A.1 mouse macrophage cells at therapeutic doses. *In vivo* efficacy studies showed that only amikacin-loaded polymeric

nanoparticles improved clearance compared to free amikacin in *M. avium* infected BALB/c mice. In general, none of the nanoparticle formulations elicited any significant microscopic lesions in the organs of infected mice at tested doses. Each nanoparticle formulation was analyzed physicochemically for size, zeta potential, amount of drug load, minimum inhibitory concentration (MIC) and stability. Both the AMK and CLA polymeric nanoparticles were below 200 nm in size and had a slightly negative overall surface charge, aerogel nanoparticles were somewhat larger in size. The amount of drug load varied between all three nanoparticles and is largely dependent on the chemical structure and interactions between the nanoparticle and drug. The AMK and CLA nanoparticles were relatively stable under varying environmental conditions and time points and had MIC ranges equivalent to the respective free drugs.

DEDICATION

I would like to dedicate this work to my daughter, Amara Jade and my son, Rubin William- you two are my everything. I would also like to dedicate this dissertation to the mice who unknowingly gave their life in the name of science.

ACKNOWLEDGEMENTS

I like to give special thanks to my family and friends for their continued support during this arduous journey. I would especially like to thank Rubin Fields for his help and countless hours of time. I would also like to thank my advisor Dr. Nammalwar Sriranganathan for his continual patience, guidance and encouragement over the years. I have learned much more than how to be a critical scientist with his help and guidance. I would also like to thank my committee members Dr. Subbiah, and Dr. Riffle who were always available to help. I especially would like to thank Dr. Falkinham for your critical eye, time, and energy, it was greatly appreciated. I would also like to give many thanks to my lab mates for their help over the years and special thanks to Kay Carlson for keeping me and our lab on track. You are a good friend and I miss you. I also wish to thank Dr. Avery, the BMVS department and the Institute for Critical Technology and Applied Sciences, Virginia Tech for their accessibility, flexibility and financial support. Additionally, I would like to thank Dr. Meng and the T32 NIH training grant for financial support.

TABLE OF CONTENTS Page #

LIST OF FIGURES

LIST OF TABLES

GENERAL INTRODUCTION

Mycobacterium tuberculosis (Mtb) is a fastidious, slow growing, hydrophobic, lipid-rich, bacterial pathogen in the family *Mycobacteriaceae* and the causative agent of most cases of tuberculosis. Mtb is responsible for the leading cause of death due to a bacterial infection in the world with over one third of the global population latently infected (1). Latency occurs after infection when *M. tuberculosis* sequesters itself inside the host's immune cells in a quiescent state until environmental conditions are favorable (2, 3) for reactivation.

Mtb is transmitted from person to person via aerosolized droplets from infected people with the active respiratory disease (4). In healthy people, infection with *Mycobacterium tuberculosis* often does not cause any symptoms. The host's immune system actively attempts to limit the spread of the bacteria by "walling off" the bacteria in the lungs forming a dynamic structure called a granuloma (5).

Treatment with antimicrobials are successful in most cases of active infection, but many people fail to complete the prescibed six to nine month course of combination antimicrobial therapy because of cost, inconvenience, or toxic side effects from the drugs (1). Patients often report feeling better early on into treatment and stop taking the medication which is a contributing factor in the development of drug resistant bacteria (6). It also increases the risk of re-emergence of active tuberculosis in the patient and aids in the spread of infection to others (6).

Mtb is a major health problem in developing countries and has also re-emerged in many industrialized countries in recent years (7). This resurgence in industrial countries like the Unites States is attributed to poor patient compliance, immigration from countries with high Mtb prevalence and also from an increased susceptibility in immune compromised individuals such as those infected with HIV/AIDS (7, 8). The risk of developing tuberculosis (TB) is estimated to be between 20-37 times greater in people living with HIV than among those without HIV infection (9). In 2011, there were 8.8 million new cases of TB, of which 1.1 million were among people living with HIV (9).

A new treatment approach that is effective, short term, safe and non-toxic, which would improve patient compliance, is urgently needed. Addressing poor patient compliance is essential in the control and treatment of *M. tuberculosis* (9). One way to improve patient compliance is to reduce the amount and frequency of dosing that is required to treat mycobacterial infections. This can be done by finding an appropriate drug carrier that has the capacity to yield a high drug load of multiple antimicrobials simultaneously while providing a sustained drug release profile that is non-toxic to patients.

Nanomedicine, a sub specialty of nanotechnology, is a promising area of science that can aid in the development of new efficacious drug delivery methods. By utilizing biocompatible nanomaterials to encapsulate antimicrobials, efficacy of current antimycobacterial treament regimens can be enhanced. Encapsulation of

antimicrobials in nanoparticles can reduce the amount, frequency of treatment and thereby undesirable side effects of a given drug (10, 11). It can also improve solubility, bioavailability and ultimately patient compliance (12, 13).

The goal of this dissertation was to explore if nanoparticles loaded with antimicrobials would reduce the amount of viable mycobacteria in murine macrophages and infected mice without causing toxic side effects. In the first chapter, an extensive literature review of *Mycobacterium tuberculosis* and Nanomedicine is discussed. Chapter two discusses the design and development on the models in cell culture and *in vivo*. Chapter three investigates the efficacy of an antibiotic loaded polymeric nanoparticle used to treat infected murine macrophages and mice using *M. avium* as a surrogate *for M. tuberculosis.* Chapter four examines the efficacy of a clarithromycin loaded polymeric nanoparticle in cell and mouse models and lastly, chapter five discusses the efficacy of aerogel particles loaded with three frontline antimicrobials used to treat tuberculosis.

References

1. World Health Organization, www.who.int/tb/publications/global_report/2011/gtbr11_full.pdf
2. Riska P. F., Carleton S. (2002). "Latent tuberculosis: models, mechanisms, and novel prospects for eradication." Semin Pediatr Infect Dis **13**(4): 263-72.
3. Talaat A. M., Ward S. K., Wu C.W., Rondon E., Tavano C. C., Bannantine J. P., Lyons R., Johnston S. A. (2007). "Mycobacterial Bacilli Are Metabolically Active During Chronic Tuberculosis in Murine Lungs: Insights from Genome-Wide Transcriptional Profiling." Journal of Bacteriology **189**(11) 4265–4274.
4. Mc Donough K. A., Kress Y., Bloom B. R. (1993). "Pathogenesis of Tuberculosis: Interaction of *Mycobacterium tuberculosis* with Macrophages." Infection and Immunity **61**(7): 2763-2773.
5. Tsai, M. C., Chakravarty, S., Zhu, G., Xu, J., Tanaka, K., Koch, C., Tufariello, J., Flynn, J. Chan, J. (2006). "Characterization of the tuberculosis granuloma in murine and human lungs: cellular composition and relative oxygen tension." Cell Microbiol. Feb; **8**(2):218-32.
6. Loddenkemper, R. Sagebiel, D. Brendel, A. 2002. "Strategies against multidrug resistant tuberculosis." Eur. Respir J. **20** Suppl. 36: 66s-77s.
7. Bermejo, A., Veeken, H., Berra, A. (1992). "Tuberculosis incidence in developing countries with high prevalence of HIV infection." AIDS. Oct: **6**(10):1203-6.

8. Meya, D. B., McAdam, K. P. (2007). "The TB pandemic: an old problem seeking new solutions." J Intern Med **261**(4):309-29.

9. World Health Organization, http://www.who.int/tb/dots/en/

10. Emerich D. F., Thanos C. G. (2008) “Targeted nanoparticle-based drug delivery and diagnosis” Journal of Drug Targeting **15**:(3) 163-183.

11. Moghimi S. M., Hunter A. C., Murray J. C. (2005) “Nanomedicine: current status and future prospects.” The FASEB Journal **19**: 311-330.

12. Gaspar M. M., Cruz A. G., Fraga A. G., Castro A. G., Cruz M. E. M., Pedrosa J. (2008) “ Developments on Drug Delivery Systems for the Treatment of Mycobacterial Infections.” Current Topics in Medical Chemistry **8**:579-591.

13. Davis M. E., Chen Z. G., Shin D. M. (2008). “Nanoparticle therapeutics: an emerging treatment modality for cancer.” Nature Reviews Drug Discovery **7** 771-782.

Chapter One

Literature Review

Global perspective

Every second, someone in the world is newly infected with *Mycobacterium tuberculosis* bacilli (1). Currently, it is estimated that about 2 billion people or one third of the world's population is already infected with *M. tuberculosis* (Mtb). Each year approximately eight million people develop active tuberculosis (TB) and three million die from the disease worldwide (2, 3, 4).

About 95% of all TB cases arise from developing countries in Asia and Africa (5). Complicating this problem is the widespread prevalence of HIV. In the year 2000, an estimated 11 million people in the world were co-infected with HIV and Mtb, with three fourths of that population living in sub-Saharan Africa (6). Even more concerning is the emergence of resistant strains of Mtb called Multi-Drug Resistant (MDR-Tb) and Extensively Drug Resistant (XDR-Tb).

MDR-Tb is defined as strains of Mtb resistant to at least rifampicin and isoniazid; first line antimicrobial TB drugs. In most cases, MDR-Tb is a result of poor patient compliance, although inadequate management and outdated control strategies also play a part (7). The management of MDR-Tb is difficult and often hospitalization is required to ensure proper isolation, infection control and medication schedule of the patient. Globally cases of MDR-Tb have occurred on

almost every continent and in 2010, 50% of MDR-TB cases worldwide were estimated to occur in China and India according to the WHO (1).

In early 2006, the term XDR-Tb was used for the first time by the Centers for Disease and Control (CDC) and WHO to describe Mtb strains that are extensively drug resistant to isoniazid, rifampicin and to at least 3-6 second line antimicrobial drugs. XDR-Tb has been reported in at least 37 countries and on every continent but predominating in sub-Saharan Africa, according to the WHO (1). In the KwaZulu-Natal province of South Africa, an outbreak of XDR-Tb occurred resulting in 98% mortality in 53 patients (8).

In the United States, Mtb has been on the decline except for increase in cases peaking in the early 1990's. The surge in cases was attributed to the HIV pandemic (9). Other factors such as immigration from countries with high TB prevalence, outdated control strategies, socioeconomic factors, poor patient compliance and emergence of MDR-Tb continue as sources for the lack of disappearance of TB. As the prevalence of HIV continued to rise along with emergence of resistance strains of Mtb, the world community refocused its attention on eradicating TB. In 1993, The WHO declared Mtb a global public health crisis. It is estimated, that nearly 1 billion people from now until 2020 will become infected, 200 million will become sick and 70 million will die from TB without newer control and management strategies (10).

Pathogenesis of infection

Mtb is a slow growing acid-fast bacterium that is rod shaped, aerobic, non-spore forming, and non-motile. When individuals are exposed to Mtb, about 10% of immune competent individuals will become infected, yet infection does not necessarily lead to active disease (11). Of those infected, about 5% will develop pulmonary or extra-pulmonary disease within two years. The other 95% develop latent disease which is defined as viable bacteria in low energy state or "dormant" within the macrophage (11). Individuals infected with latent Mtb have a 5% chance of reactivating Mtb and developing clinical signs within their lifetime.

Transmission of this facultative intracellular pathogen occurs via aerosolized respiratory secretions from person-to-person (12). One droplet of infected liquid from a sneeze, for example, is capable of transporting between 1-3 bacilli into the air to be inhaled by a susceptible individual (12) where as a cough can expel many more bacilli. Once the droplet enters the respiratory tract, it settles in the alveoli of the lung where alveolar macrophages are among the first cells of the immune system to encounter the microbe. This encounter stimulates the process of phagocytosis and the release of immune-modulators which stimulate migration of other inflammatory cells such as neutrophils, T-lymphocytes and other monocytes to the site (13).

Once the microbe is phagocytized, the macrophage attempts to kill the intracellular bacteria with mechanisms such as phagolysosomal fusion,

respiratory bursts and release of hydrolytic enzymes (14). Mycobacteria have several mechanisms to escape destruction within the macrophage. These include; downregulation of the host macrophage's ability to release chemokines that induce a cellular immune response, inhibition of phagolysosomal fusion by inhibiting proteins that shuttle lysosomal compartments and inhibition of acidification of the phagolysosome (15, 16). Modification to the phagolysosome facilitates survival, replication and possible escape into the cytoplasm. Survival within the macrophage can result in active infection and subsequent development of clinical signs or become the source of latent infection. These survival mechanisms and a thick lipid rich mycobacterial cell wall, make mycobacterial infections difficult to treat by conventional drugs that do not accumulate in the macrophage where the pathogen is sequestered. Furthermore, it is recognized that the ability of Mtb to enter macrophages and subvert the normal immune response in order to survive intracellularly is a major key to its virulence (17).

Granuloma Formation

When phagocytic cells such as macrophages and dendritic cells become infected, mycobacterial antigens will be processed and presented to specialized lymphocytes called T-cells. This will initiate the cellular immune response which is crucial to the control and elimination of Mtb (2). Activation of the cellular immune response will ultimately result in the formation of a granuloma surrounding infected macrophages. A granuloma can take 4 -6 weeks to form

post infection and its purpose is to stop the spread of infection (18). The human granuloma is a highly organized structure with a complex mixture of CD4 and CD8 T-lymphocyte cells, macrophages and other immune cells contained in the center (19). A thick fibrotic wall with a ring of lymphoid cells lines the outer surface. Recent research reveals that the surrounding lymphoid surface is an active site of host-pathogen interactions. It is not the walled off structure it was once thought to be but rather a dynamic entity in constant communication with host cells (20). The containment of mycobacteria within the granuloma is in constant balance. If the immune system is unable to control the infection adequately, the granuloma will continue to enlarge eventually developing a necrotic center of dead cells. The granuloma can then become unstable and rupture causing liquefaction and cavitation, which can result in leakage into the airways. This is the development of active disease. It is also the source of infection to nearby cells and through coughing, eventual transmission to the outside world (21).

Latent TB

In a normal, immunocompetent individual, the granuloma will be stable thus containing the bacteria and preventing spread. Inside the granuloma, many mycobacteria will be killed by the macrophages but some will persist in a latent state. The term latency refers to the ability of the organism to cause disease at a later date when environmental conditions favor its growth. In this state of latency, Mtb is considered viable but many biochemical pathways have been

downregulated (22). Mycobacteria have the ability to survive in an acidic, avascular, nutrient, and oxygen deprived state of latency for years (23). During this period, the infected individual is not contagious and will not exhibit clinical symptoms (24), but will have a positive tuberculin skin test. Reactivation can occur if the infection can no longer be contained by the host's immune system as is the case with elderly individuals or persons suffering from immunosuppression due to cancer, cancer chemotherapy, or co-infection with HIV.

Immunology of Infection

Protection against Mtb is primarily mediated through the cellular immune response, although there is a complex interplay between innate and adaptive immunity. During a cellular immune response, antigen-presenting cells (APCs) such as macrophages or dendritic cells ingest foreign material, such as bacteria or viruses. The initial response of a macrophage to infection with Mtb is to activate CD4 T-helper lymphocyte cells to release interferon gamma (IFN-γ), a cytokine, via the TH1 pathway (18). The release of IFN-γ stimulates surrounding macrophages to ingest Mtb. IFN-γ also stimulates endothelial binding and emigration of more T-lymphocyte cells to infected areas. IFN-γ is crucial to the successful elimination or control of Mtb. In fact, when transgenic mice were unable to produce IFN-γ they became more susceptible to infection (25). After activation, T helper cells begin to proliferate through the secretion of another cytokine, IL-2, which results in clonal expansion and activation of more APCs. IL-2 is also important for memory T cells especially with vaccine-induced long-

lived immunity. Other cytokines like tumor necrosis factor (TNF) alpha, IL-12, and IL-17 are also essential in resistance to Mtb (20, 26).

After activation and proliferation, some T helper lymphocyte cells mature and express a surface protein CD4, which is essential for participating in cell to cell communication by linking to a specialized receptor, MHC class II, on APC's surface. After APCs ingest Mtb, peptide fragments from bacterial antigens bind to major histocompatibility complex (MHC) class II molecules, which then translocate to the cell surface to mediate presentation of Mtb peptides to $CD4^+$ T cells (27, 28). Mtb peptides are also presented by MHC class I molecules on APC's to $CD8^+$ T lymphocyte cells. CD4 lymphocytes are imperative during acute infections, and CD8 lymphocytes have been shown to be just as important in the latter stages of infection primarily through cytotoxic activity (29). The result of this complex immune cell activity is the elimination of the bacteria through microbial digestion or containment by the formation of a granuloma.

Receptor Mediated Recognition in the Macrophage

Mtb utilizes many receptors to gain entrance in the macrophage. Initially Mtb enters a cell through receptor mediated phagocytosis (18). In the alveolar macrophage, Mtb enters through complement receptors, primarily CR3 but can also enter via Toll like receptors, mannose receptors, and type A scavenger receptors (30). F_c gamma receptors only play a role in phagocytosis after antibody production is present from previous exposure of Mtb.

Complement Receptors

Complement is important in the phagocytosis of Mtb. The complement receptors (CR) involved are CR1 (CD35), CR3-the leukocyte integrins (CD 11b/CD18) and CD4 (CD11c/CD18) (31). Macrophages secrete complement that opsonize or coat particles to enhance phagocytosis. Some components of the Mtb cell wall also enhance opsonization via C3 acceptor molecules (31).

CR3 is a major integrin of phagocytic cells on mononuclear cells, neutrophils, NK cells and small set of lymphocytes. CR3 also mediates migration of leukocytes in inflamed tissue. CR4 plays a major role in phagocytosis of human alveolar macrophages. It has been reported that Mtb uses complement receptors preferentially because a strong superoxide production is not triggered through this receptor (32). However, additional research has shown that whichever receptor is used to gain entry in the macrophage, there is little impact on Mtb survival. For example, mice lacking CR3 receptors had a similar bacterial burden and host response to those mice that had functional CR3 receptors (2).

Toll- Like Receptors

Toll-like receptors (TLRs) are a family of pattern recognition receptors and associated adaptor proteins that have a conserved intracellular sequence region that is necessary for signal transduction. TLR's are expressed on macrophages, mast cells, eosinophils, dendritic cells, respiratory and intestinal epithelial cells (33). There are many different types of TLR and the binding of these receptors of specific molecules like bacterial antigens elicits a varied immune response.

Therefore TLRs are critical in orchestrating the immune response between adaptive and innate immunity. For example, TLR2 recognizes bacteria components like peptidoglycan, lipoproteins, and mycobacterial glycolipids such as lipoarabinomannan which stimulates an innate immune response (34). TLR4 stimulation results in the activation of adaptive immunity by inducing macrophages to produce cytokines and chemokines which recruit other immune cells to the area.

Some TLRs associate with each other in a synergist and regulatory way. For example, TLR1 associates with TLR2 to recognize mycobacterial lipoprotein (33). Once binding occurs, a signal is initiated that activates genes to synthesize and release cytokines.

Mannose Receptors

The mannose receptor (MR) recognizes mannose- and fructose-containing glycol-conjugates which are found on the surface of a variety of bacteria. Different components of Mtb cell wall like LAM, arabinomannans, mannas, and mannoproteins can serve as ligands for these receptors which are present on alveolar macrophages, dendritic cells, and tissue macrophages (18). MR can serve as a link between innate and adaptive immunity and MR activity is increased by IL-4, IL-13 and inhibited by IFN-γ (33).

Cholesterol

In recent studies, it has become clear that cholesterol plays a part in the host - pathogen interaction of Mtb. Cholesterol rafts have been shown to accumulate around phagocytic receptors and are required for Mtb uptake. Depleting cells of cholesterol prevents Mtb internalization (2). It is unclear what the exact advantage is for pathogen or host but more research is needed.

Phagolysosome Arrest

After phagocytosis, Mtb is internalized by the macrophage into a vesicle called the phagosome. The phagosome containing Mtb can mature by fusing with lysosomes to form a phagolysosome (14). The bacteria are then subjected to attack by hydrolytic enzymes from the lysosomes, and to an acidic environment that lacks many essential nutrients required for bacterial growth. This hostile milieu should result in killing of the ingested bacteria and its subsequent elimination. However, the phagolysosome is a dynamic structure and Mtb has evolved various mechanisms to arrest the development of a mature phagolysosome and modify the microenvironment of the phagosome to its advantage. This attribute has also been seen in other pathogenic bacteria like *M. bovis, M. avium paratuberculosis* and *M. leprae* (31).

Mtb are able to halt the maturation process by disrupting the trafficking and tethering of molecules involved in lysosomal fusion (37). Normal membrane fusion between two compartments requires assemblage of a complex protein that facilitates lysosomal fusion. This protein is called SNARE and also requires

multiple smaller tethering proteins. Mtb is able to retain a small protein involved in this process called Rab5, a small GTPase binding protein (39). Rab 5 binds to Vps34, a class III phosphatidylinositol 3-kinase (PI 3-P) on the cytosolic face of the vacuole. PI-3P, in turn, acts as an acceptor molecule for the early endosomal antigen, EEA1, which also complexes with Rab5. EEA1 binds to calmodulin which stimulates calcium release. EEA1 accumulation is necessary for the acquisition of Rab7 another small GTPase that is enriched on lysosomes (39).

Another way Mtb inhibits phagosomal maturation in addition to blocking tethering of proteins at the Rab 5 stage, is to inhibit sphingosine kinase activity and subsequent Ca 2+ signaling pathways which is necessary to recruit hvps35 to membrane organelles. Protein kinase g from Mtb has also been shown to inhibit phagolysosomal fusion (37). Mycobacteria are also able to utilize host molecules for their own survival inside the macrophage by interfering with the host's cell signaling process. A protein formerly called TACO (Tryptophan aspartate containing coat protein) also known as P57 and now called coronin 1, is a protein normally responsible for inhibiting phagosome-lysosome fusion through calcium dependent calcineurin signaling pathway in the host. Studies have shown that phagosomes containing live mycobacteria had an exclusive presence of this protein whereas phagosomes containing dead mycobacteria did not indicating that coronin 1 is an important host factor involved in inhibition of phagolysosomal fusion (38).

Mycobacterial Cell Envelope

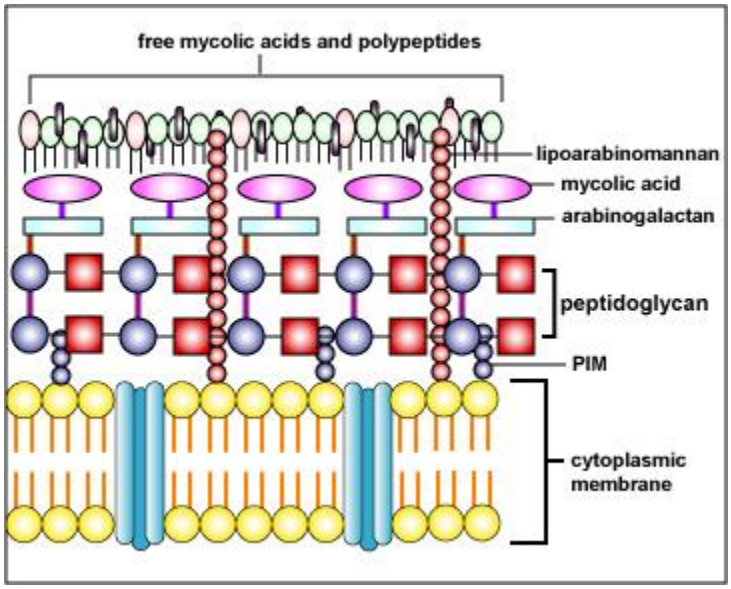

http://faculty.ccbcmd.edu/courses/bio141/labmanua/lab16/diseases/mtuberculosis/u1fig11.html

The envelope of mycobacteria consists of three major components; a capsule-like outermost layer, a cell wall, and a plasma membrane (40). The capsule layer is rich in polysaccharides and proteins with only a small amount of lipids. The main polysaccharide components are glucan, arabinomannan, and mannan. The capsule is not covalently bound to the rest of the structure and during an active infection it is replaced as the macrophage attempts to destroy it (42). Not much is known about the function of capsule but it is presumed to be protective (42).

The mycobacterial cell wall is a structure that affords certain unique characteristics onto mycobacterial cells. It consists of an impermeable, outer membrane layer which contains porins and mycolic acids that are covalently linked to an inner structural peptidoglycan layer via the arabino-mannan polymer

(41). The peptidoglycan biosynthesis and function is similar across species of bacteria but the arabinogalactan and mycolic acids are unique to the genus *Mycobacterium* (41). The outer membrane provides a hydrophobic barrier that protects Mtb from antibiotics and disinfectants, with concomitant reduction in permeation of hydrophilic nutrients. It is also a major contributor to the slow growth of Mtb and enables the cell to resist drying out, extreme ph and other environmental stressors (40). The mycolic acids of the outer membrane layer are also responsible for the "acid fastness" of the bacteria or resistance to decolorization during Ziehl-Neelson staining. Together, these components are responsible for the size and shape of the cell.

The plasma membrane of Mtb is considered to be structurally and functionally similar to other bacterial plasma membranes. This is the site of respiration and the electron transfer chain. In the literature, no recent developments have occurred to increase the knowledge base in this area.

Surveillance and Diagnosis of *M. tuberculosis*

A widely used screening method for latent tuberculosis is the intradermal test in which a crude extract of cell wall components called tuberculin, is injected under the skin. This purified protein derivative (PPD) of the mycobacterial cell wall stimulates a cellular immune response if the individual has had a previous exposure which results in inflammation at the site of injection and therefore, a positive result. The immunological conversion of this delayed type

hypersensitivity occurs within a month of exposure and in most cases, exists for a lifetime (43).

Complications with the PPD test are low sensitivity and specificity. False positives can occur in individuals infected with other species of *Mycobacterium* as well as those who previously received the BCG vaccine. False negatives can occur from an overwhelming disseminated infection with Mtb or if there is severe immune suppression as is the case in individuals suffering from HIV- AIDs. Another problem with the PPD test is a 48-72 hour delay before test can be officially read. Although the skin TB test has low sensitivity and specificity to latent TB bacterial infection, there have been some recent advances to improve the specificity of the test by using multiple antigens and a filtrate protein that is not present in nonpathogenic Mtb or Bacillus Calmette-Guerin (43).

Another screening and diagnostic tool used is called QuantiFERON-TB GOLD Test. This test which has been approved by the Food and Drug Administration (FDA) in 2005 for aiding in the diagnosis of latent and active Mtb, examines the levels of gamma interferon using whole blood. Although, the interferon gamma test has been noted to be equivalent in sensitivity to skin test for latent bacteria (4), it can be useful to detect active infection. Elevated levels of IFN-γ are produced by T-lymphocyte cells and NK cells and can indicated active infection with greater sensitivity than the skin test (43).

In developing and developed countries methods for diagnosis of Mtb can vary widely. In developing countries, the microscopic examination of sputum for acid fast bacteria and thoracic radiography are the most common tests used. However, in infected patients the acid fast smear (AFS) has a sensitivity rate that varies from 40% to 60% (44). Concerns with the effectiveness of the AFS involve the necessity to test clinical patients at least three times before an accurate negative test can be reported. In the case of patients with low bacterial burden or those who have extra-pulmonary TB, their results could be reported as false negatives (44).

In developed countries, TB diagnosis is based on microscopic detection of acid fast bacteria, culture and use of nucleic acid amplification tests of sputum samples and a chest X-ray (31). In the mid 1990's, the FDA approved the use of two nucleic acid amplification tests the have shown to be rapid and sensitive for the detection of Mtb in clinical samples; AMPLICOR and Amplified Mycobacterium Direct (MTD) via the Polymerase Chain Reaction (PCR). The amplification of the genetic target 16s rRNA is most commonly performed (31).

Although amplification tests are highly accurate, the gold standard of diagnosis and selectivity of proper antimicrobials remains the direct culture of Mtb bacteria on selective media. This process is often performed on inspissated egg based culture medium (Lowenstein-Jensen), non-egg based agar (Middlebrook 7H10), and egg based culture media (Herrold's media) prepared on slants to allow for

humidity control. Mature colonies begin to form after 14-21 days. Despite using multimodal diagnostic approaches, diagnosis still takes several days for definitive diagnosis in AFS positive TB cases and several weeks for smear negative cases (44).

Vaccines for *M. tuberculosis*

Bacille Calmette Guérin (BCG) is a live attenuated bacterial vaccine derived from *Mycobacterium bovis.* The BCG is the only vaccine available today for protection against TB. It was developed in 1920 and since that time has been given to over 1 billion people worldwide (1). Although protection is variable in adults (45), it is effective in protecting children from severe TB. The variability of efficacy in the vaccine is attributable to genetic variance within multiple sub-cultured strains, genetic diversity within the host as well as regional differences in the TB strains themselves (46).

In areas where the TB prevalence is high such as Africa and Asia, the vaccine is given routinely. In the U.S., however, the vaccine is not recommended unless there is a high risk of TB exposure as is the case with certain health care workers or travelers to TB positive countries with a stay of 3 months or greater (47). Since the TB vaccine is a live vaccine, there is a small risk that it may cause disease such as TB meningitis, or disseminated TB, which can occur at a rate of 0.06 to 1.56 cases per 1 million vaccinated (45).

The race to design a more effective vaccine has been underway for many years now. There are three basic approaches being explored; development of non-living vaccines such as subunit vaccines or DNA vaccines, development of living vaccines by genetically improving BCG or by attenuating Mtb strains and using viral vectors such as Adenovirus or Vaccinia virus to express immunodominant antigens (48, 49, 50). Each vaccine approach has produced a vaccine candidate(s) now in clinical trials, phase I/II trials, or entering field trials in Africa or Asia funded by organizations such as the Bill and Melinda Gates Foundation. Hopefully, a new vaccine for TB will be entering the market within 5-10 years.

Although these vaccines hold tangible promise for an improved vaccine against TB, the field as a whole is still limited by the lack of understanding of the complexities of protective immunity to Mtb. Many researchers acknowledge that our knowledge of this immunity remains incomplete and is essential to developing the most efficacious vaccine for TB.

Treatment for *M. tuberculosis*

The case fatality rate of people with untreated clinical TB can be as high 50% (51). However, in most cases the treatment of Mtb is curative of disease symptoms but the protocol is long, costly and has low patient compliance. The CDC and WHO recommend a treatment protocol called Directly Observed Therapy (DOT's) that describes a 95% cure rate when followed (52). DOTS is highly effective in treating TB, preventing spread of infection to others and

development of drug resistant bacteria. The program encourages completion of a six-month drug regimen by providing drugs for free and observing patients taking the chemotherapeutics for the first two months. This internationally approved drug program comprises of first line and second line drugs. First line drugs are isoniazid and rifampin, pyrazinamide and ethambutol. Second line drugs include; para amino-salicylate, kanamycin, cycloserine, ethionamide, amikacin, capreomycin, thiacetazone and fluroquinolones. Currently, the standard drug protocol for TB patients without drug resistant strains is 6-9 months of chemotherapy beginning with isoniazid, rifampin, pyrazinamide and ethambutol for 2 months followed by 4-7 months of isoniazid and rifampin (31, 52). The use of the multi-drug regimen was created to avoid drug resistant strains of Mtb from developing since it was noticed from the early days of TB treatment, that drug resistance could quickly develop within months with use of one drug.

By 2001 over 60% of the global population was covered by DOTS and by the end of 2002 over 10% people have been treated (31). Since the rise of MDR-Tb, an amended protocol was developed called DOTS Plus which utilizes second line TB drugs to combat resistant strains. However, DOTS Plus is more expensive, therapy takes longer and has significant side effects (52).

Treatment of latent mycobacteria

The drug isoniazid is recommended for people latently infected with Mtb. It is prescribed for 6-12 months and has an estimated efficacy of 75-93% when taken

correctly (4). Isoniazid is effective against latent bacteria because it targets mycolic acid synthesis in the cell wall. Even though latent bacilli are at a low metabolic rate they, at least occasionally, attempt to grow and replicate (4). Even though individuals latently infected will not have clinical signs or be contagious it is still recommended to treat because of a 5% chance of reactivation within their lifetime. Although there has been no new TB drugs released into the marketplace in the last 40 years, several possibilities have been in development. Currently in phase III clinical trials there are several fluroquinolones, rifamycins and a few new drug compounds (53). There are still more in phase I/II trials as well as preclinical development. Hopefully these research efforts will produce newer and better drug combinations to effectively treat TB.

Cost of *M. tuberculosis* treatment

In the United States, treatment of a person with uncomplicated Mtb can range into the thousands (31). Complicated cases of *Mycobacterium tuberculosis* involving antimicrobial resistant strains (MDR) and (XDR) are much more costly to manage.

The management of MDR-Tb is difficult and often hospitalization is required to ensure proper isolation, infection control and medication schedule of the patient. In individuals with MDR treatment can be as high as 250,000 per person (9). In the early 1990's in New York City, an outbreak of MDR-Tb had emerged that cost

the city over 1 billion dollars to contain (52). Patients infected with XDR-Tb have a much worse prognosis. It is estimated by the CDC that in-hospital treatment of an individual with XDR-Tb can cost over five hundred thousand dollars to manage.

Challenges of *M. tuberculosis* treatment

Treatment of mycobacterial infections are challenging. The intracellular location of mycobacteria makes it difficult for penetration of drugs and elimination of bacteria. Additionally Mtb are able to survive and persist inside the host macrophage creating a state of latency. Therefore, the treatment of Mtb requires lengthy treatment periods with multiple drugs that are able gain access to the intracellular milieu where the pathogen resides.

Patient compliance is another major obstacle in the successful treatment of Mtb (55). Mycobacteria have slow generation times which necessitate prolonged therapy involving multiple drugs. These drugs act both on inhibiting protein and cell wall synthesis. Major disadvantages of these drugs are their toxicities. When taken for prolonged periods of time which is needed in Tb therapy, liver and kidney damage can occur. Also, common dose related side effects that may stop people from taking the antimicrobials are nausea and GI distress (54). According to Zhang et al. 2002, approximately one-half of the people who have TB do not complete their treatment regimen as prescribed (52). Treatment in developing countries is often complicated by the high rate of HIV prevalence, drug resistant strains and a negative social stigma. Even though there are

established DOTS programs, people still decline treatment because of lack of information or accessibility to treatment (55).

Drug Delivery and nanomedicine

Even with years of attention, Mtb still remains a formidable pathogen and yet the goals of therapy are simple; elimination of the organism from the host in the shortest time possible without toxic side effects thus preventing latent disease or drug resistance. Over the past several decades, as we strive for the above goal, many different drug delivery systems to treat mycobacterial infections have been explored including liposomes, solid lipids and polymeric nanoparticles (56-59). Liposomes are microscopic vesicles composed of phospholipid bilayers surrounded by aqueous compartments (60) and have been used extensively as a drug carrier (61-63). After a liposome encounters a macrophage, it becomes adsorbed to the surface of the macrophage, engulfed through an energy dependent mechanism and finally degraded in phagolysosomal compartments. Properties that enhance phagocytosis of liposomes are surface charge and presence of a surface protein or carbohydrate. Positively charged liposomes are phagocytized best, with negatively charged particles being taken up better than neutral ones (64). Size is also critical for uptake of liposomes and the optimal size range is between 0.05-0.1 micrometers. Complications using liposomes included lack of stability in the presence of serum proteins, especially when loaded with hydrophilic drugs (65). Other limitations include low encapsulation efficiency and poor storage stability (66).

Starting in the 1990's, the use of Solid Lipid Nanoparticles (SLN) as drug delivery carriers has appeared in the literature (67). Solid lipid nanoparticles are lipid based submicron colloidal carriers (68) that are similar to nanoemulsions except SLN's consist of a solid hydrophobic core surrounded by a monolayer of phospholipids stabilized by surfactants. Since the basic components of SLN are already used in industry, they have an advantage over other carrier systems like liposomes because they have large "scale up" feasibility and presumably less concern of toxicity (69, 70). Disadvantages include rapid release of drugs from the particle or "burst release phenomenon" and poor stability. Entrapping antimycobacterial drugs in solid lipid nanoparticles is a novel strategy to combat TB infections, yet many formulations are still in the early development and experimental phase.

Nanomedicine, a sub specialty of nanotechnology, is a promising area of science that can aid in the development of new efficacious drug delivery methods to treat mycobacterial infections. By utilizing biocompatible nanomaterials such as polymeric nanoparticles to encapsulate antimicrobials, efficacy of current antimycobacterial treament regimens can be enhanced. There are hundreds of publications in the literature describing the production, composition, functions and efficacy of various types of nanoparticles as drug carriers. Very few address the importance and impact of using nanoparticles entrapped with antimycobacterial drugs to treat TB (71, 72). Encapsulation of antimicrobials in

nanoparticles can decrease the frequency of which the drug must be taken for the same therapeutic affect and increase the amount of drug delivered to a site, thereby reducing undesirable systemic side effects (73, 74). A study performed by Pandey et al. (75), examined the treatment of three frontline TB drugs encapsulated with the polymer PLG versus conventional antimycobacterial drugs in mice infected with TB. Following a single oral administration of the drug loaded nanoparticle, a prolonged therapeutic release was noted. Drug levels in the plasma of mice were maintained above the MIC for 6-9 days as compared to the conventionally treated group of which no amount of drug could be detected beyond 12 hours. Furthermore, encapsulation of polymeric nanoparticles is known to have an increase in drug load over other carrier systems (76). In the same study, the particle size of this nanoparticle was determined to be approximately 200nm and the encapsulation efficiency was determined to be 60-70%.

Encapsulation of antimicrobials in nanoparticles can also improve solubility, bioavailability and ultimately patient compliance (77, 78). Since nanoparticles, when taken orally, are known to cross the intestinal permeability barrier directly through the transcellular-paracellular pathway, the bioavailability increases over conventional drugs because the nanoparticle can deliver the drug intact to the circulation.

Encapsulation of antimicrobials with polymeric nanoparticles offers several advantages over other experimental treatment approaches. Polymeric nanoparticles can be tailored to the routes of administration. Oral, topical, ocular and inhaled have all been investigated with promising results (79, 80, 81, 82). The surface chemistry of polymeric nanoparticles can be altered to improve cellular uptake, prolong circulation time or regulate release of drugs (78, 83, 84).

The process of opsonization is an effective and automatic method of increasing cellular uptake (85). As a general rule, opsonization of hydrophobic particles occurs more quickly as compared to hydrophilic ones (64). Also, as demonstrated in *in vitro* research, surface charge also plays a role in opsonization with neutrally charged particles having a lower opsonization rate than charged particles (64). To prolong circulation time, polymeric nanoparticles can be coated with polymers such as PEG to become “stealth” or resistant to opsonization and thus prolong circulation time. Lastly the release of drugs from the nanoparticle can be regulated by modifying surface charge and chemistry and/or prolonging or encouraging opsonization. For example, following uptake, nanoparticles are transported through early endosomes to sorting endosomes. A fraction of the nanoparticles recycles back to the cell exterior while another fraction is transported to secondary endosomes or lysosomes (83). Here the antimicrobial encapsulated nanoparticles can either be broken down by hydrolytic enzymes thus releasing drugs, or escape into the cytoplasm depending on their surface charge (83) to release drugs there. However, as with any drug delivery

system, there are disadvantages or challenges to overcome and with polymeric nanoparticles, poor scale up feasibility and storage stability are the most common.

Polymeric nanoparticles represented in the literature are considered relatively safe and non-toxic (83, 86). If the nanoparticle is biocompatible and biodegradable like FDA approved PGLA or PLA, eventually the nanoparticle will be broken down into lactic acid and glycolic acid and eliminated via the tri-carboxylic acid cycle (83). If the polymeric particle is not biodegradable, it will accumulate in the organs of the liver and spleen. This deposition has been associated with toxicity and cell death (83, 64).

Since the pipeline for new anti-TB drugs is slow to emerge to the market, investigation of novel carrier systems that deliver current effective antimycobacterial drugs to the intracellular environment of the infected macrophage may prove to be beneficial in mycobacterial treatment. Nanomedicine could hold the key to this process and provide new efficacious drug delivery methods that are safe and improves patient compliance.

References

1. World Health Organization, www.who.int/tb/publications/global_report/2011/gtbr11_full.pdf
2. Bhatt, K., Salgame, P. (2007). "Host Innate Immune Response to *Mycobacterium tuberculosis.*" J Clin Immunol. Jul; **27**(4):347-62.
3. Gelperina, S., Kisich, K. et al. (2005). "The potential advantages of nanoparticle drug delivery systems in chemotherapy of tuberculosis." Am J Respir Crit Care Med **172**(12):1487-90.
4. Riska, P. F., Carleton, S. (2002). "Latent tuberculosis: models, mechanisms, and novel prospects for eradication." Semin Pediatr Infect Dis **13**(4):263-72.
5. Bermejo, A., Veeken, H., Berra, A. (1992). “Tuberculosis incidence in developing countries with high prevalence of HIV infection.” AIDS. Oct: **6**(10):1203-6.
6. Meya, D. B., McAdam, K. P. (2007). "The TB pandemic: an old problem seeking new solutions." J Intern Med **261**(4):309-29.
7. Loddenkemper, R. Sagebiel, D. Brendel, A. 2002. “Strategies against multidrug resistant tuberculosis.” Eur. Respir J. **20** Suppl. 36: 66s-77s.
8. Migliori, G. B., Loddenkemper, R. et al. (2007). "125 years after Robert Koch's discovery of the tubercle bacillus: the new XDR-TB threat. Is "science" enough to tackle the epidemic?" Eur Respir J **29**(3):423-7.
9. Brudney, K., Dobkin, J. (1991). “Resurgent tuberculosis in New York City: Human Immunodeficiency Virus, homelessness, and the decline of

tuberculosis control programs." American Review of Respiratory Disease Oct; **144**(4):745-749.

10. Pasqualoto, K. F. M., Ferreira, E. I. (2001). "An Approach for the Rational Design of New Anti-tuberculosis Agents." Current Drug Targets, Dec; **2**(4):427-437.
11. Skeiky, Y. A., Sadoff, J. C. (2006). "Advances in tuberculosis vaccine strategies." Nat Rev Microbiol **4**(6):469-76.
12. Mc Donough, K. A., Kress, Y., Bloom, B. R. (1993). "Pathogenesis of Tuberculosis: Interaction of *Mycobacterium tuberculosis* with Macrophages." Infection and Immunity **61**(7):2763-2773.
13. Sawant, K. V., McMurray, D. N. (2007). "Guinea pig neutrophils infected with *Mycobacterium tuberculosis* produce cytokines which activate alveolar macrophages in noncontact cultures." Infect Immun **75**(4):1870-1877.
14. Vieira, O. V., Botelho, R. J., Grinstein, S. (2002). "Phagosome maturation: aging gracefully." Biochem. J. Sep 15;**366**(Pt 3):689-704
15. Armstrong, J. A., Hart, P. D. (1975). "Phagosome-lysosome interactions in cultured macrophages infected with virulent tubercle bacilli. Reversal of the usual non-fusion patterns and observations on bacterial survival." J. Exp. Med. Jul; **142**(1): 1–16
16. Hestvik, A. L., Hmama, Z., Av-Gay, Y. (2005). "Mycobacterial manipulation of the host cell." FEMS Microbiol. Rev. **29**:1041-1050.

17. Sharma, A., Pandey, R., Sharma, S., Khuller, G. K. (2004) "Chemotherapeutic efficacy of poly (DL-lactic-co-glycolide) nanoparticle encapsulated anti-tubercular drugs at sub-therapeutic dose against experimental tuberculosis" Int. J. Antimicrob. Agents Dec; **24**(6):599-604.
18. Flynn, J. L., Chan, J. (2001). "Immunology of Tuberculosis." Annu. Rev. Immunol. **19**:93-129.
19. Tsai, M. C., Chakravarty, S., Zhu, G., Xu, J., Tanaka, K., Koch, C., Tufariello, J., Flynn, J. Chan, J. (2006). "Characterization of the tuberculosis granuloma in murine and human lungs: cellular composition and relative oxygen tension." Cell Microbiol. Feb; **8**(2):218-32.
20. Salgame, P. (2005). "Host innate and Th1 responses and the bacterial factors that control *Mycobacterium tuberculosis* infection." Curr Opin Immunol **17**(4):374-380.
21. Saunders, B. M., Brittion, W. J. (2007). "Life and death in the granuloma: immunopathology of tuberculosis." Immunol. Cell Biol. **85**:103-111.
22. Talaat, A. M., Ward, S. K. Wu, C. W., Rondon, E., Tavano, C. C., Bannantine, J. P., Lyons, R., Johnston, S. A. (2007). "Mycobacterial Bacilli Are Metabolically Active During Chronic Tuberculosis in Murine Lungs: Insights from Genome-Wide Transcriptional Profiling." Journal of Bacteriology **189**(11) 4265–4274.
23. Rustard, T. R., Harrell, M. I., Liao, R., Sherman, D. R. (2008). "The enduring hypoxic response of *Mycobacterium tuberculosis*." PloSOne **3**:e1502.

24. Opie, E., Aronson, J. (1927). “Tubercle bacilli in latent tuberculosis lesions and in
lung tissue without tuberculosis.” J. Path. Lab. Med. **4**:1-21.
25. Flynn, J. L., Chan, J., Triebold, K. J., Dalton, D. K., Stewart, T. A., Bloom, B. R. (1993). “An essential role for IFN-y in resistance to *M. tuberculosis* infection. “ J. Exp Med. Dec 1; **178**(6):2249-54.
26. Flynn, J. L., Goldstein, M. M., Chan, J., Triebold, K. J., Pfeffer, K., Lowenstein, C. J., Schreiber, R., Mak, T. W., Bloom, B. R. (1995). “Tumor necrosis factor–alpha is required in the protective immune response against *Mycobacterium tuberculosis* in mice.” Immunity Jun; **2**(6):561-572.
27. Kaufman, S. H., Schaible, U. E. (2005). “Antigen presentation and recognition in bacterial infections.” Curr. Opin. Immunol. Feb; **17**(1):79-87.
28. Boom, W, H., Canaday, D. H., Fulton, S. A., Gerhing, A. J., Rojas, R. E., Torres, M. (2003). “Human immunity to *M. tuberculosis*: T cell subsets and antigen processing.” Tuberculosis(Edinb) **83**(1-3):98-106.
29. van Pinxteren, L. A., Cassidy, J. P., Smedegaard, B. H., Agger, E. M., Anderson, P. (2000). “Control of latent *Mycobacterium tuberculosis* infection is dependent on CD8 T cells.” Eur. J. Immunol. Dec; **30**(12):3689-3698.
30. Ernst, J. D. (1998). “Macrophage Receptors for *Mycobacterium tuberculosis.”* Infect Immun. April; **66**(4):1277–1281.
31. Cole, S. T. Tuberculosis and the Tubercle Bacillius. Washington, DC: American Society for Microbiology, 2004.

32. Nicod, L. P. (2007). “Immunology of Tuberculosis.” Swiss Med Weekly **137**:357-362.

33. Tizard, I. R. Veterinary Immunology: An introduction 7th edition. Philadelphia, PA: Elsevier, 2004.

34. Harding, C. V., Boom, W. H. (2010). “Regulation of antigen presentation by *Mycobacterium tuberculosis*: a role for Toll-like receptors”. Nat Rev Microbiol April; **8**(4):296-307.

35. Tufariello, J. M., Chan, J., Flynn, J. L. (2003). Latent tuberculosis: mechanisms of host and bacillus that contribute to persistent infection. Lancet Infect. Dis. Sep; **3**(9)**:**578-590.

36. Xu, J., Laine, O., et al. (2007). "A unique *Mycobacterium* ESX-1 protein co-secretes with CFP-10/ESAT-6 and is necessary for inhibiting phagosome maturation." Mol Microbiol **66**(3): 787-800.

37. Clemens, D. L. (1996). “Characterization of the *Mycobacterium tuberculosis* phagosome.” Trends Microbiol. Mar; **4**(3):113-118.

38. Pieters, J. (2008). “*Mycobacterium tuberculosis* and the macrophage: maintaining the balance” Cell, Host and Microbe. Jun **8**:399-407.

39. Vergne, I., Chua, J., Singh, S. B., Deretic, V. (2004). “Cell biology of *Mycobacterium tuberculosis* phagosome.” Annu Rev Cell Dev Biol. **20:**367-94.

40. Brennan, P. J. (2003). “Structure, function and biogenesis of the cell wall of *Mycobacterium tuberculosis.”* Tuberculosis **83**(1-3):91-97.

41. Jarlier, V., Nikaido, H. (1994). “Mycobacterial cell wall: Structure and role in natural resistance to antibiotics.” FEMS Microbiology Letters Oct. **123**(1-2):11-18.
42. Daffé, M., Etienne, G. (1999). “The capsule of *Mycobacterium tuberculosis* and its implications for pathogenicity.” Tubercle and Lung Disease Jun; **79**(3):153-169.
43. Wilkinson, K. A., Kon, O. M. et al. (2006). "Effect of treatment of latent tuberculosis infection on the T cell response to *Mycobacterium tuberculosis* antigens." J Infect Dis **193**(3): 354-9.
44. Chan, E. D., Heifets, L., Iseman, M. D. (2000). “Immunologic diagnosis of tuberculosis: a review.” Tubercle and Lung Disease **80**(3):131-140.
45. Fine, P. E. (1995). “Variation in protection by BCG: implications of and for heterologous immunity.” Lancet **346**:1339-1345.
46. Anderson, P., Doherty, T. M. (2005). “The success and failure of BCG: implications for a novel tuberculosis vaccine.” Nat. Rev. Microbiol. Aug; **3**(8):656-662.
47. Houston, S. (1997). “Tuberculosis risk and prevention in travelers-what about BCG?” J. Travel Med. Jun 1; **4**(2):76-82.
48. Doherty, T. M., Anderson, P. (2005). “Vaccines for Tuberculosis: Novel Concepts and Recent Progress.” Clin Microbiol Rev **18**(4):687-702.
49. Lin, M. Y., Ottenhoff, T. H. (2008).” Not to wake a sleeping giant: new insights into host-pathogen interactions identify new targets for vaccination

against latent *Mycobacterium tuberculosis* infection: Vaccines in the pipeline a review." Biol Chem May; **389**(5):497-511.

50. Young, D., Dye, C. (2006). "The development and impact of tuberculosis vaccines. Cell Feb 24; **124**(4):683-7.
51. Gomez, J. E., McKinney, J. D. (2004). "*M. tuberculosis* persistence, latency, and drug tolerance." Tuberculosis (Edinb) **84**(1-2): 29-44.
52. Zhang, Y., Amzel, L. M. (2002). "Tuberculosis drug targets." Curr Drug Targets **3**(2): 131-54.
53. Global Alliance for Tb Drug Development, http://www.tballiance.org/pipeline/discovering-new-drugs.php
54. Primm, T. P., Franzblau, S. G. (2007). "Recent Advances in Methodologies for the Discovery of Antimycobacterial Drugs." Current Bioactive Compounds **3**(3):1-8.
55. Raviglione, M. C., Smith, I. M. (2007). "XDR tuberculosis--implications for global public health." N. Engl. J. Med. **356**(7):656-9.
56. Avgoustakis, K. (2004). "Peglated Poly(lactide) and Poly(lactide-co-glycolide) Nanoparticles: Preparation, properties and possible applications in drug delivery." Current Drug Delivery **1**: 321-333.
57. Muller, R. H., Mader, K., Gohla, S. (2000). "Solid lipid nanoparticles (SLN) for controlled drug delivery- a review of the state of the art." European Journal of Pharmaceutics and Biopharmaceutics **50**:161-177.
58. Barrow, W. W. (2004). "Microsphere Technology for Chemotherapy of Mycobacterial Infections. " Current Pharmaceutical Design **10**:3275-3284.

59. Klemens, S. P., Cynamon, M. H., Swenson, C. E, Ginsberg, R. S. (1990). “Liposome encapsulated gentamicin therapy of *Mycobacterium avium* complex infection in beige mice” Antimicrobial Agents and Chemotherapy June; **34**(6): 967-970.
60. Ahsan, F., Rivas, I. P., et al. (2002). "Targeting to macrophages: role of physicochemical properties of particulate carriers--liposomes and microspheres--on the phagocytosis by macrophages." J Control Release **79**(1-3):29-40.
61. Vyas, S. P., Khatri, K. (2007). “Liposomal-based drug delivery to alveolar macrophages.” Expert Opin. Drug Delivery **4**(2):95-99.
62. Gelpernia, S., Kisich, K., Iseman, M. D., Heifets, L. (2005). “The Potential Advantages of Nanoparticle Drug Delivery Systems in Chemotherapy of Tuberculosis” Am J Respir Crit Care Med **172:**1487–1490.
63. Leitzke, S., Bucke, W., Borner, K., Muller, R., Hahn, H., Ehlers, S. (1998). “Rationale for Efficacy of Prolonged-Interval Treatment Using Liposome-Encapsulated Amikacin in Experimental *Mycobacterium avium* Infection.” Antimicrobial Agents and Chemotherapies Feb; **42**(2):459-461.
64. Owens, D. E., Peppas, N. A. (2006). “Opsonization, biodistribution, and pharmacokinetics of polymeric nanoparticles.” International Journal of Pharmaceutics, Jan; **307(**1):93-102.
65. Prior, S., Gander, B. et al. (2002). "In vitro phagocytosis and monocyte-macrophage activation with poly(lactide) and poly(lactide-co-glycolide) microspheres." Eur J Pharm Sci **15**(2):197-207.

66. Soppimath, K. S., Aminabhavia, T. M., Kulkarnia, A. R., Rudzinski, W. E. (2001). “Biodegradable polymeric nanoparticles as drug delivery devices.” Journal of Controlled Release **70**:1-20.

67. Mukherjee, S., Ray, S., Thakur, R. S. 2009. “Solid lipid nanoparticles: A modern formulation approach in drug delivery system.” Indian J Pharm Sci 71(**4**): 349-358.

68. Emerich, D. F., Thanos, C. G. (2008). “Targeted nanoparticle-based drug delivery and diagnosis” Journal of Drug Targeting **15**(3):163-183.

69. Muller, R. H, Mader, K., Gohla, S. (2000). “Solid lipid nanoparticles (SLN) for controlled drug delivery- a review of the state of the art.” European Journal of Pharmaceutics and Biopharmaceutics **50**:161-177.

70. Uner, M., Yener, G. (2007). “Importance of solid lipid nanoparticles (SLN) in various administration routes and future perspectives.” International Journal of Nanomedicine **2**(3):289-300.

71. Barrow, E. L. W., Winchester, G. A., Staas, L. K., Quenelle, D. C., Barrow, W. W. (1998). “Use of microsphere technology for targeted delivery of rifampin to *Mycobacterium tuberculosis* infected macrophages” Antimicrobial Agents and Chemotherapy Oct; **42**:(10):2682-2689.

72. Pandey, R., Sharma, S., Khuller, G. K. (2006). “Chemotherapeutic efficacy of nanoparticle encapsulated antitubercular drugs” Drug Delivery **13**:287-294.

73. Emerich, D. F., Thanos, C. G. (2008). “Targeted nanoparticle-based drug delivery and diagnosis” Journal of Drug Targeting **15**(3):163-183.

74. Moghimi, S. M., Hunter, A. C., Murray, J. C. (2005). “Nanomedicine: current status and future prospects.” The FASEB Journal **19**:311-330.

75. Pandey, R., Ahmed, Z., Sharma, S., Khuller, G. K 2003.” Nanoparticle encapsulated antitubercular drugs as a potential oral drug delivery system against murine tuberculosis.” Tuberculosis (Edinb) **83**:373-378.

76. Pandey, R. (2011). “Nanomedicine and experimental tuberculosis: facts, flaws, and future.” Nanomedicine: nanotechnology, biology and medicine **7**:259-272.

77. Gaspar, M. M., Cruz, A. G., Fraga, A. G., Castro, A. G., Cruz, M. E. M., Pedrosa, J. (2008). “Developments on Drug Delivery Systems for the Treatment of Mycobacterial Infections.” Current Topics in Medical Chemistry **8**:579-591.

78. Davis, M. E., Chen, Z. G., Shin, D. M. (2008). “Nanoparticle therapeutics: an emerging treatment modality for cancer.” Nature Reviews Drug Discovery **7**:771-782.

79. Pandey, R., Khuller, G. K. (2007). “Nanoparticle based oral drug delivery system for an injectable antibiotic-streptomycin. “Evaluation in a murine tuberculosis model.” Chemotherapy **53**:437-441.

80. Pawar, K. R., Babu, R. J. (2010). “Polymeric and lipid based materials for topical nanoparticle delivery systems.” Crit. Rev. Ther. Drug Carrier Syst. 27(**5**):419-59.

81. Nagarwal, R. C., Kant, S., Singh, P. N., Maiti, P., Pandit, J. K. (2009). “Polymeric nanoparticulate system: A potential approach for ocular drug delivery.” Journal of Controlled Release. **136**:2-13.

82. Pandey R., Khuller G. K. (2005). “Antitubercular inhaled therapy: opportunities, progress and challenges.” Journal of Antimicrobial Chemotherapy **55**:430-435.

83. Panyam, J., Labhasetwar V. (2003). “Biodegradable nanoparticles for drug and gene delivery to cells and tissue.” Advanced Drug Delivery Reviews **55**:329-347.

84. Kakizawa Y., Kataoka, K. (2002). “Block copolymer micelles for delivery of gene and related compounds.” Advanced Drug Delivery Reviews **54**:203-222.

85. Moghimi, S. M., Hunter A. C., Murray, C. (2001). “Long Circulating and Target-Specific Nanoparticles: Theory to Practice.” Pharmacol Rev **53**:283 318.

86. Caruthers, S. D., Wickline-Lanza, G. M. (2007). “Nanotechnology applications in medicine.” Current Opinion in Biotechnology **18**:26-30.

Chapter Two

Standardization of *M. avium* Infection Model in Cell Culture and Mice

Abstract

Various biochemical tests for mycobacterial identification and a 10 day growth curve in bacterial media of *Mycobacterium avium* subspecies *hominissuis* strain 49601 were performed. Standardization of *M. avium* infection in cell culture with J774A.1 murine macrophages was also done. When a multiplicity of infection of 1 was used, ~1 x 10^5 CFU/mL of viable *M. avium* can be consistently recovered from the macrophages. Also by reducing the percent of fetal bovine serum in the media and by infecting the cells in the original culture flask, the cell culture infection experiment can be extended up to 6 days. Standardization experiments with BALB/c mice reveal an infective dose of 1 x 10^6 CFU/mL, given intra-peritoneally, was able to yield recoverable *M. avium* organisms consistently and cause microscopic granulomas in liver tissue.

Introduction

Mycobacterium avium is an opportunistic pathogen that is ubiquitous in distribution and capable of causing disease in both animals and humans (1, 2). *Mycobacterium avium hominissuis* is the sub species that is isolated from humans whereas *Mycobacterium avium* subsp. *avium* is reserved for infections originating from animals. *M. avium* is a member of the *Mycobacterium avium*

complex (MAC), where *M. avium* subspecies *paratuberculosis* (MAP), *M. avium* subspecies *silvaticum* and *M. intracellulare* also belong (3). In animals, *M. avium* can be transmitted via ingestion or aerosolized secretions (3). In humans, aerosolized water, drinking water, swimming pools and hot tubs are important sources of infection (4).

Once inside the body, *M. avium* passes through the mucosal epithelium and infects resident macrophages. Within macrophages, *M. avium* cells are carried to local lymph nodes via the lymphatic system. If the host has a robust and competent immune system, the infection will then be eliminated or controlled. This is the case with the majority of transient infections. However in the case of individuals with immune suppressive diseases like HIV, *M. avium* will spread rapidly via the blood, multiply unchecked and cause disseminated disease (3). In fact, members of MAC are the main source for non-tuberculous mycobacterial (NTM) infections in individuals suffering from acquired immune deficiency syndrome (AIDS) in developed countries (5).

M. avium is a difficult microorganism to treat with antimicrobials and typically treatment involves multiple drug therapy for extended periods of time (6). The innate resistance is due, in part, to the presence of a thick, mycolic acid-rich outer membrane (7). The mycobacterial outer membrane is comprised of lipids, waxes and mycolic acids (i.e., long chain fatty acids (C_{60}-C_{80}) and are unique to the genus *Mycobacterium* (8). Consequently, mycobacterial cells are resistant to

many disinfectants. In addition, NTM are relatively resistant to high temperature, high salt concentrations, acidic environments, and, can grow at low oxygen levels.

Members of the genus *Mycobacterium* share many similarities with respect to biological processes, architecture, and if pathogenic, similar disease processes and pathology in the host. Therefore for this dissertation, *M. avium* will be used as a surrogate for *M. tuberculosis.* *M. avium* is considered a lower risk opportunistic pathogen and can be maintained in Bio-Safety Level 2 laboratories. However, the knowledge gained from these research efforts may apply to *M. tuberculosis* or other mycobacteria as well.

Materials and methods

The majority of experiments involving infection models were performed using *Mycobacterium avium* subspecies *hominissuis* strain 49601 obtained from American Type Culture Collection (ATCC) (Manassas, VA, USA). Some experiments performed used *Mycobacterium avium* subspecies *hominissuis* strain A5, which was provided by Dr. Falkinham, Biology Department, at Virginia Tech. This strain was isolated from an AIDS patient and was used in biochemical classification experiments and some *in vivo* effort.

Growing Stock M. avium Cultures

A loop of rehydrated stock *M. avium* strain 49601 from ATCC was added to 2 mL of Middlebrook 7H9 Broth containing 10% (vol/vol) oleic acid- albumin-dextrose-catalase (OADC) enrichment (Difco Laboratories, Detroit, MI, USA) and incubated at 37° C in a rotary shaker for 7 days. The resulting culture was streaked on several Middlebrook 7H10 agar plates and incubated at 37° C for 7-10 days. Under 10-fold magnification by light microscopy, transparent colonies were selected and either re-streaked on Middlebrook 7H10 agar plates for later stock culture preparation, or added to 2 mL of M7H9 broth and incubated at 37° C with aeration for 7 days. Next, 1 mL of bacterial culture was transferred to 9 mL of fresh Middlebrook broth and placed back into the rotary shaker for an additional 4 days to achieve mid log growth, before being aliquoted into 1 mL tubes and frozen at -18° C. After one week, a frozen 1 mL tube was thawed, vortexed for several seconds, and streaked onto TSA plates to check for contamination. Additionally, the bacterial suspension was streaked onto M7H10 agar to assess the percentage of transparent colonies present within the culture and to determine the colony forming units per mL by serial dilution. Only cultures containing 90% transparent colonies were used in macrophage or mouse experiments.

Biochemical Classification of M. avium

Acid Fast Staining (Ziehl Neelson)

One colony of *M. avium* A5 was smeared onto a slide to which a drop of water was added. After air drying, the slide was passed quickly through a flame to fix

the cells. A piece of paper towel was affixed to the slide to prevent the dye from spilling over. Next, carbofuschin dye was added and the slide was placed over a flame until steam was produced. For the next eight minutes, flaming was continued resting periodically as to not boil the dye. More dye was added as needed. Next, the paper towel piece was removed and the slide was rinsed with water, before flooding with acid-alcohol for twenty seconds. After rinsing again with water the counter stain, methylene blue, was added for one minute. The slide was rinsed one final time and left to air dry before microscopic examination with an oil immersion lens.

The Catalase Drop Method

Equal volumes of 30% hydrogen peroxide and 10% of sterilized Tween 80 were mixed together. One drop of the mixture was added to visible growth on a Middlebrook agar plated streaked with *M. avium* strain A5 and observed for the presence of “bubbling” around the colonies.

Nitrate Reduction Test

In a sterile screw cap test tube, a loopful of broth containing *M. avium A5* was added to 4 mL of distilled water and 2 mL of NaNO3 substrate solution. After shaking the tube gently by hand, the tube was incubated in a water bath for 2 hours at 37°C. Next, one drop of 3 separate reagents was added; Reagent one consisted of a 1:2 dilution of concentrated HCL in water, Reagent two was 0.2% sulfanilamide and Reagent three was 0.1% aqueous N-(1-naphthyl)

ethylenediamine dihydrochloride. Observations of color development were recorded.

Tellurite Reduction Test

A turbid broth culture of *M. avium* strain A5 was inoculated with 2 drops of potassium tellurite solution and incubated for 4 days at 37°C. Development of a black solution was considered positive and recorded.

Tween Hydrolysis Test

A solution containing 100 mL of phosphate buffer 0.067M, 0.5 mL of Tween 80, and 2 mL of 0.1% aqueous neutral red stock solution was autoclaved for 15 minutes at 121° C before a loopful of actively growing *M avium A5* was added and incubated for up to 10 days. Presence of a red color was recorded day 1, 5, and 10.

Arylsulfatase Test

2.5 mL of tri-potassium phenolphthalein 0.08M was added to 200 mL of dubios broth media and aliquoted in 2 mL amounts into a screw cap test tube. Approximately 0.1mL of a barely turbid culture of *M. avium A5* was added to the mixture and incubated for 3 days at 37° C. After three days, 6 drops of 1M Na_2CO_3 was added to the tube and observations of color, if any, was recorded.

M. avium Growth Curve in Broth Culture

Five (5) mL of a 7 day culture of *M. avium* strain A5 was inoculated into a side arm flask containing 45mL of M7H9 incubated on a rotary shaker at 37° C. The optical density was measured using a Klett colorimeter (Klett-Summerson colorimeter; Klett Manufacturing, Brooklyn, N.Y.) with the blue filter, twice daily for 10 days. Samples of the bacterial culture were collected every 24 hours, diluted and 0.1 mL of each dilution spread on M7H10 agar in triplicate, sealed with parafilm and placed in an incubator at 37° C for 7-10 days to determine the colony forming units (CFU)/mL.

In Vitro J774A.1 Murine Macrophage Infection Model with M. avium strain 49601

For intracellular infection studies with *M. avium* in this dissertation, the murine macrophage cell line J774A.1 was used. This macrophage cell line is the predominate type represented in the literature for *in vitro* mycobacterial research (9, 10,11). The cell line was isolated from a tumor in a female BALB/c mouse. It is easily maintained in the laboratory setting, has strong phagocytic ability and produces copious amounts of lysosomal enzymes (19). Development of the *M. avium* infection model was based essentially according to Barrow et al. and Wright et al. (9, 10, 11) with some modifications.

Murine macrophage cell line, J774A.1, was acquired from ATCC and grown as monolayers in 75 cm^2 tissue culture flasks (Corning, Inc., Corning, NY) in a humidified incubator with 5% CO_2 atmosphere at 37° C. Cells were maintained in

Dulbecco's modified Eagle's medium (DMEM) from Sigma-Aldrich (St. Louis, MO) containing 10% (vol/vol) fetal bovine serum (FBS), L-glutamine (4mM), $NaHCO_3$, (0.44M) pyridoxine-HCl, 4500 mg/L glucose and 1% penicillin-streptomycin solution (Mediatech, Inc. Manassas, VA). At 90% confluence, the medium in the flask was removed and replaced with approximately 5 x 10^6 colony forming units/mL of *M. avium* suspended in 10 mL of DMEM supplemented with 10% FBS for a MOI of 1:1. After 4-6 hours of incubation, macrophages were rinsed twice with Hanks Balanced Salt Solution, then collected by gently scraping the flask with 10 mL of DMEM with 10% FBS. Next, the cell suspension was centrifuged at 156xg for 3 minutes (Sorvall Legend RT Plus, UK) to remove non-adherent mycobacteria by discarding the supernatant suspension. The pelleted cells were then suspended in 38 mL of DMEM containing 10% (vol/vol) FBS. The cell suspension was then seeded in 1 mL samples into 12 well plates at a concentration of 2 x 10^5 macrophages per well, previously determined by Trypan Blue Dye Exclusion Assay. Plates were then incubated at 37° C in 5 % CO_2 for twenty-four hours to allow attachment of infected cells. Then, every twenty-four hours, samples were withdrawn and cells were lysed with 0.1% (vol/vol) Triton X-100. The lysate was then plated by serial dilution on M7H10 agar medium to quantify the number of *M. avium* organisms in CFU/mL.

In Vivo Murine Infection Model with M. avium 49601

Typically, for *in vivo* studies with *M. avium*, beige mice are the predominant mice strain used (21, 22) but BALB/c and C57BL/6 are also represented in the

literature (23, 24, 25). Beige mice require special care and husbandry because they lack functional immune cells such as T lymphocytes and Natural Killer (NK) cells, which are crucial in the control of infection. In contrast, BALB/c mice are considered immune- competent and remain healthy for a significant amount of time, even at high infective doses. In this dissertation, BALB/c mice were chosen based on current literature, availability, cost, temperament and previous laboratory experience with this strain. The standardization of *M. avium* infection in mice was adapted from Fattorini et al. (12, 13).

Female BALB/c mice (Charles River, ME) were housed as per Institutional Animal Care and Use Committee (IACUC) approved protocol in an animal biosafety level (ABSL) 2 facility with food and water *ad libitum.* Mice were placed into 3 groups, with each group containing 15 mice except for a negative control group, which contained 5. According to group assignment (Table 2.1), 8-10 week old mice received 200 µl intra-peritoneally of either 5×10^6 CFU/mL, or 5×10^7 CFU/mL of *M. avium* strain 49601, grown to mid-log phase and containing at least 90% translucent colonies.

All mice were individually marked and weighed weekly throughout the experiment. At weeks 2, 4, and 10 weeks post infection, 5 mice from groups two and three were sacrificed and liver, spleen, kidney and lung tissue were collected for quantification of CFU/organ. In addition, two mice from groups two and three, at each time point, had approximately half of each organ collected and placed in

10% formalin for histopathological analysis. An impression smear of any visible granuloma on an organ was obtained for acid fast staining. At ten weeks, 5 mice from group one, the non-infected negative controls, were sacrificed and liver, spleen, kidney and lung tissue were collected for quantification of CFU/organ and histological analysis.

Measurement of M. avium counts in tissues

Mice were euthanized via CO_2 asphyxiation and cervical dislocation before lung, liver, kidneys and spleen were collected to measure colony forming units per organ. The organs were aseptically removed, weighed, and if needed, halved and placed into 10% formalin. Otherwise whole or halved organs were placed in separate 50mL tubes containing 2mL of M7H9 broth. Organs were homogenized for 1-2 minutes using a Tissuemiser homogenizer (Fisher Scientific, USA), 200µl of organ homogenate was placed into well of 96 well plate and serially diluted in M7H9 broth to a maximum of 10^{-5} dilutions, plated on M7H10 agar and incubated for 7-14 days at 37° C. The number of colonies per dilution were counted, calculated and reported in CFU/organ.

Results

Biochemical Classification

Acid Fast Staining (Ziehl Neelson)

After performing the standard acid fast staining procedure, several bright pink rod shaped organisms were observed under 100X magnification indicating the presence of *M. avium* (Figure 2.1).

Biochemical Analysis

Routine biochemical analyses were performed to aid in the identification of *M. avium.* All biochemical tests yielded expected outcomes (Table 2.2) which included a positive tellurite reduction and catalase drop test. The nitrate reduction, tween hydrolysis and arylsulfatase test were negative.

M. avium A5 Growth Curve in Broth Culture

A standard growth curve of *M. avium* in Middlebrook 7H9 Broth containing 10% (vol/vol) oleic acid- albumin-dextrose-catalase (OADC) enrichment was performed for ten days. Every twenty four hours, a sample of the culture was obtained and processed to determine the numbers of colony forming units per mL. After a ten day period, *M. avium* organisms increased their growth by about one log (Figure 2.2).

Standardization of Infection Model in Murine Macrophages with M. avium 49601

The intracellular growth of *M. avium* in J774A.1 macrophages was standardized by using a multiplicity of infection of 1. *M. avium* infected murine macrophages were seeded in 1 mL aliquots into 12 well plates at a concentration of 2×10^5

macrophages per well. Every twenty four hours, cells were processed to determine the numbers of colony forming units per mL. During the initial two day period, intracellular growth increased by about 1/3rd of a log (Figure2.3). On day three, growth decreased slightly and then stabilized through day five.

Standardization of Infection Model in BALB/c Mice with M. avium 49601

The effect of duration of infection and inoculum size of *M. avium* was examined in the spleen and liver of BALB/c mice. At two weeks post infection, there was a lack of reduction in the bacterial load in the liver using an inoculum dose of 5 x10^{6} *M. avium* organisms. By 4 weeks post infection, the bacterial load was reduced by one log without the use of antibiotics. At 10 weeks post infection, the bacterial load had remained the same at 1 x 10^{5} without antibiotics. Also, when an inoculum dose of 5 x10^{7} of *M. avium* was given to the mice, the bacterial load recovered in the liver at 2 weeks post infection, was reduced by about 1.5 logs (with a large standard of error). At 4 and 10 weeks post infection, the bacterial load had remained fairly consistent without the use of antibiotics (Figure 2.5).

Also at two weeks post infection, there was a lack of reduction in the bacterial load in the spleen using an inoculum dose of 5 x10^{6} *M. avium* organisms (Figure 2.4). At 4 weeks post infection, the bacterial load was reduced by 1/2 log without the use of antibiotics. At 10 weeks post infection, the bacterial load was reduced by 1 log without antibiotics. When an inoculum dose of 5 x10^{7} of *M. avium* was given to the mice, the bacterial load recovered in the spleen at 2 weeks post

infection, was slightly more than 2 logs although a large standard of error was present. At 4 weeks post infection, the bacterial load had increased slightly for a total of a 2 log reduction with a small standard of error. At 10 weeks post infection, it appeared as if the bacterial load increased although a large standard of error was present. Additionally, throughout the experiment, all mice appeared bright alert and reactive and continued to gain weight. Also, no macroscopic granulomas were seen at either dose in any of the organs upon necropsy.

Discussion

There are many biochemical analyses that can be performed to aid in the classification and identification of bacteria. In the laboratory setting, the acid fast staining test (Ziehl Neelson) is a rapid, low cost and reliable method to assist in the diagnosis of mycobacterial infections. Under examination with a light microscope, the presence of red colored rods indicates a positive result (See Figure 2.1). Acid fast organisms like *Mycobacterium* get their “acid-alcohol fastness” from large amounts of lipid substances within their cell walls called mycolic acids. These acids resist staining by ordinary methods such as the Gram stain.

Although other closely related bacteria like *Nocardia* can also stain acid fast, examination of colony morphology and further analysis of simple biochemical tests can quickly establish the presence of a mycobacterial organism (14). One easy test to perform is the catalase drop method. Almost all mycobacteria are

positive except for a few mutant strains resistant to isoniazid (15). Catalase is a common enzyme found in many living organisms and catalyzes the breakdown of hydrogen peroxide to water and oxygen. When a few drops of the enzyme were placed on *M. avium* colonies, the presence of “bubbling” was observed indicating a positive result.

The nitrate reduction test is a biochemical test that is useful to determine between *M. tuberculosis* and *M. bovis* (15). The test reveals if a mycobacterial species can utilize nitrite as an energy source from nitrogen. A lack in the development indicates a negative result. *M. avium* is considered to be negative for this test, although research has shown that *M. avium* can reduce nitrate but at much slower rate than the test is able to detect (16).

The tellurite reduction test is a valuable test to differentiate between slow or fast growing *Mycobacterium.* Of the slow growers, only *M. avium* and *M. intracellulare* are able to reduce tellurite to metallic tellurium which is then deposited in the cell membrane resulting in black color and a positive test.

Some mycobacteria are able to hydrolyze Tween 80 and release oleic acid. This can aid in the identification between *M. scrofulaceum* or *M. avium* which are negative, seen as a lack of the development of a red color.

The arylsulfatase test is useful to distinguish between fast or slow growing mycobacteria. Fast growing mycobacteria like *M. scrofulaceum* strains can hydrolyze the added chemical phenolphthalein disulfate (PPDS) to produce a pink or red color within a few days where as slow growing organisms like *M. avium* or *M. intracellulare* will take much longer, if at all (17).

Growth curve

The bacterial generation time is the time it takes to double the population from beginning to completion of the replication cycle. For *M. avium* it is about 10-12 hours which is why it is considered a slow growing organism. For comparison, *M. smegmatis,* a fast growing *Mycobacterium*, has a generation time of 2 hours (18).

In examining the growth curve of *M. avium* in this experiment (Figure 2.2), it appears very similar to what is expected with a lag phase and a logarithmic growth phase, yet the stationary and decline phase seem to be elusive. Perhaps this is attributable to the amount of media in the flask still being capable of supporting continued growth beyond 10 days, which is the typical length of a *M. avium* growth curve.

In vitro infection studies with *M. avium* in J774A.1 cells are difficult to pursue due to the slow growth of *M. avium* and the short life cycle of the macrophage. In order to overcome this challenge and extend the life of the macrophages, Fetal

Bovine Serum (FBS), a common nutrient in cell culture medium was reduced from the standard 10% to 1% of the media (9, 10). This adjustment can slow the replication rate of the macrophages allowing for more time to study the intracellular activities of *M. avium*. Also, by infecting macrophages in the flask instead of in the 12 well plate, a step in the protocol can be eliminated thus allowing for more time to collect additional data points.

A multiplicity of infection (MOI) of 1 occurred as a result of infecting the macrophages in the flask. Ideally a MOI of 1 represents a ratio between the numbers of infectious organisms to the numbers of target cells present. As the MOI increases, the percentages of target cells infected with at least one bacterium or virus increases. A MOI of 1 translates into about 65% of macrophages being infected with at least 1 *Mycobacterium*. Typical MOI's used in mycobacterial infection studies are 5 or 10 (10). Yet a MOI of 1 in this procedure was able to consistently recover viable *M. avium* organism at 2×10^6 CFU/mL (Figure 2.3).

Observations from multiple infection experiments with *M. avium* in J774A.1 cells has shown that on day 1 of infection, the amount of viable *M. avium* recovered from infected macrophages is typically $1/3^{rd}$ to $2/3^{rd}$ logs lower than original inoculum. Potentially, two reasons for this observation are the natural phagocytic ability of macrophage to kill *M. avium* organisms and the loss of infected macrophages from the seeding process. Also noted in Figure 2.3, there is

typically little increase in intracellular growth of *M. avium* in J774A cells throughout the course of the 6-day experiment. These observations have also been noted by others, but not all, *M. avium* strains including strain 49601 using similar infection doses (28, 29).

If higher inoculums are used, the risk of causing detachment and death of the macrophages from super infection increases. In the host, macrophages and other phagocytic cells are able to initiate cell death via apoptosis in response to overwhelming intracellular infection. This is the cell's last resort to control the infection by exposing it to the external environment. In cell culture media, macrophage death can occur by self-induced apoptosis or by necrosis, which is caused by catastrophic destruction of the cellular components both of which can be caused by super infection with *M. avium* or other infectious agents.

For this *in vivo* standardization experiment, two infection doses were chosen based on previous publications (12, 13) and data collected from earlier dose titration experiments with other *M. avium* strains such as A5. At both doses of 5 $x10^6$ or 5 $x10^7$, *M. avium* could be consistently recovered from the liver and spleen of mice. Also, the mice in this study did not become ill or die. In fact they continued to gain weight throughout the study. As illustrated in Figure 2.4 and 2.5, an inoculum dose of 5 $x10^6$ CFU/mL is reduced in both the spleen and liver by approximately 1 log by 4 weeks post infection and did not increase in bacterial burden when examined at 10 weeks post infection. This bacterial stabilization

has been seen in other infection models using BALB/c mice with *M. avium* for up to 90 days (13, 23) and possibly much longer. The BALB/c mouse has functional CD4 T cells, which are essential for the control of infection and thus a great model to use when studying infections with *M. avium.*

As seen in Figure 2.6, an infiltration of macrophages appeared in the liver parenchyma and began to cluster around the periphery of the central lobules. This is likely the early formation of a granuloma. In comparison to the highly structured granuloma of humans, mice granulomas are less organized with a loose accumulation of macrophages, neutrophils and lymphocytes in the lesion. Also, caseation is less common in the mouse and if present, occurs more slowly.

In earlier experiments with strain A5, granulomas were evident on the surface of the liver and spleen at 8-10 weeks post infection at similar doses, yet the same was not seen at 4 or 10 weeks with strain 49601 at an infection dose of 5×10^6 or 5×10^7 (Figure 2.7). It is known that there are differences in pathogenicity between strains and it is likely that strain A5 is more virulent than 49601 with respect to induction of granuloma formation in mice (26, 27).

Conclusion

One major goal of these experiments was to standardize an infection model *in vivo* and *in vitro* with *M. avium* 49601. It is necessary to standardize research experiments to reliably predict the course of disease in an infection model and

consistently recover a known amount of viable microorganisms for a given dose. In the standardization experiment with macrophages, it was shown that J774A.1 cells can survive up to 6 days by reducing the percent of FBS in the media, and by infecting the cells in the flask before seeding into the 12 well plates. When a multiplicity of infection of 1 was used, 1×10^5 CFU/mL of viable *M. avium* were consistently recovered. In mice an infective dose of 5×10^6 was able to yield recoverable *M. avium* organisms consistently and cause microscopic granulomas.

References

1. Thoen C. O. (1994). "*Mycobacterium avium* infections in animals" Res Microbiol **145**(3):173-7.
2. Falkinham III J. O. (1996). “Epidemiology of Infection by Nontuberculous Mycobacteria” Clinical Microbiology Reviews Apr; **9**(2):177-215.
3. Inderlied C. B., Kemper C. A., Bermudez L. E. (1993). “The *Mycobacterium avium* complex” Clinical Microbiology Reviews July; **6**(3):266-310.
4. Falkinham III J. O., Norton C. D. LeChevallier M. W. (2001). “Factors influencing numbers of *Mycobacterium avium, Mycobacterium intracellulare*, and other mycobacteria in drinking water distribution systems.” Appl Environ Microbiol **67**:1225-1231.
5. Nightingale S. D., Byrd L. T., Southern P. M., Jockusch J. D., Cal S. X., Wynne B. A. (1992). “Incidence of *Mycobacterium avium-intracellulare* complex bacteremia in human immunodeficiency virus-positive patients.” J Infect Dis **165**:1082-1085.
6. Griffith D. E., Aksamit T. Brown-Elliott B A., Catanzaro A., Daley C., Gordin F., Holland S. M., Horsburgh R., Huitt G., Iademarco M. F., Iseman M., Olivier K., Ruoss S., von Reyn C. F., Wallace Jr. R. J., Winthrop K. (2007). “American Thoracic Society Documents: An official ATS/IDSA statement: diagnosis, treatment, and prevention of nontuberculous mycobacterial diseases.” Am. J. Respir. Crit. Care Med. Feb.; **175**(4):367-416.

7. Chatterjee D. (1997). “The mycobacterial cell wall: structure, biosynthesis drug action and sites of drug action.” Curr Opin Chem Biol. Dec; **1**(4):579-88.
8. Cole S.T. *Tuberculosis and the Tubercle Bacillius*. Washington, DC: American Society for Microbiology, 2004.
9. Barrow E. L. W., and W. W. Barrow. (2007). “Efficacy of Rifabutin loaded microspheres for treatment of *Mycobacterium avium* infected macrophages and mice” Drug Delivery **14**:119-127.
10. Barrow E. L. W., Winchester G. A., Staas L. K., Quenelle D. C., Barrow W. W. (1998) “Use of microsphere technology for targeted delivery of rifampin to *Mycobacterium tuberculosis* infected macrophages.” Antimicrobial Agents and Chemotherapy **42**(10): 2682-2689.
11. Wright E. L., Quenelle D. C., Suling W. J., Barrow W. W. (1996) “Use of Mono Mac 5 Human Monocytic cell line and J774 Murine Macrophage cell line in parallel antimycobacterial drug studies” Antimicrobial Agents and Chemotherapy Sept; **40**(9): 2206-2208.
12. Fattorini L., Mattei M., Placido R., Iona E., Agrimiz U., Colizzi V., Orefici G. (1999). “*Mycobacterium avium* infection in BALB/c and SCID mice” J. Med. Microbiol. **48**:577-583.
13. Fattorini L., Nisini R., Fan Y., Li Y.J., Tan D., Mariotti S., Teloni R., Iona E., Orefici G.(2002). “Exposure of BALB/c mice to low doses of *Mycobacterium avium* increases resistance to a subsequent high-dose infection.” Microbiology Oct; **148**(10):3173-3181.

14. Leao S. C., Martin A., Mejia G. I., Palomino J. C., Robledo J., Telles M. A. S., Portaels F. (2005). *Practical handbook for the phenotypic and genotypic identification of mycobacteria.* Brugge, Belgium, Van den Broele.
15. Hugo, D. (1976). *Bacteriology of the mycobacteriosis.* U.S. Dept. of Health, Education, and Welfare, Public Health Service, Center for Disease Control, Bureau of Laboratories, Bacteriology Division, Mycobacteriology Branch, Atlanta GA.
16. McCarthy C. M. (1987). "Utilization of nitrate or nitrite as single nitrogen source by *Mycobacterium avium*." J Clin Microbiol. Feb; **25**(2): 263–267.
17. Falkinham III J. O. (1990). "Arylsulfatase Activity of *Mycobacterium avium, M. intracellulare,* and *M. scrofulaceum"* International Journal of Systemic Bacteriology." **40**(1):66-70.
18. Williams K. J., Chung G. A. C., Piddock L. J. V., (1998). "Accumulation of Norfloxacin by *Mycobacterium aurum and Mycobacterium smegmatis*. Antimicrobial Agents and Chemotherapy Apr; **42(**4):795–800.
19. American Type Culture Collection, http://www.atcc.org/.
20. Quenelle D. C., Staas J. K., Winchester G. A., Barrow E. L. W, Barrow W. W. "Efficacy of microencapsulated rifampin in *Mycobcaterium tuberculosis* infected mice" (1999). Antimicrobial Agents and Chemotherapy. Oct;**43**(5): 1144-1151.

21. Klemens S. P., Cynamon M. H., Swenson C. E., Ginsberg R. S. (1990). "Liposome encapsulated gentamicin therapy of *Mycobacterium avium* complex infection in beige mice" Antimicrobial Agents and Chemotherapy Jun;**34**(6): 967-970.
22. Duzenges N., Perumal V. K., Kesavalu L., Goldstein J. A., Debs R. J., Ganagadharam P.R.J. (1988) "Enhanced effect of liposome encapsulated amikacin on *Mycobacterium avium- M. intracellulare* complex" Antimicrobial Agents and Chemotherapy Sept;**32**(9): 1401-1411.
23. Roque S., Nobrega C., Appelberg R., Correia-Neves M. (2007). "IL-10 Underlies Distinct Susceptibility of BALB/c and C57BL/6 Mice to *Mycobacterium avium* Infection and Influences Efficacy of Antibiotic Therapy." Journal of Immunology Jun;**178**(12): 8028-8035.
24. Chung S. W., Choi S. H., Kim T. S. (2004). "Induction of persistent in vivo resistance to *Mycobacterium avium* infection in BALB/c mice injected with interleukin-18-secreting fibroblasts." Vaccine **22**: 398-406.
25. de Steenwinkel J. E., van Vianen W., Ten Kate M. T., Verbrugh H. A., van Agtmael M. A., Schiffelers R. M., Bakker-Woudenberg I. A. (2007). "Targeted drug delivery to enhance efficacy and shorten treatment duration in disseminated *Mycobacterium avium* infection in mice." J Antimicrob Chemother. Nov;**60**(5):1064-73.
26. Birkness K. A., Swords E. W., Huang P. H., White E. H., Dezzutti C. S, Lal R. B., Quinn F. D. (1999) "Observed Differences in Virulence-Associated

Phenotypes between a Human Clinical Isolate and a Veterinary Isolate of *Mycobacterium avium*." Infect Immun. Sept.;**67**(9):4895–4901.

27. Amaral E. P., Kipnis T. L., de Carvalho E. C. Q., da Silva W. D., Leão S. C., et al. (2011). "Difference in Virulence of *Mycobacterium avium* Isolates Sharing Indistinguishable DNA Fingerprint Determined in Murine Model of Lung Infection." PLoS ONE **6**(6):e21673.
28. Gaspar, M. M. Neves S., Portaels F., Pedrosa J., Silva M. T., Cruz M. E. (2000). "Therapeutic efficacy of liposomal rifabutin in a *Mycobacterium avium* model of infection." Antimicrob Agents Chemother. Sep;**44**(9):2424-30.
29. Onyeji C. O., Nightingale C. H., Nicolau D. P., Quintiliani R. (1994). "Efficacies of liposome-encapsulated clarithromycin and ofloxacin against *Mycobacterium avium-M. intracellulare* complex in human macrophages." Antimicrob Agents Chemother Mar;**38**(3):523-7.

Tables and Figures

Treatment Groups and dose*		No. of mice per group	No. of mice sacrificed @ 2 weeks	No. of mice sacrificed @ 4 weeks	No. of mice sacrificed @ 10 weeks
1.	Negative Control	5	0	0	5
2.	*M. avium* 5 x 10^6 CFU/mL	15	5	5	5
3.	*M. avium* 5 x 10^7 CFU/mL	15	5	5	5

*Note: Mice were housed 5 to a box.

Table 2.1. *Experimental Design of BALB/c mice infected with M. avium 46901*

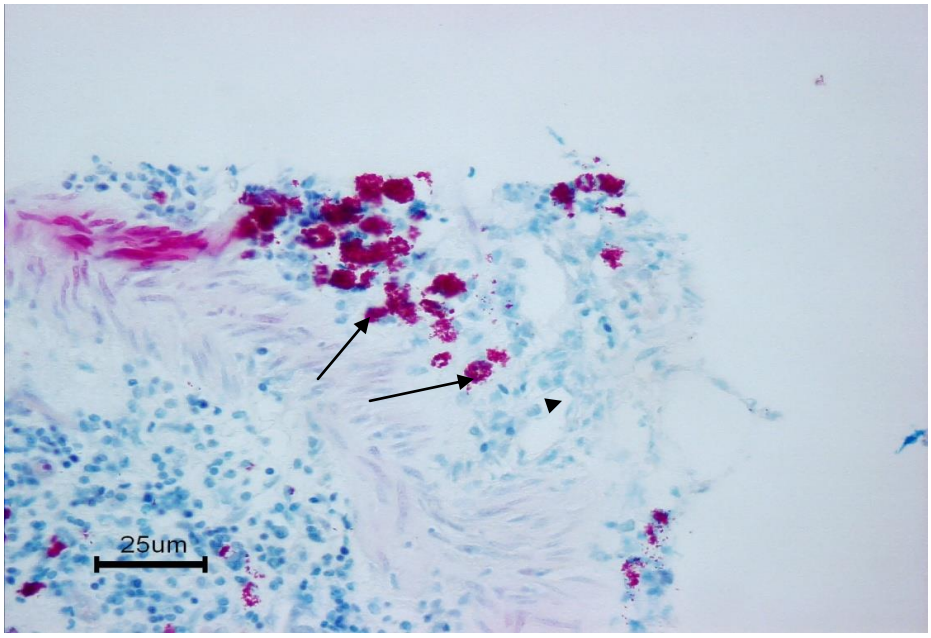

Figure 2.1. Acid fast stain of liver tissue infected with *M. avium* in BALB/c mice at 2 weeks post infection. Arrows indicate pink, rod shaped *M. avium* organisms.

Biochemical Analysis	Result
Catalase drop test	Positive
Nitrate reduction test	Negative
Tellurite Reduction test	Positive
Tween Hydrolysis test	Negative
Arylsulfatase test	Negative

Table 2.2 Standard biochemical tests to assist in identification of *M. avium.* Strain A5 was the isolate used in this analysis.

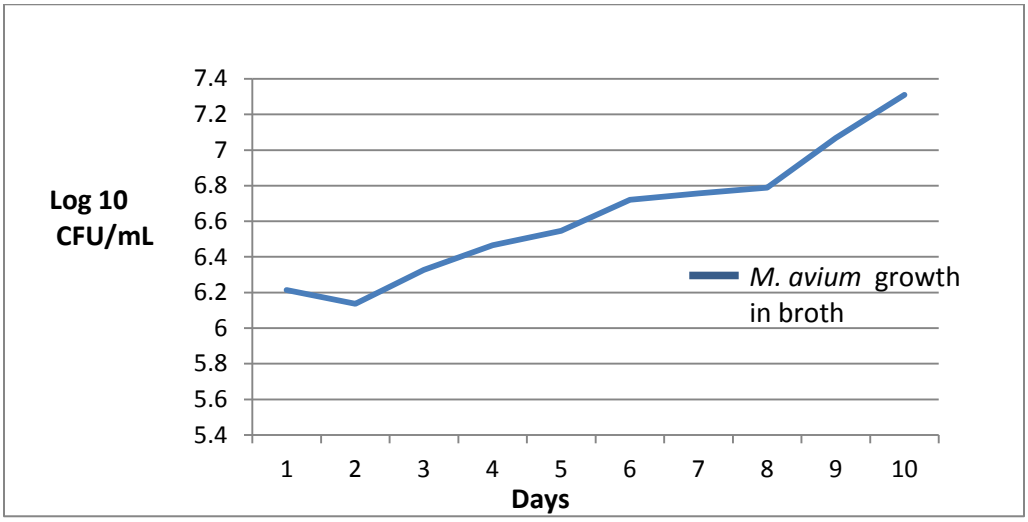

Figure 2.2 Growth curve in broth of *M. avium* determined by serial dilution in colony forming units per mL over a ten day period.

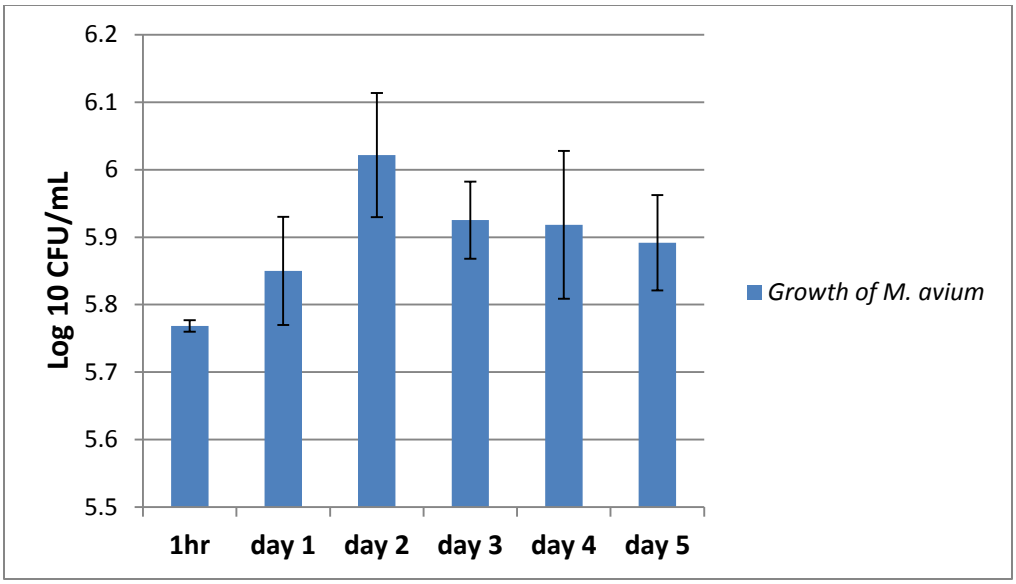

Figure 2.3. Intracellular growth of *M. avium* 49601 in J774A.1 murine macrophages. Macrophages were infected at a MOI of 1 and harvested each day to quantify the number of *M. avium* in colony forming units per mL by serial dilution. Tests were performed in triplicate, N=3.

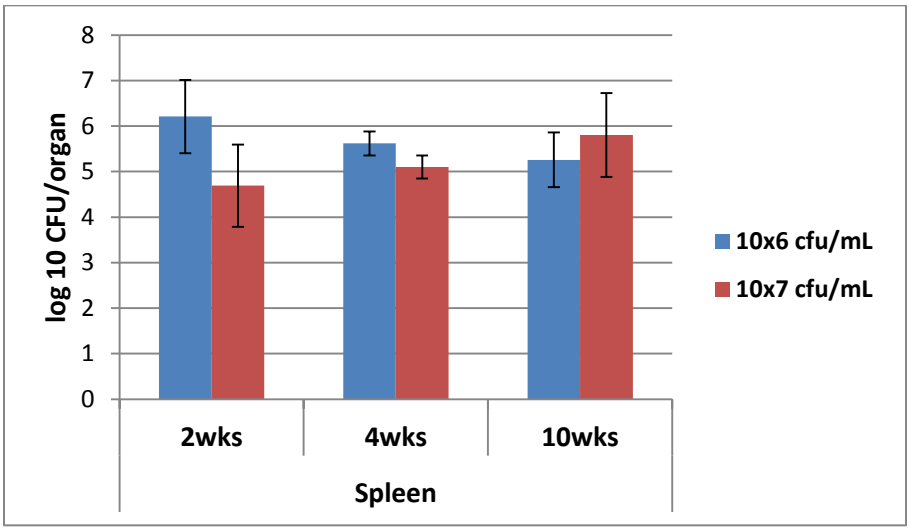

Figure 2.4 Standardization of infection model of *M. avium* 49601 in the spleen of BALB/c mice. The effect of duration and inoculum size of *M. avium* infection in

the spleen of mice was analyzed at 2, 4, and 10 weeks post infection, using two different inoculum dilutions; 5 x10^6 and 5 x10^7

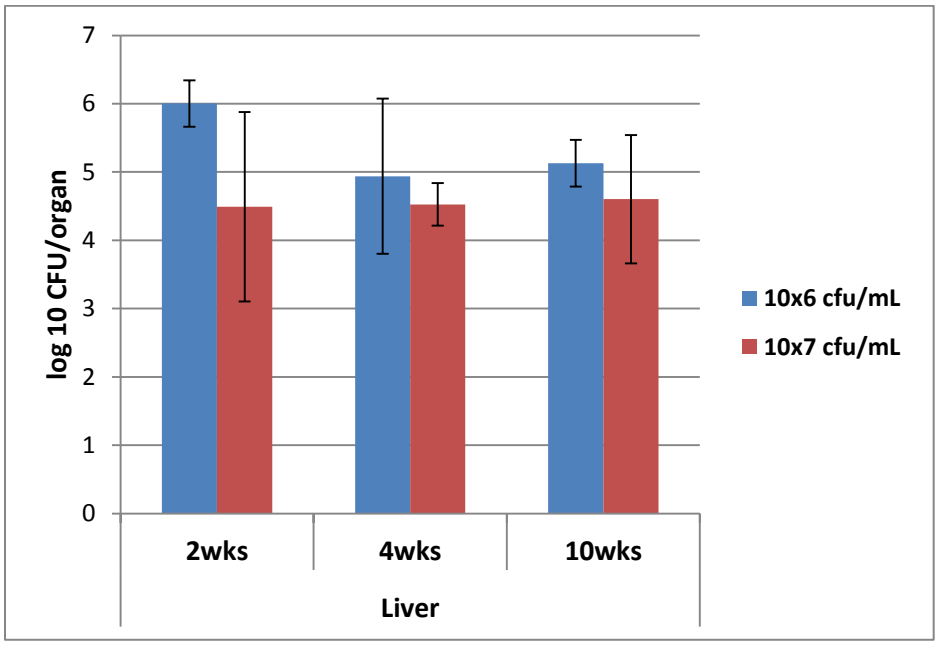

Figure 2.5. Standardization of infection model of *M. avium* 49601 in the liver of BALB/c mice. The effect of duration and inoculum size of *M. avium* infection in the liver of mice was analyzed at 2, 4, and 10 weeks post infection, using two different inoculum dilutions; 5 x10^6 and 5 x10^7 .

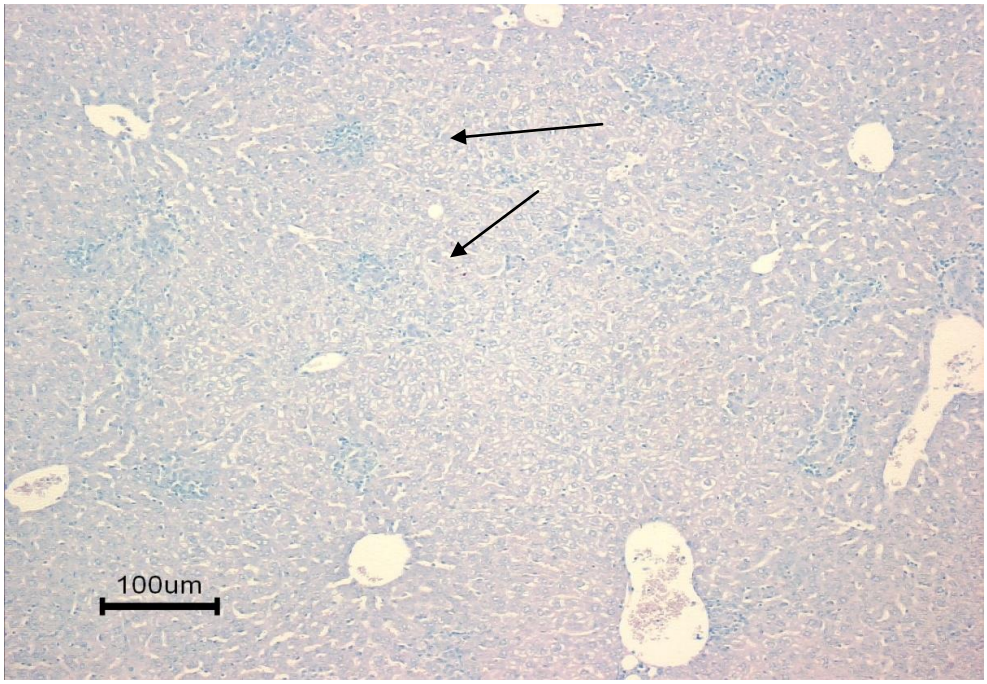

Figure 2.6. Histological analysis of liver from *M. avium* infected BALB/c mice at 4 weeks. Arrows indicated areas of accumulated *M. avium* infected macrophages in liver parenchyma.

Chapter Three

Efficacy of Amikacin Encapsulated Polymeric Nanoparticles in *Mycobacterium avium* Infected Murine Macrophages and Mice

Abstract

Currently, about one third of the world's population is latently infected with *Mycobacterium tuberculosis* and about 4 million people die from the disease annually worldwide. Although treatment with antimicrobials can be curative of disease symptoms, many people fail to complete the prescribed therapeutic regimen which can increase the risk of disease re-emergence, spread of infection to others and development of drug resistance. An improved treatment approach is urgently needed. Development of safe and effective colloidal drug delivery systems may reduce the amount and frequency of antimicrobial therapy needed, which can lead to better patient compliance and effective treatment of tuberculosis. The goal of this research effort is to explore if polymeric nanoparticles loaded with amikacin would reduce mycobacteria in murine macrophages and infected mice without toxic side effects. *In vitro* efficacy studies with amikacin loaded nanoparticles showed a statistically significant reduction in *M. avium* as compared to untreated controls. Free amikacin appears to work slightly better, but statistically identical to amikacin-loaded nanoparticles. Cytotoxicity assays revealed polymeric nanoparticles loaded with amikacin were non-toxic in J774A.1 cells. *In vivo* efficacy studies using amikacin loaded

polymeric nanoparticles in *M. avium* infected BALB/c mice demonstrated statistically significant improved clearance as compared to free amikacin. Histopathological studies of both kidneys showed amikacin nanoparticles to be non-toxic at a dose of 50mg/kg body weight in mice. Intensity-average diameter of amikacin nanoparticles was 162 nm ±19 with a zeta potential of -16 ±1 mV and an average drug content of the nanoparticle was 27% by weight, respectively.

Keywords: tuberculosis, nanoparticles, amikacin

Introduction

Mycobacterium tuberculosis is an intracellular pathogen that currently infects more than 3 billion people worldwide, making it the number one cause of death due to a bacterial infection in the world (1). *M. tuberculosis* has the ability to cause overt disease in a host or sequester itself inside the host's immune cells in a quiescent state until environmental conditions are favorable (2). Treatment with antimicrobials are successful in most cases of active infection, but many people fail to complete the prescibed 6-9 month course of combination therapy because of cost, inconvenience, or toxic side effects from the drugs (1). Patients often report feeling better early on into treatment and stop taking the medication which is a contributing factor in the development of drug resistant bacteria (3). It also increases the risk of re-emergence of active tuberculosis in the patient and aids in the spread of infection to others (4, 5). A new treatment approach that is

effective, short term, safe and non-toxic, which would improve patient compliance, is urgently needed.

Nanomedicine, a sub specialty of nanotechnology, is a promising area of science that can aid in the development of new efficacious drug delivery methods. By utilizing biocompatible nanomaterials such as polymeric nanoparticles to encapsulate antimicrobials, efficacy of current antimycobacterial treament regimens can be enhanced. A study performed by Pandey et al. (6), examined the treatment of *M. tuberculosis* infected mice with three frontline TB drugs encapsulated with the polymer poly(lactic-*co*-glycolic acid (PLGA) versus the free form of the same antimicrobials. Following a single oral administration of the drug loaded nanoparticle, a prolonged therapeutic release was noted. Drug levels in the plasma of mice were maintained above the MIC for 6-9 days as compared to the conventionally treated group, of which no amount of drug could be detected beyond 12 hours.

Furthermore, encapsulation of antimicrobials in nanoparticles can reduce the amount, frequency of treatment and thereby undesirable side effects of a given drug (7, 8). It can also improve solubility, bioavailability and ultimately patient compliance (9, 10). Many different drug delivery systems have been explored over the past several decades including liposomes, microspheres, solid lipids and polymeric nanoparticles (11, 12, 13). Each has advantages and disadvantages as a drug delivery system (15, 16, 17). Encapsulation of

antimicrobials with polymeric nanoparticles offers several advantages over other experimental treatment approaches. Advantages include; the ability to manipulate the surface chemistry of polymeric nanoparticles to improve cellular uptake, prolong circulation time or regulate release of drugs (10, 22, 23). Also, polymeric nanoparticles can be tailored to different routes of administration. Oral, topical, ocular, and inhaled have all been investigated with promising results (18, 19, 20). Polymeric nanoparticles, especially natural polymers, represented in the literature are considered relatively safe and non-toxic (22, 24). However some challenges exist when using polymeric nanoparticles as a drug delivery system including poor scale-up feasibility and variable stability on storage.

Several frontline TB drugs including rifampin, ethambutol and isoniazid have been encapsulated by various types of polymeric nanoparticles and explored as a delivery system with limited success (25, 26). However, research investigating the efficacy of amikacin loaded polymeric nanoparticles is lacking. Amikacin is a potent aminoglycoside antimicrobial that is bactericidal against mycobacteria *in vitro* and *in vivo* (27-30). Amikacin has limited clinical use as an antimycobacterial agent because it can only be given parentally and has a narrow safety range. Amikacin also has a short circulation time in the body and poor cell membrane permeability. Encapsulation of amikacin into polymeric nanoparticles would be advantageous to improve drug bioavailability and

solubility by gaining better access to the macrophage and intracellular environment where mycobacteria reside (31, 32).

The polymeric nanoparticles used in this study were constructed from commercially available hydrophobic and hydrophilic block co-polymers, poly (ethylene oxide)-poly (propylene oxide)-poly (ethylene oxide) (PEO-*b*-PPO-*b*-PEO) with anionic poly acrylic acid (PAA) grafted onto the polymer. These amphiphilic block copolymers are able to self-assemble into micelles in aqueous solution and encapsulate amikacin, a cationic drug, through electrostatic interactions with PAA (33, 34). The polymeric nanoparticles are unique in that they create an inner core architecture that provides a natural carrier state for amikacin through ionic forces with an amphiphillic shell that aids in cellular membrane permeability and particle stabilization.

Materials and methods:

Mycobacterial Strain

A single transparent colony of strain *Mycobacterium avium subspecies hominissuis* (MAH), ATCC 49601, was grown in Middlebrook 7H9 Broth containing 10% (vol/vol) of albumin-dextrose-catalase (ADC) enrichment with 2% glycerol (Difco Laboratories, Detroit, MI, USA) to mid log phase before being frozen at minus 20ºC in aliquots containing ~5 x 10^6 cfu/mL. Sterility checks and verification of colony forming units (CFU) by serial dilutions were done in triplicate before each use. The minimal inhibitory concentration (MIC) of amikacin in these studies was found to be 2 µg/mL for MAH 49601.

Development of Amikacin Nanoparticles

In this study, pluronic triblock plus pentablock copolymers comprised of poly(ethylene oxide) (PEO) terminal blocks with a poly(propylene oxide) (PPO) central block-(PEO-*b*-PPO-*b*-PEO) were fabricated to form the shell of the nanoparticle (Fig. 3.1) as described previously (33) with cores containing amikacin complexed with polyacrylate anions (PAA). The amikacin sulfate was obtained from Sigma Chemical Co. (St. Louis, Mo.). Next, the polymer solution was placed in a sonication bath and the amikacin sulfate solution 10.0 mg/mL, equal to 30 mg amikacin, (3.5×10^{-4} eq of cations) was added via syringe to form a turbid dispersion (36). Any non-complexed free amikacin sulfate was removed by dialysis against 4 L of deionized (DI) water at 4ºC for 24 hours and the core-shell nanostructures were recovered by freeze-drying.

Physico-chemical Characterization of Amikacin Nanoparticles

Dynamic Light Scattering (DLS)

The solute sizes and zeta potentials of the complexes were characterized by DLS using the Zetasizer Nano ZS at 25 ± 0.1 °C. Samples were diluted in de-ionized water to 1 mg/mL and sonicated using a water bath sonicator (Model 8890, Cole-Parmer, Chicago, IL) for 10 minutes before analysis. The intensity-average diameter (*DI*), polydispersity index (PDI) and zeta potential were recorded for each sample and averaged from three measurements following the directions of the manufacturer.

Measurement of Drug Content by HPLC and Bioassay

The amount of amikacin loaded into the nanoparticles was determined by HPLC and bioassay using a micro-dilution method (37, 38). For HPLC analysis, the nanoparticle was dissolved in 0.1M borate buffer pH 10.5, derivatized with FDNB (1-fluoro-2,4-dinitrobenzene), before passage in a HPLC column (Phenomenex Synergi Fusion-RP, dimensions: 100 x 3.0 mm, 2.5µ) and detected at 365nm with UV spectroscopy. For the bioassay, *Bacillus subtilis* ATCC 6633 was used to measure amikacin concentrations as the minimum inhibitory concentration (MIC) of the amikacin-loaded nanoparticles in broth as compared to the free drug in µg/mL. Briefly, 1mg/mL stock solutions of free amikacin, amikacin-loaded nanoparticle, and copolymer with appropriate controls were serially diluted in a 96 well plate to which $7x10^5$ cfu/mL of *B. subtilis* was added. After 24 hours of incubation at 37º C, turbidity was scored by eye and recorded. The MIC was defined as the lowest concentration of drug able to completely inhibit growth.

Preparation of Amikacin Nanoparticles for in vitro and in vivo studies

Freeze dried amikacin nanoparticles were reconstituted with molecular grade, de-ionized, distilled water to a working concentration of 1mg/mL for cell culture studies and 5mg/mL for the *in vivo* study. A sterility check was performed on all solutions; amikacin nanoparticle, copolymer, free amikacin, and water used for injection by plating 100 µl on Trypticase Soy agar (TSA) (Beckton, Dickinson, and Company, Sparks, MD, USA), in triplicate, and incubating at 37°C overnight.

The pH of the amikacin nanoparticle, copolymer, and free drug was determined using a pH meter (Accumet Basic, Fisher Scientific, USA) and recorded. Stability studies using MIC of the amikacin-loaded nanoparticle in solution with appropriate controls were performed on days 5, 10, and 22 of suspensions incubated at 4ºC, 25ºC, and 37º C. The MICs of the 'freeze dried' nanoparticle stored at 4ºC for 6 weeks before reconstitution were also measured with samples of empty nanoparticle and free amikacin to evaluate stability.

Macrophage Viability Assay

Cell toxicity was determined by an MTS (3-(4,5-dimethylthiazol-2-yl)-5-(3-carboxymethoxyphenyl)-2-(4-sulfophenyl)-2H-tetrazolium) Cytotoxicity Assay (Promega Corporation) as described by Ranjan et al. (39). Experiments were performed in triplicate and data was analyzed using the Student's *t* test.

Growth and Infection of J774A.1 Macrophages with M. avium

Cell preparation and infection was adapted from Barrow et al. (17, 40) with the following modifications. Murine macrophage cell line, J774A.1, was acquired from American Type Culture Collection and grown as monolayers in 75 cm^2 tissue culture flasks (Corning, Inc.) in a humidified incubator with 5% CO^2 atmosphere at 37°C. Cells were grown in Dulbecco's modified Eagle's medium (DMEM) from Sigma-Aldrich containing 10% (vol/vol) fetal bovine serum (FBS), L-glutamine (4mM), $NaHCO_3$, (0.44M) pyridoxine-HCl, 4,500 mg/L and 1%

penicillin-streptomycin solution (Mediatech, Inc., Manassas, VA). At 90% confluence, the medium was replaced with 3 x 10^6 colony forming units/mL of *M. avium* suspended in 10mL of DMEM containing 10% FBS. After 4-6 hours of incubation, macrophages were rinsed twice with Hanks Balanced Salt Solution, then collected by gently scraping the flask with 10mL of DMEM with 10% FBS without antibiotics. Next, the cell suspension was centrifuged at 156 x g for 3 minutes (Sorvall Legend RT Plus, UK) to remove extracellular bacteria and then re-suspended with 38mL of DMEM containing 10% FBS. The cell suspension was then added in 1mL aliquots into 12 well plates at a density of 2 x 10^5 cells per well. Plates were incubated at 37^{o}C in 5 % CO_2 for twenty-four hours to allow attachment of infected and uninfected J774 A.1 cells.

After twenty-four hours, the media was replaced with DMEM with 1% FBS, containing 25 µg/mL of; free amikacin, amikacin nanoparticles, or empty nanoparticles, along with untreated controls, and allowed to incubate at 37^{o}C in 5% CO_2. At days 0, 3 and 6, cells were lysed with 0.1% Triton X-100 and *M. avium* cells were enumerated as colony forming units (cfu)/mL by plating serial dilutions of each lysate on Middlebrook agar containing 10% (vol/vol) oleate-albumin-dextrose-catalase (OADC) and 5% glyercol (Difco Laboratories, Detroit, MI, USA). On day 3, the media was replaced with DMEM with 1% FBS. Experiments were performed in triplicate. Statistical analysis was performed between the groups with Student's *t* tests. A *P* value of <0.05 was considered statistically significant for all of the experiments.

Infection and Treatment of Mice

Prior to any animal work, this research protocol was approved by the institution's animal welfare committee (Institutional Animal Care and Use Committee (IACUC)). Female BALB/c mice, purchased from Charles River, were housed in an Animal Biosafety Level 2 facility with food and water *ad libitum.* At 13 weeks of age, 21 mice, weighing approximately 25 grams each, were infected intraperitoneally (IP) with 200µL of $6x10^6$ cfu/mL of *M. avium* strain ATCC 49601. One week post infection, 3 groups of mice, containing 5 mice per group, were treated IP with 50mg/kg of either free amikacin, or amikacin-loaded nanoparticle or copolymer thrice weekly for 4 weeks. As a positive control, 3 infected mice were treated with 250 µL of sterile de-ionized water IP. As a negative control, three uninfected mice were treated with 250 µL of sterile de-ionized water IP.

Tissue M. avium Counts

Four days after the last treatment, mice were sacrificed to determine the cfu per organ from liver, lungs, and spleen. The organs were removed aseptically from each mouse and placed separately into 50mL tubes containing 2mL of Middlebrook broth 7H9 supplemented with 10% (vol/vol) ADC enrichment. The organs were homogenized for 1-2 minutes using a Tissuemiser homogenizer (Fisher Scientific, USA). Next, aliquots of each organ homogenate were serially diluted in Middlebrook broth to a maximum of five ten-fold dilutions, plated on Middlebrook 7H10 agar plates supplemented with 10% OADC enrichment and

incubated for 7-14 days at 37°C. The number of colonies per dilution were counted and reported as cfu/organ. An unpaired, two tailed student's *t* test was performed and a *P* value of < 0.05 was considered statistically significant.

Histopathology

Kidneys from each mouse were collected, fixed in 10% neutral buffered formalin, trimmed, routinely processed and embedded in paraffin blocks. Five (5) micron thick sections were cut with a microtome, fixed on a glass slide and stained with hematoxylin and eosin. In a blinded study, two veterinary pathologists examined the kidney samples independently and scored changes (degeneration/necrosis, inflammation, hemorrhage, edema) using a scale from 0 to 4. The degree of pathological change was recorded as; (0) = unremarkable, (1) = minimum, (2) = mild, (3) = moderate, and (4) = marked.

Hematology Analysis

Blood was obtained from each mouse via the retro orbital plexus while under general anesthesia (1.5% isofluran and 1.5 L/min of oxygen), just before euthanasia. Blood was collected into a micro hematocrit tube to determine Total Protein (TP) and Packed Cell Volume (PCV) which accesses hydration and the volume percentage of red blood cells present in whole blood.

Results

Physico-chemical Characterization of Amikacn-Loaded Nanoparticles

Dynamic Light Scattering (*DLS)*

Several physico-chemical properties were measured by DLS (Table 3.1). The relative size or intensity-average diameter of the amikacin-loaded nanoparticle was found to be 162 nm (±19). The zeta potential or surface, charge was anionic at -16mV (± 1). Lastly, the polydispersity index (PDI), which measures the variance of size of the nanoparticle was 0.215 (± 0.042).

The variance of the amikacin-loaded nanoparticle's size distribution in 1 mg/mL solution was assessed by DLS. Results indicate the presence of one symmetrical peak which occurs with nanoparticle particle size uniformity (Table 3.2). After DLS analysis, a routine quality control report was also performed to assess the validity of the DLS results. The raw correlation data (Table 3.3) of amikacin-loaded nanoparticles in 1mg/mL solution generated a uniform S shaped curve.

Measurement of Amikacin Content by HPLC and Bioassay of amikacin loaded nanoparticle

The drug content of amikacin-loaded nanoparticles was 27% by weight with an encapsulation efficiency of 60%. The MIC of the amikacin loaded nanoparticles using *B. subtilis* as an indicator organism was 2 µg/mL; the same as free amikacin. The pH of a 1 mg/mL solution of amikacin-loaded nanoparticle was measured at 6.0, the free amikacin at 6.4 and the empty nanoparticle or copolymer at 7.0 (Table 3.4).

Storage Studies via bioassay with B. subtilis.

The stability of the nanoparticles was measured as a function of the ability of the nanoparticles to inhibit growth of *B. subtilis* during MIC analysis (Table 3.5). Results show the MIC for both the free drug and amikacin-loaded nanoparticle at 37°C increased after 5 days incubation (N=3). There was a slightly longer maintenance of biological activity of the amikacin-loaded nanoparticles versus the free drug at 4^0C. After 6 weeks of storage at 4º C, freeze dried nanoparticles were reconstituted, tested and MIC was found to be 2 µg/mL (results not shown).

Macrophage Toxicity Assay

The cyto-toxicity of amikacin-loaded nanoparticles in J774A.1 cells was measured using the MTS assay and statistically analyzed using a Student's *t* test. Results showed cell viability remained above 90% at varying concentrations up to 50 µg/mL and no statistical difference in the means (Figure 3.3). The experiment was repeated three times and each group had a sample size of 6.

In Vitro Efficacy Study in Macrophages

In vitro efficacy studies of amikacin-loaded nanoparticles against *M. avium* infected J774A.1 cells were done. Macrophages were infected at a MOI of 1 and treated with 25 µg/well of free amikacin, amikacin-loaded nanoparticles or copolymer until harvest on Day 6. Results show 0.88 log reduction by amikacin nanoparticles and a 1.2 log reduction by free amikacin as compared to control

(Figure 3.4). The copolymer did not have any killing activity on *M. avium* (results not shown). Results were performed in triplicate. N=3, ** P value < 0.001.

In Vivo Efficacy Study in Mice

Efficacy of treatment using amikacin-loaded nanoparticles compared to free amikacin and untreated controls in liver, spleen, and lungs of *M. avium* infected BALB/c mice were done. Mice were treated thrice weekly at a dose of 50mg/kg body weight for 4 weeks. Results show a reduction of 1.7 log in spleen, 1.2 log in liver, and 1.7 log in lungs of mice treated with amikacin nanoparticles as compared to controls (Figure 3.5). Although it appears the free drug reduced the bacterial load in the organs compared to controls, the results are not statistically significant. * = P < 0.05, ** = P< 0.001.

Histopathology

Histopathology results showed no inflammatory changes in either the amikacin-loaded nanoparticle or the free drug at 50mg/kg (Table 3.6). Results also showed minimal inflammation in the peri-renal area of samples of infected mice left untreated and mice treated with the copolymer alone. However, inflammation localized to the peri-renal area common findings in histopathological evaluation of kidneys.

Hematology Analysis

Hematology results of the PCV and TP for the amikacin-loaded nanoparticle and the co-polymer groups were within normal range. However, the PCV and TP of the free amikacin group was elevated (Table 3.7).

Discussion

The amikacin-loaded nanoparticle (AMK NP) has several physicochemical properties that promotes cellular uptake and thus increases its suitability as an ideal carrier for drug delivery of antimicrobials. One important physicochemical property that can enhance cellular uptake is size. As seen in Table 3.1, the AMK NP is an ideal size for macrophage uptake. According to Gelpernia et al., when nanoparticles near the size range of 200 nm are given intravenously, they follow the same process of engulfment into macrophages as intracellular pathogens (41). To confirm that amikacin-loaded nanoparticles follow an intracellular pathway, future studies would include adding a targeting agent to the shell of the nanoparticle and analyzing cellular uptake by flow cytometry.

In addition to size, the shape of a nanoparticle can influence the process of cellular uptake. It is speculated that the shape of the amikacin-loaded nanoparticle is spherical (Figure 3.1) due to its amphiphilic composition that forms micelles in solution (34, 36). Doshi and Mitragotri (42) showed that nanoparticles resembling rod shaped bacteria within the size range of 100 nm or less are engulfed most readily with spherical shaped particles in the same size range being second. It is also important to note that smaller nanoparticles less

than 50 nm are more readily taken up by macrophages than larger ones of the same shape but a higher degree of cytotoxicity was observed (43).

A spherical shape is also supported when one considers that the accuracy of dynamic light scattering is dependent on the particle being spherical in solution. Table 3.2 supports this theory by depicting one uniform, symmetrical peek of the nanoparticle in solution. If significant agglomeration, variance in size or a non-spherical shape in solution did in fact occur, an error report would have been generated by the Zetasizer during analysis. Additionally, Table 3.3 depicts a smooth curve indicating a good quality control report. Analysis such as transmission electron microscopy would be the next step to confirm shape.

Another important factor in the process of cellular uptake is the surface charge or zeta potential of a particle. Zeta potentials greater than ± 30 mV enhance particle stabilization and facilitation of cellular uptake (43). The zeta potential of the amikacin-loaded nanoparticle was negative 16mV (+/-1), which is ideal for cellular uptake. In the same study by Bhattacharjee et al., (43) the role of surface charge and cellular uptake was examined. They found that polymeric anionic nanoparticles 100 nm or less are more efficiently engulfed than polymeric cationic particles of the same size range and that neutral particles have the slowest rate of macrophage engulfment. Lastly, the polydispersity index (PDI), which measures the variance of size of the nanoparticle, was below 0.2 indicating relative size uniformity (43).

After HPLC analysis of the nanoparticles, the drug load was calculated to be 27% by weight with an encapsulation efficiency of 60%. The amount of drug load determined by HPLC was confirmed by biological activity through MIC analysis. The MIC of the amikacin loaded nanoparticles and free amikacin using *B. subtilis* as an indicator organism was both 2 µg/mL after 24 hours. This indicates that the amount of amikacin available and released was at least as much as the free drug since both MIC's were equivalent. When nanoparticles were reconstituted and then stored in solution under various environmental conditions, a slow increase in the MIC values were observed over 22 days indicating that the reconstituted amikacin loaded nanoparticle and free drug begin to degrade and become less biologically active as a function of time. However, as seen in Table 3.5, the amikacin-loaded nanoparticle remains biologically active longer than the free drug which may be from a continuous release of amikacin from the nanoparticle or the polymer is providing some protection against degradation of amikacin. Finally, stability studies show that after 6 weeks of storage at 4º C, freeze dried nanoparticles were biologically active as determined by MIC analysis using *B. subtilis* as the indicator organism.

The MTS cytotoxicity assay showed no significant differences in percentage mean absorption between various treatment groups, which indicate the amikacin loaded nanoparticle, copolymer and free drug were non-toxic to J774A.1 at doses ranging from 15 to 50µg/mL.

In the treatment of *M. avium* infected J774A.1 murine macrophages, the amikacin-loaded nanoparticle reduced the bacterial load by 0.88 log as compared to untreated controls. Treatment of active mycobacterial infections requires administration of several drugs in combination to be effective. In the literature, monotherapy typically reduces the bacterial load by 0.3 to 1 log (44, 45). The results of this cell culture experiment may be considered successful as amikacin was the only antimicrobial used. Also in this experiment, free amikacin achieved a 1.2 log reduction as compared to the untreated controls. One possible factor that might account for the greater reduction of *M. avium* organisms seen in the free drug group versus the nanoparticle group is the drug release pattern of the nanoparticle. If the amikacin-loaded nanoparticle has a slow drug release pattern, an extended incubation period beyond a week may be required to yield a dramatic reduction in mycobacterial organisms as compared to controls. Unfortunately, the period of incubation was limited by the life span of macrophages in cell culture, which is typically about 3-6 days (17, 40). In addition, *M. avium* is a slow growing organism with a doubling time of about 24 hours and although it tends to grow faster in macrophages, it is also considered a "slow dying" organism. The thick lipid rich cell wall renders it relatively impermeable to many antibiotics and therefore treatment to eliminate *M. avium in vitro* or *in vivo* can be lengthy (9). It was noted, however, that during MIC stability analysis, the amikacin-loaded nanoparticle was able to maintain a therapeutic MIC for 10 days in various environments including an elevated

temperature that is similar to the human body. In the future, a drug release profile of the amikacin loaded nanoparticles may provide essential information to bolster the hypothesis of a slow release of amikacin from the nanoparticle.

In mice, amikacin loaded nanoparticles were able to successfully reduce viable *M. avium* numbers in the spleen by 1.7 log, in the liver by 1.2 log and in the lungs by 1.7 log as compared to untreated controls. In contrast, the free amikacin group did not reveal a statistically significant reduction in *M. avium* numbers compared to untreated controls indicating that the amikacin nanoparticle was more effective in killing *M. avium* in infected animals than the free drug in these experiments. The standard effective dosing schedule of free amikacin is twice daily (46). However in this study, a dosing schedule of thrice weekly was used and perhaps is too infrequent of a dosing schedule for free amikacin to be effective. Perhaps the lack of reduction in the number of viable *M. avium* in mice occurred in the free amikacin group because the half-life of free amikacin is short lasting only 2-4 hours (46) and there was simply not enough antibiotic present to decrease the bacterial load. However, in the encapsulated amikacin group, the bacterial load was reduced by more than a log as compared to untreated controls suggesting a slow release of amikacin from the nanoparticle over time. A logical next step would be the determination of the release kinetics of this nanoparticle. Although the amount of drug released from the nanoparticle over time was not determined, drug release studies were performed on a similar nanoparticle formulation by Ranjan et al (47). In their study using similar polymeric

nanoparticle encapsulated gentamicin, a structurally similar aminoglycoside, was found to have slow drug release kinetics with 25-30% released within 24 hours (47). It is possible that the amikacin-polymeric nanoparticle may have similar release characteristics, although further testing is needed.

Histopathology of the kidneys revealed no signs of toxicity in any of the groups of mice treated with free amikacin, encapsulated amikacin or copolymer alone. This indicates a dose of 50mg/kg body weight given IP thrice weekly for 4 weeks is non-toxic in BALB/c mice. Amikacin shows dose dependent nephrotoxicity in humans and animals (46, 48). In mice, a dose greater than 120mg/kg has been shown to cause adverse changes in the renal parenchyma indicative of toxicity (29). A dose of 50mg/kg was chosen because it will effectively reduce viable *M. avium* organisms by approximately one log without toxic side effects (29).

In the groups treated with copolymer (empty nanoparticle) and untreated controls, an infiltration of white blood cells was noted in the adipose tissue surrounding the kidneys. This infiltration is an indication of mild inflammation of the body cavity lining most likely from repeated injections. It is interesting that this mild inflammation was not noted in the free drug or encapsulated nanoparticle group. It has been represented in the literature that certain macrolide and aminoglycoside antimicrobials like amikacin have systemic anti-inflammatory properties (49) and although only speculative, this may account for

why mild inflammation is seen only in the polymer control groups and not the drug treated groups.

Other parameters that were investigated and can indicate renal dysfunction is an elevated Packed Cell Volume (PCV), which measures the percent of red blood cells in blood and a decrease in the amount of Total Protein (TP) in blood. Mice treated with encapsulated amikacin nanoparticle and copolymer alone had PCV and TP values that are within normal range showing no signs of renal dysfunction. Mice treated with free amikacin and infected untreated mice did show a mild elevation in PCV and TP values, which indicates hemoconcentration most likely due to dehydration, not dysfunction. Analysis of urine specific gravity or hematological analysis of kidney enzymes would further assist in differentiating between dehydration or from early renal dysfunction. Clinically, none of the mice showed any abnormal signs of illness such as lethargy, rough hair coat or weight loss.

Conclusion

The results obtained in this study reveal that amikacin loaded nanoparticles are a safe and effective drug delivery system in the treatment of experimental infection with *M. avium* in J774A.1 murine macrophages and BALB/c mice. The formulation of this polymeric nanoparticle is unique and provides an inner molecular architecture that serves as a carrier for amikacin through electrostatic forces along with an amphiphillic shell that promotes particle stabilization and

membrane penetration in an aqueous environment. By exploiting the natural propensity of macrophages to phagocytize foreign material, polymeric nanoparticles can be used to improve transport of antimicrobials with poor membrane permeability such as amikacin, gentamicin, kanamycin etc., into cells to aid in the elimination of intracellular bacteria. Furthermore, using novel nanoparticles targeted to the macrophage will also provide an opportunity to re-investigate older antimicrobials that were once passed over due to poor solubility, bioavailabilty or toxicity.

References

1. World Health Organization, www.who.int/tb/publications/global_report/2011/gtbr11_full.pdf
2. Talaat A. M., Ward S. K., Wu C. W., Rondon E., Tavano C. C.,. Bannantine J. P., Lyons R., Johnston S. A. (2007). "Mycobacterial Bacilli Are Metabolically Active During Chronic Tuberculosis in Murine Lungs: Insights from Genome-Wide Transcriptional Profiling." Journal of Bacteriology **189**(11) 4265–4274.
3. Loddenkemper, R. Sagebiel, D. Brendel, A. 2002. "Strategies against multidrug resistant tuberculosis." Eur. Respir J. **20** Suppl. 36: 66s-77s.
4. Riska, P. F. and Carleton S. (2002). "Latent tuberculosis: models, mechanisms, and novel prospects for eradication." Semin Pediatr Infect Dis **13**(4): 263-72.
5. Brown D. H., Miles B. A., Zwilling B. S. (1995) "Growth of *Mycobacterium tuberculosis* in BCG-Resistant and Susceptible Mice: Establishment of Latency and Reactivation." Infection and Immunity **63** (6): 2243-2247.
6. Pandey, R., Ahmed, Z., Sharma, S., Khuller, G. K 2003." Nanoparticle encapsulated antitubercular drugs as a potential oral drug delivery system against murine tuberculosis." Tuberculosis (Edinb) **83**:373-378.
7. Emerich D. F., Thanos C. G. (2008) "Targeted nanoparticle-based drug delivery and diagnosis" Journal of Drug Targeting **15**:(3) 163-183.

8. Moghimi S. M., Hunter A. C., Murray J. C. (2005) “Nanomedicine: current status and future prospects.” The FASEB Journal **19**: 311-330.

9. Gaspar M. M., Cruz A. G., Fraga A. G., Castro A. G., Cruz M. E. M., Pedrosa J. (2008) “ Developments on Drug Delivery Systems for the Treatment of Mycobacterial Infections.” Current Topics in Medical Chemistry **8**:579-591.

10. Davis M. E., Chen Z. G., Shin D. M. (2008). “Nanoparticle therapeutics: an emerging treatment modality for cancer.” Nature Reviews Drug Discovery **7** 771-782.

11. Avgoustakis K. (2004) “Peglated Poly(lactide) and Poly(lactide-co-glycolide) Nanoparticles: Preparation, properties and possible applications in drug delivery.” Current Drug Delivery **1**: 321-333.

12. Muller R. H., Mader K., Gohla S. (2000) “Solid lipid nanoparticles (SLN) for controlled drug delivery- a review of the state of the art.” European Journal of Pharmaceutics and Biopharmaceutics **50**: 161-177.

13. Barrow W. W. (2004) “Microsphere Technology for Chemotherapy of Mycobacterial Infections. “ Current Pharmaceutical Design **10**: 3275-3284.

14. Klemens S. P., Cynamon M. H., Swenson C.E., Ginsberg R. S. (1990) “Liposome encapsulated gentamicin therapy of *Mycobacterium avium* complex infection in beige mice” Antimicrobial Agents and Chemotherapy June; **34**:(6) 967-970.

15. Saito H., Tomioka H. (1989) “Therapeutic efficacy of liposome entrapped rifampin against *Mycobacterium avium* complex infection induced in mice” Antimicrobial Agents and Chemotherapy April; **33**:(4) 429-433.

16. Pandey R., Sharma S., Khuller G. K. (2005) “Oral solid lipid nanoparticle based chemotherapy” Tuberculosis **85**: 415-420.

17. Barrow E. L. W., Barrow W. W. (2007) “Efficacy of Rifabutin loaded microspheres for treatment of *Mycobacterium avium* infected macrophages and mice” Drug Delivery **14:** 119-127.

18. Pandey R., Khuller G. K. (2007). “Nanoparticle based oral drug delivery system for an injectable antibiotic-streptomycin. Evaluation in a murine tuberculosis model.” Chemotherapy **53**:437-441.

19. Pawar K. R., Babu R. J. (2010). “Polymeric and lipid based materials for topical nanoparticle delivery systems.” Crit. Rev. Ther. Drug Carrier Syst. 27(**5**)419-59.

20. Nagarwal R. C., Kant S., Singh P. N., Maiti P., Pandit J. K. (2009). “ Polymeric nanoparticulate system: A potential approach for ocular drug delivery.” Journal of Controlled Release. **136:** 2-13.

21. Pandey R., Khuller G. K. (2005). “Antitubercular inhaled therapy: opportunities, progress and challenges.” Journal of Antimicrobial Chemotherapy **55**: 430-435.

22. Panyam, J., Labhasetwar V. (2003). “Biodegradable nanoparticles for drug and gene delivery to cells and tissue.” Advanced Drug Delivery Reviews **55**:329-347.

23. Kakizawa Y., and Kataoka K. (2002) “Block copolymer micelles for delivery of gene and related compounds.” Advanced Drug Delivery Reviews **54**: 203-222.

24. Caruthers S. D., Wickline Lanza G. M. (2007) “Nanotechnology applications in medicine.” Current Opinion in Biotechnology **18**: 26-30.

25. Barrow E. L. W., Winchester G. A., Staas L. K., Quenelle D. C., Barrow W. W. (1998) “Use of microsphere technology for targeted delivery of rifampin to *Mycobacterium tuberculosis* infected macrophages” Antimicrobial Agents and Chemotherapy Oct;**42**:(10) 2682-2689.

26. Pandey R., Sharma S., Khuller G. K. (2006) “Chemotherapeutic efficacy of nanoparticle encapsulated antitubercular drugs” Drug Delivery **13**: 287-294.

27. Sharma A., Pandey R., Sharma S., Khuller G. K. (2004) “Chemotherapeutic efficacy of poly (DL-lactic-co-glycolide) nanoparticle encapsulated antitubercular drugs at sub-therapeutic dose against experimental tuberculosis” Int. J. Antimicrob. Agents **24**: 599-604.

28. Pekkegrin I., Maugein J., Lapeyre C., Barbeau P., Leng B., Pellegrin J. L. (1996) “Activity of rifabutin, clarithromycin, ethambutol, sparfloxacin and

amikacin alone and in combination against *Mycobacterium avium* complex in human macrophages." Journal of Antimicrobial Chemotherapy **37**:501-510.

29. Duzenges N., Perumal V. K., Kesavalu L., Goldstein J. A., Debs R. J., Ganagadharam P. R. J. (1988) "Enhanced effect of liposome encapsulated amikacin on *Mycobacterium avium- M. intracellulare* complex" Antimicrobial Agents and Chemotherapy Sept; **32**:(9):1401-1411.

30. Peterson, E.A., Grayson J. B., Hersh E. M., Dorr R. T., Chiang S. M., Koa M., and Proffitt R. T. (1996) "Liposomal amikacin: improved treatment of *Mycobacterium avium* complex in the beige mouse model." Journal of Antimicrobial Chemotherapy **38**: 819-828.

31. Dhillon J., Fielding R., Adler- Moore J., Goodall R. L., Mitchison D. (2001) "The activity of low- clearance liposomal amikacin in experimental murine tuberculosis." Journal of Antimicrobial Chemotherapy **48**: 869-876.

32. Mc Donough K. A., Kress Y., Bloom B. R. (1993) "Pathogenesis of Tuberculosis: Interaction of *Mycobacterium tuberculosis* with macrophages." Infection and Immunity **61**(7): 2763-2773.

33. Tian Y., Bromber L., Lin S. N., Hatton T. A., Tam K. C. (2007) "Complexation and release of doxorubicin from its complexes with pluronic P-85-*b*-poly(acrylic acid) block copolymers." Journal of Controlled Release **121**: 137-145.

34. Batrakova E. V., Li S., Li Y., Alakhov V. Y., Elmquist W. F. Kabanov A. V. (2004) “Distribution of a micelle-forming block copolymer Pluronic P85.” Journal of Controlled Release **100**: 389-397.

35. Heifets, L. (1996). “Susceptibility of *Mycobacterium avium* complex Isolates” Antimicrobial Agents and Chemotherapy **40**(8):1759-1767.

36. Ranjan A., Pothayee N., Seleem M. N., Sriranganathan N., Markis M., Kasimanickam R., Riffle J. S. (2009) “ In vitro Trafficking and Efficacy of Core Shell Nanostructures for treating Intracellular Salmonella Infections.” Antimicrobial Agents and Chemotherapy Sept.;**53**(9):3985-3988.

37. Telles, M. A. S., and Yates M. D. (1994). ”Single and double drug susceptibility testing of *Mycobacterium avium* complex and mycobacteria other than tubercule (MOTT) bacilli by a microdilution broth minimum inhibitory concentration (MIC) method.” Tubercule and Lung Disease **75:** 286-290.

38. Wallace Jr. R. J., Nash D. R., Steele L. C, and. Steingrube V. (1986). “Susceptibility Testing of Slowly Growing Mycobacteria by a Microdilution MIC Method with 7H9 Broth.” Journal of Clinical Microbiology **24**(6): 976-981.

39. Ranjan A., Pothayee N.,. Vadala T. P,. Seleem M. N, Restis E., Sriranganathan N., Riffle J. S and Kasimanickam R. (2010). “Efficacy of Amphiphillic Core Shell Nanostructures Encapsulating Gentamicin in an *In Vitro Salmonella* and *Listeria* Intracellular Infection Model.” Antimicrob. Agents Chemother. Aug;**54**(8):3524-6.

40. Wright E. L., Quenelle D. C., Suling W. J., Barrow W. W. (1996) “Use of Mono Mac 5 Human Monocytic cell line and J774 Murine Macrophage cell line in parallel antimycobacterial drug studies” Antimicrobial Agents and Chemotherapy Sept; **40** (9):2206-2208.

41. Gelpernia S., Kisich K., Iseman M. D., Heifets L. (2005). “The Potential Advantages of Nanoparticle Drug Delivery Systems in Chemotherapy of Tuberculosis” Am J Respir Crit Care Med **172:**1487–1490.

42. Doshi N., Mitragotri S. (2010). “Macrophages Recognize Size and Shape of Their Targets.” PLoS One. **5**(4): e10051.

43. Bhattacharjee S., Ershov D., Fytianos K., van der Gucht J., Alink G. M., Rietjens I. M., Marcelis A. T., Zuilhof H. (2012). “Cytotoxicity and cellular uptake of tri-block copolymer nanoparticles with different size and surface characteristics.” Part Fibre Toxicol. Apr ;**9**(11):1-19.

44. Bermudez E., Young L. S. (1988). “Activities of Amikacin, Roxithromycin, and Azithromycin Alone or in Combination with Tumor Necrosis Factor against *Mycobacterium avium* Complex.” Antimicrobial Agents and Chemotherapy Aug; **32**(8):1149-1153.

45. Pellegrin I., Maugein J., Lapeyre C., Barbeau P., Leng B., Pellegrin J.L. (1996) “Activity of rifabutin, clarithromycin, ethambutol, sparfloxacin and amikacin alone and in combination against *Mycobacterium avium* complex in human macrophages.” Journal of Antimicrobial Chemotherapy **37**:501-510.

46. Turnidge J. “Pharmacodynamics and dosing of aminoglycosides.” (2003). Infect Dis Clin N Am **17**:503–528.

47. Ranjan A., Pothayee N., Seleem M., Jain N., Sriranganathan N., Riffle J. S., Kasimanickam R. (2010). “Drug Delivery using novel nanoplexes against a *Salmonella* mouse infection model.” J Nanopart Res **12**:905-914.

48. Brion N., Barge J., Godefroy I., Dromer F., Dubois C.,Contrepois A., Carbon C. (1984). “Gentamicin, Netilmicin, Dibekacin, and Amikacin Nephrotoxicity and Its Relationship to Tubular Reabsorption in Rabbits.” Antimicrobial Agents and Chemotherapy Feb;**25**(2):168-172.

49. Tauber S. C., and Nau R. (2008) “Immunomodulatory Properties of Antibiotics.” Current Molecular Pharmacology **1**(1):68-79.

Tables and Figures

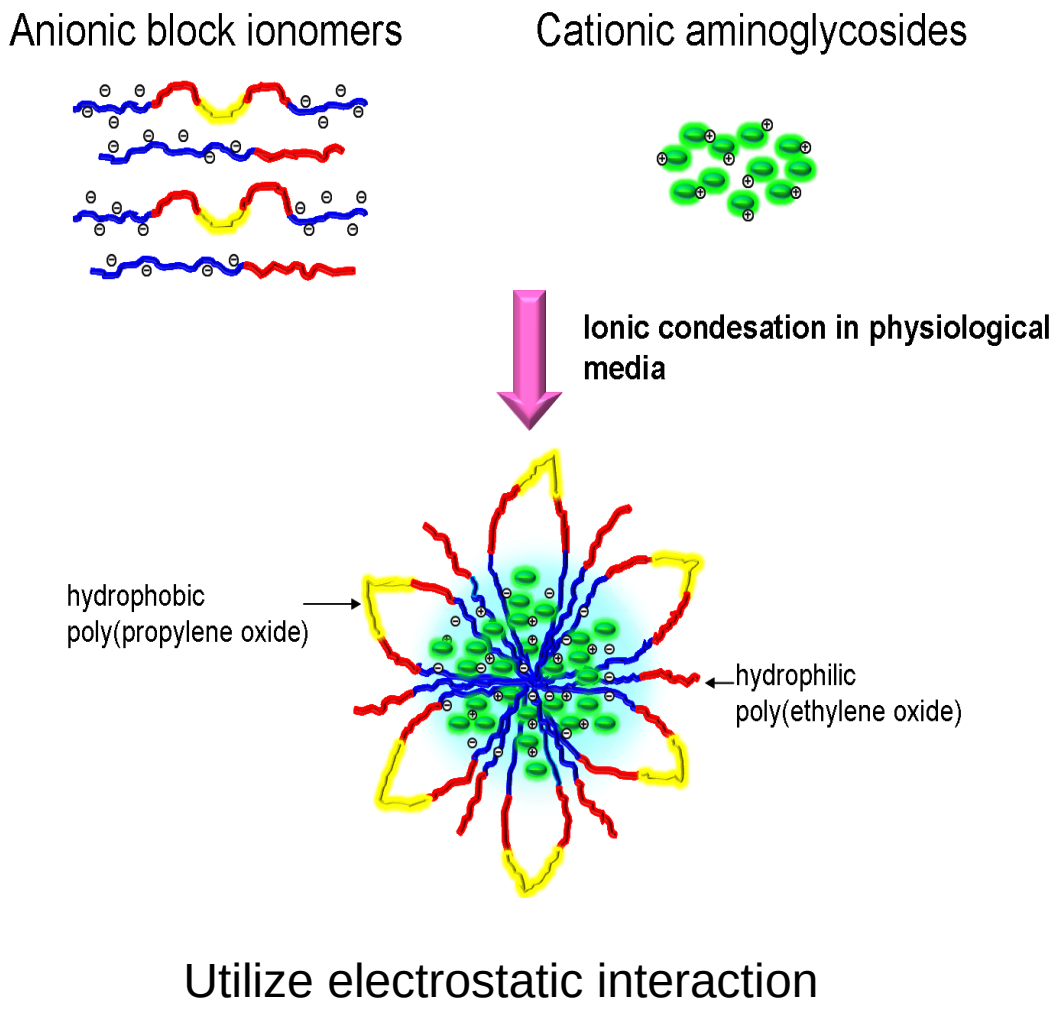

Figure 3.1 Amphiphilic block copolymers are able to self-assemble into micelles in aqueous solution and encapsulate amikacin, a cationic drug, through electrostatic interactions with anionic poly acrylic acid (PAA).

Name	**Intensity Diameter (nm)** ± SD	**Zeta Potential (mV)** ± SD	**PDI** ± SD
AMK NP	162 ±19	-16 ±1	0.215 ±0.042

SD = Standard deviation

Table 3.1. Physico- chemical characterization of amikacin-loaded polymeric nanoparticles by dynamic light scattering at 1mg/mL

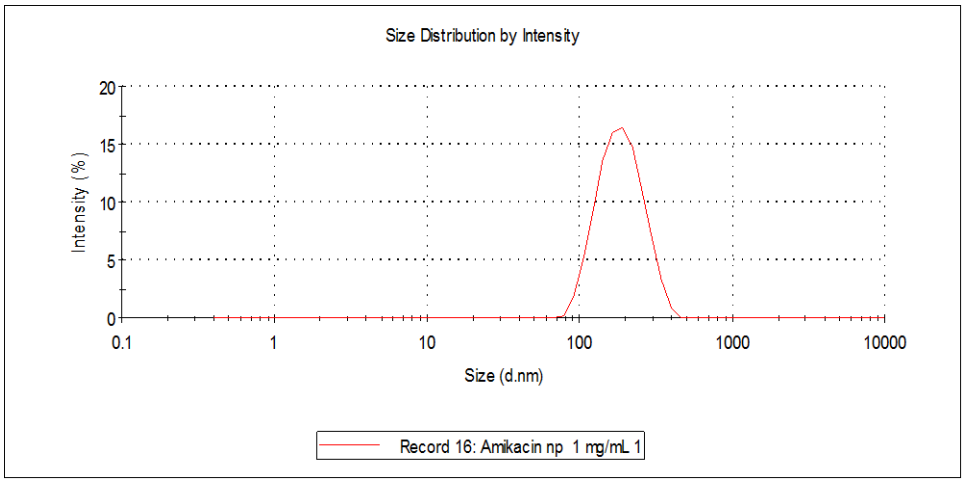

Table 3.2 Size distribution by intensity of amikacin-loaded nanoparticle by dynamic light scattering at 1mg/mL

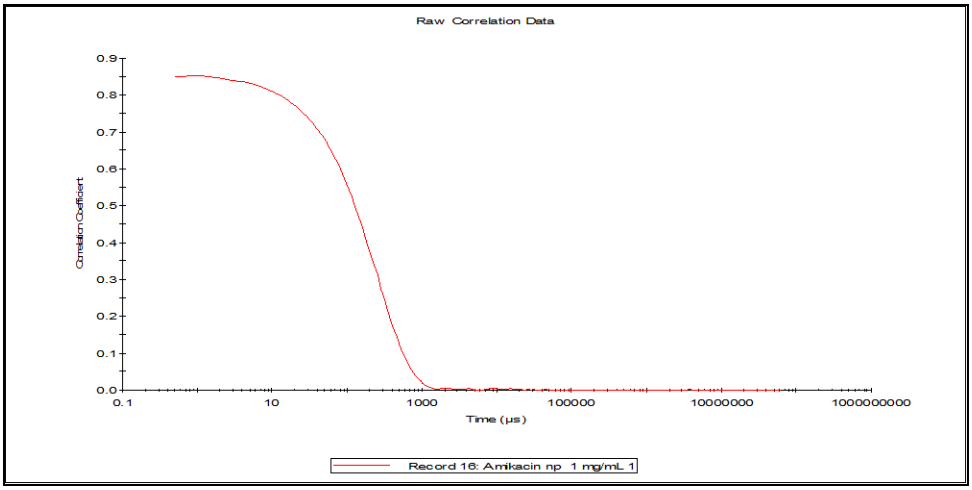

Table 3.3 Raw correlation data of amikacin-loaded nanoparticle in 1mg/mL solution by dynamic light scattering

AMK NP	Free AMK	Copolymer
6.0	6.4	7.4

Table 3.4 pH of solutions (1mg/mL) for injection in mice

MIC of AMK NP in µg/mL following storage at			
Incubation Period	**4^0C**	**25^0C**	**37^0C**
Day 5	2	2	2
Day 10	2	4	2
Day 22	2	2	4

MIC of Free AMK in µg/mL following storage at			
Incubation Period	**4^0C**	**25^0C**	**37^0C**
Day 5	2	2	1
Day 10	4	2	8
Day 22	4	4	4

Table 3.5 Storage Studies via bioassay with *B. subtilis.* Results show the MIC for both the free drug and amikacin loaded nanoparticle at 37°C increased after 5 days incubation (N=3). After 6 weeks of storage at 4º C, freeze dried nanoparticles were reconstituted, tested and MIC was found to be 2 µg/mL (results not shown).

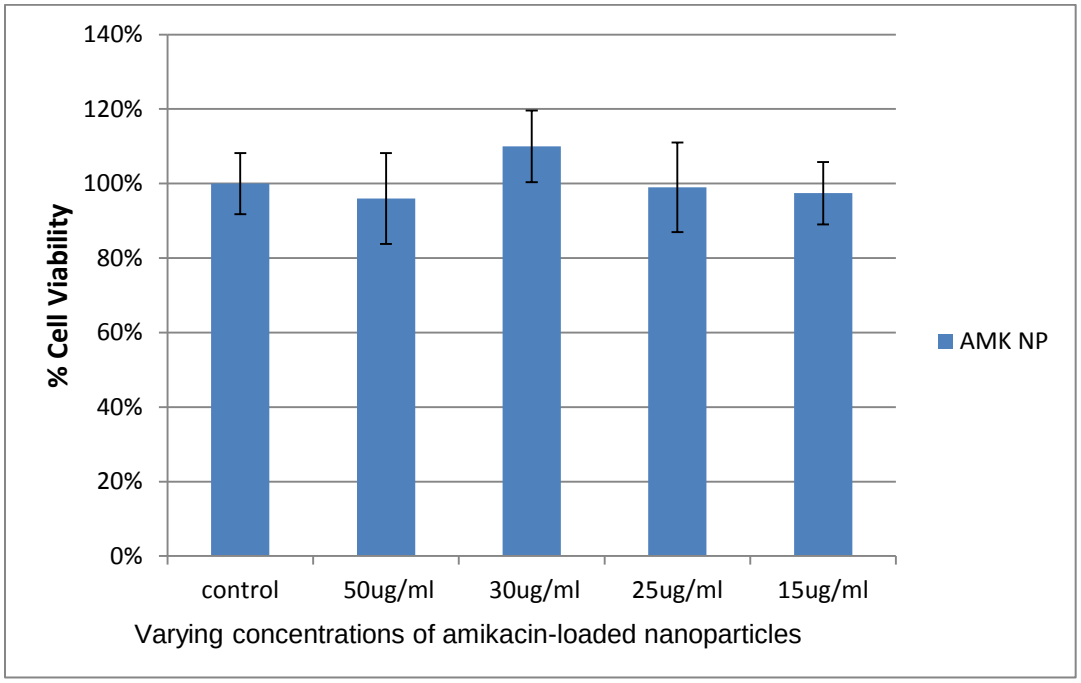

Figure 3.3 Cytotoxicity of amikacin-loaded nanoparticles in J774A.1 cells. Macrophages were incubated with amikacin-loaded nanoparticles overnight.

Results show no statistical difference in the means. Experiments were done in triplicate, N=6.

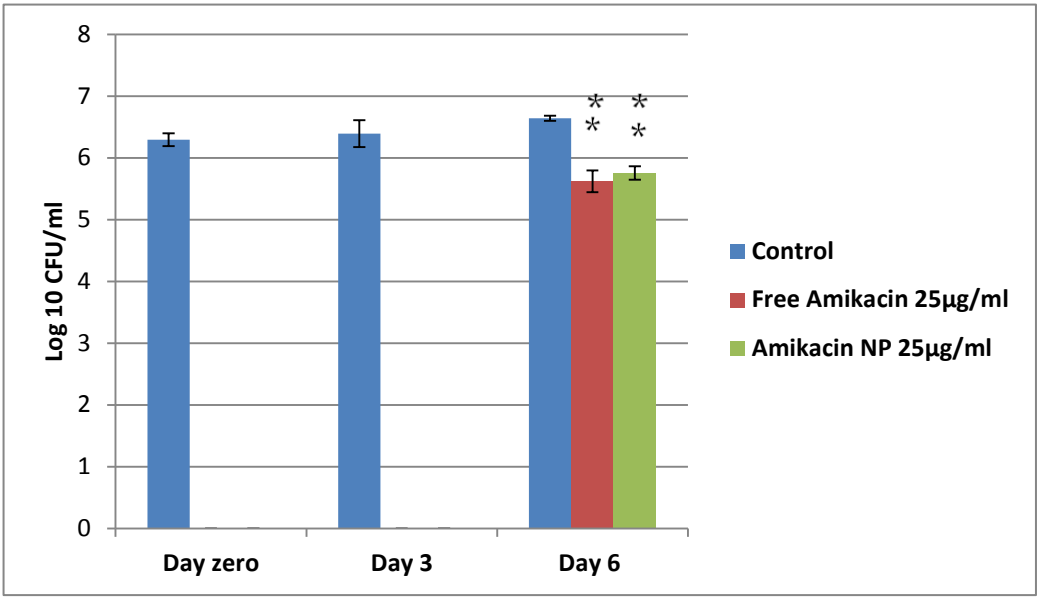

Figure 3.4 Amikacin-loaded nanoparticles against *M. avium* infected J774A.1 cells at 25 µg/mL. Macrophages were infected at a MOI of 1 and treated with either; free amikacin, amikacin-loaded nanoparticles or copolymer until harvest on Day 6. Results show 0.88 log reduction by amikacin nanoparticles and a 1.2 log reduction by free amikacin as compared to untreated control. The copolymer did not have any killing activity on *M. avium* (results not shown). Results were performed in triplicate. N=3, ** P value < 0.001.

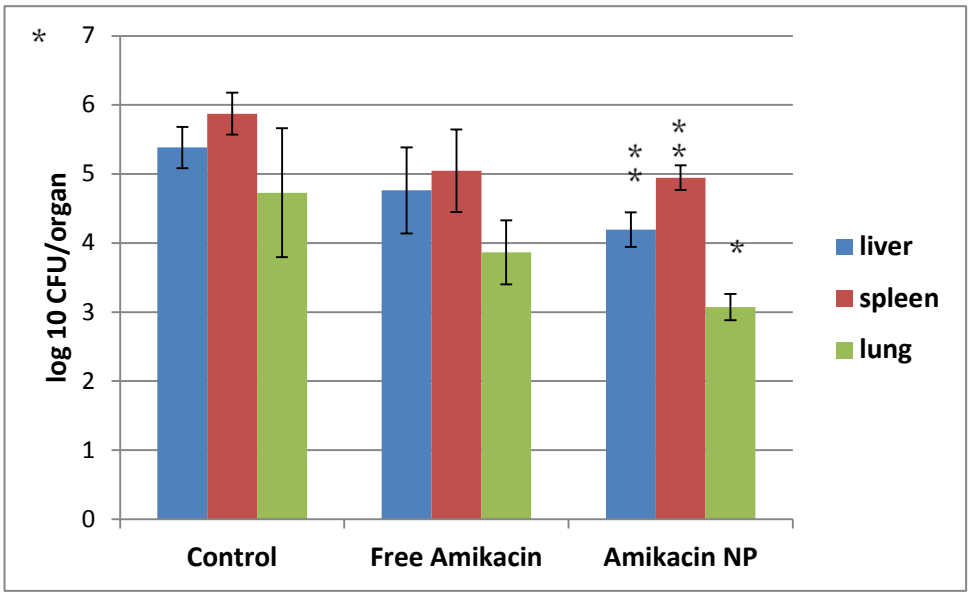

Figure 3.5 Efficacy of treatment of amikacin-loaded nanoparticles in liver, spleen, and lungs of *M. avium* infected mice BALB/c mice compared to free amikacin and untreated controls. Mice were treated thrice weekly at a dose of 50mg/kg body weight for 4 weeks. Results show a log reduction of 1.7 in spleen, 1.2 in liver, and 1.7 in lungs of mice treated with amikacin nanoparticles as compared to controls. Although it appears the free drug reduced the bacterial load in the organs compared to controls, the results are not statistically significant. * = $P < 0.05$, ** = $P < 0.001$.

Kidney no	Kidney score AMK NP		Kidney score Free AMK		Kidney score Empty AMK NP		Kidney score Untreated	
	1st pathologist	2nd pathologist	1st pathologist	2nd pathologist	1st pathologist	2nd pathologist	1st pathologist	2nd pathologist
1	0	0	0	0	**1**	**1**	**1**	**1**
2	0	0	0	0	0	0	0	0
3	0	0	0	0	0	0	0	0
4	0	0	0	0	0	0	0	0
5	0	0	0	0	0	**1**	0	0
6	0	0	0	0	0	**2***	0	0
7	0	0	0	0	0	0	-	-
8	0	0	0	0	0	0	-	-
9	0	0	0	0	0	0	-	-
10	0	0	0	0	**1**	**1**	-	-

* aggregates of leukocytes in the peri-renal fat

Table 3.6 Scoring by individual pathologist of *M. avium* infected kidneys. Mice were treated with 50 mg/kg body weight of either free amikacin, amikacin-loaded nanoparticles or empty amikacin nanoparticle (copolymer alone). One group remained infected but left untreated with any drugs or nanoparticles. Results show no inflammatory changes in both the amikacin loaded nanoparticle or the free drug at 50 mg/kg. Results also show minimal to mild inflammation in several samples of infected mice left untreated and mice treated with the copolymer alone. Kidney scores were as follows: 0 - normal; 1 - minimal inflammation; 2 - mild inflammation; 3 - moderate inflammation; 4 - marked inflammation

Category	Mean Pack Cell Volume (PCV) in % ± SD	Mean Total Protein (T.P.) in g/dL ± SD
AMK NP Group N=5	48.6 ± 3.0	5.9 ± 0.13
Free AMK Group N=5	59.6 ± 1.5	7.9 ± 0.13
Empty AMK NP Group N=5	43.8 ± 5.5	6.1 ± 0.14
Negative control N=3	48.6 ± 0.5	5.7 ± 0.2
Positive control N=3	55 ± 2.6	6.1 ± 0.17

SD = Standard deviation

Table 3.7 Packed cell volume and total protein of mice treated with free amikacin, amikacin-loaded nanoparticle, copolymer and controls. PCV and TP are within normal limits of amikacin loaded nanoparticle group and are elevated in both the free amikacin and infected untreated mouse group. The normal range of PCV in mice is 39-49% and TP is 3.5-6.5.

Chapter Four

Efficacy of Clarithromycin Encapsulated Polymeric Nanoparticles against *Mycobacterium avium*

Abstract

M. avium is an opportunistic pathogen that can cause disease in immune-compromised individuals such as those with HIV/AIDS. Treatments with antimicrobials are complicated and often unrewarding. An improved treatment modality is desperately needed to aid in the elimination *M. avium* infections. We tested the efficacy of clarithromycin-loaded nanoparticles against *M. avium* infection in mice. Average intensity diameter of clarithromycin nanoparticles was 174 nm ±2 and the zeta potential was -4 mV ±0.6. The encapsulation efficiency of the clarithromycin nanoparticle was calculated to be greater than 98%. *In vitro* efficacy studies with clarithromycin loaded polymeric nanoparticles showed a statistically significant reduction in *M. avium*. Cytotoxicity assay revealed clarithromycin-loaded nanoparticles (CLA NP) were non-toxic in J774A.1 cells at doses ranging from 8 µg/mL to 60 µg/mL. *CLA NP* demonstrated a reduction of *M. avium* load in the spleen by 0.8 log but not the liver of infected mice. No histopathological lesions were noticed in the kidneys of mice at a dose of 100 mg/kg of clarithromycin-loaded nanoparticles, suggesting absence of toxicity *in vivo*.

Keywords: tuberculosis, *M. avium*, nanoparticles, clarithromycin

Introduction

Mycobacterium avium is an opportunistic pathogen that is ubiquitous in distribution and capable of causing disease in both animals and humans (1, 2). *M. avium* is primarily transmitted via ingestion and aerosolized secretions (3). Once inside the body, *M. avium* can penetrate the mucosal epithelium and infect resident macrophages (3). Hidden within macrophages, *M. avium* organisms are transported to local lymph nodes via the lymphatic system where they begin to replicate. If a robust and competent immune system is present, the infection will be eliminated or controlled. If immune suppression is present as is the case for individuals also infected with human immunodeficiency virus (HIV), then *M. avium* will spread rapidly via the blood, multiplying unchecked and causing disseminated disease (3). It is estimated that most, if not all, HIV positive patients will eventually become infected with *M. avium* if they do not succumb to other opportunistic infections first (4).

M. avium is a difficult microorganism to treat with antimicrobials due to the presence of a thick, waxy cell wall and a slow growth phase (5, 6). Typically treatment involves taking multiple drugs simultaneously for extended periods of time. Although combination therapy is best, clarithromycin (CLA) has shown to be a potent first line drug used to treat *M. avium* infections (7). Clarithromycin is

a macrolide antibiotic and has shown dose dependent bactericidal activity in *M. avium* infected cell culture and mice (8, 9, 10, 11). This lipophilic antimicrobial can easily cross cell membranes and accumulate tenfold inside cells including macrophages (12). Some limitations of CLA include a short half-life of 4 hours and low bioavailability of ~45-50% when taken orally (13). In order to improve bioavailability and increase the bactericidal activity of CLA without toxic side effects, encapsulation with a novel polymeric nanoparticle was explored and tested in *M. avium* infected macrophages and mouse model.

Encapsulation of antimicrobials by nanoparticles for drug delivery is a burgeoning area of nanotechnology. Utilization of polymeric nanoparticles to encapsulate antimicrobials offers several advantages over other experimental carrier systems. Polymeric nanoparticles are versatile and can be fabricated for different routes of administration. Oral, topical, ocular, parentral and inhaled have all been investigated with promising results (14, 15, 16). Also the surface chemistry of polymeric nanoparticles can be altered to improve cellular uptake, prolong circulation time or regulate the release of drugs (17, 18, 19). Lastly, polymeric nanoparticles are considered relatively safe and non-toxic (18, 20). Although various drugs have been investigated (21, 22, 23), CLA remains largely unexplored as part of a polymeric drug delivery method.

The polymeric nanoparticles used in this study were constructed from commercially available hydrophobic and hydrophilic block co-polymers, poly

(ethylene oxide)-poly (propylene oxide)-poly (ethylene oxide) (PEO-*b*-PPO-*b*-PEO) with polycaprolactone (PCL) grafted onto the polymer. These amphiphilic block copolymers are able to self-assemble into micelles in aqueous solution during a process called nano-precipitation (24) and encapsulate CLA through hydrophobic interactions with PCL. The polymeric nanoparticles are unique in that they create an inner core architecture that provides a natural carrier state for CLA with an amphiphilic shell that aids in particle stabilization and cellular membrane permeability.

Materials and methods

Mycobacterial Strain

A single transparent colony of strain *Mycobacterium avium subspecies hominissuis*, ATCC 49601, was grown with aeration in Middlebrook 7H9 Broth supplemented with 10% (vol/vol) of albumin-dextrose-catalase (ADC) enrichment with 2% glycerol (Difco Laboratories, Detroit, MI, USA) to mid log phase before being frozen at minus 20ºC in aliquots containing ~5 x 10^6 cfu/mL. Sterility checks and verification of colony forming units by serial dilutions were done in triplicate before each use. The minimal inhibitory concentration (MIC) of CLA was 0.12 µg/mL for *M. avium* 49601. This is in agreement with other *M. avium* strains that are susceptible to CLA (25).

Development of Clarithromycin Nanoparticles

Clarithromycin-loaded nanoparticles (CLA NP) were fabricated (Fig 4.1 and 4.2) via the dialysis method (24) by dissolving the polymer and drug in tetrahydrofuran (THF), a solvent, then dialyzed (MWCO 1000 g/mol) against 10 mM phosphate buffer pH 7.4 for 24 hours with 3 changes of buffer. The solution was then filtered through 0.45 µm Teflon filter to remove aggregates and stored at 4^{o} C until usage. For *in vitro* and *in vivo* work the CLA NP were diluted with molecular grade, de-ionized, distilled water to a working concentration of 1 mg/mL for cell culture studies and 10 mg/mL for *in vivo* mouse studies.

Physico-chemical Characterization of Clarithromycin Nanoparticles

Dynamic Light Scattering (DLS)

The average intensity diameter and zeta potential of the CLA NP and "empty" clarithromycin nanoparticles or co-polymers were characterized by DLS using the Zetasizer Nano ZS at 25 ± 0.1 °C. Samples were diluted in de-ionized water to 1 mg/mL and sonicated using a water bath sonicator (Model 8890, Cole-Parmer, Chicago, IL) for 10 minutes before analysis. The intensity-average diameter (*DI*), polydispersity index (PDI) and zeta potential were recorded for each sample and averaged from three measurements.

Determination of Drug Content by HPLC and Bioassay

The amount of clarithromycin loaded into the nanoparticle was determined by HPLC and bioassay using the microdilution method (26, 27). After fabrication of the clarithromycin-loaded nanoparticles, the dialyzed solution was centrifuged at

3700 x *g* for 1 hour to separate drug loaded nanoparticles from free un-encapsulated CLA. The supernatant containing free drug was submitted to the veterinary bioscience department at Virginia Tech for HPLC analysis using a reverse phase column (C18) with UV detection at 210 nm. The encapsulation efficiency was then calculated from the equation: EE= total drug- free drug/total drug x 100%.

In the bioassay, *Micrococcus luteus* ATCC 9341 was used as the indicator organism to determine the Minimum Inhibitory Concentration (MIC) of the clarithromycin loaded nanoparticle in broth as compared to the free drug at µg/mL. Briefly, 1 mg/mL stock solutions of free CLA, clarithromycin-loaded nanoparticle and copolymer were serially diluted in a 96 well plate to which $5x10^6$ cfu/mL of *M. luteus* was added. After 24 hours of incubation at 37º C, turbidity was scored by eye and recorded. The MIC was defined as the lowest concentration of drug able to completely inhibit growth.

The pH of the clarithromycin loaded nanoparticle, free drug, and copolymer that was used for *in vivo* effort was determined using a pH meter (Accumet Basic, Fisher Scientific, USA) and recorded. Stability studies via MIC determination of the clarithromycin- nanoparticle in solution with appropriate controls was performed on days 5, 10, and 22 after reconstitution and storing at temperatures of 4ºC, 25ºC, and 37º C.

Macrophage Viability Assay

Cell toxicity was determined by an MTS (3-(4,5-dimethylthiazol-2-yl)-5-(3-carboxymethoxyphenyl)-2-(4-sulfophenyl)-2H-tetrazolium) Cytotoxicity Assay (Promega Corporation) as described by Ranjan et al., (28). Briefly, J774A.1 macrophages were incubated at 37°C in a humidified 5% CO_2 atmosphere overnight with several concentrations of free CLA, clarithromycin-loaded nanoparticles, empty nanoparticles (copolymer) and untreated controls. A 96-well ELISA plate reader (SoftMax Pro Inc., USA) was used to record absorbance at 490 nm. Results were expressed as the percentage mean absorbance by cells upon incubation with various treatments (free CLA, clarithromycin nanoparticle or copolymer) with respect to untreated controls. Experiments were performed in triplicate and data was analyzed using the Student's *t* test. A "P" value of < 0.05 was considered significant.

Growth and Infection of J774A.1 Macrophages with M. avium

Cell preparation and infection was adapted from Barrow et al. (29, 30) with the following modifications. Murine macrophage cell line, J774A.1, was acquired from American Type Culture Collection (ATCC) and grown as monolayers in 75 cm^2 tissue culture flasks (Corning, Inc.) in a humidified incubator with 5% CO_2 atmosphere at 37°C. Cells were grown in Dulbecco's modified Eagle's medium (DMEM) from Sigma-Aldrich containing 10% (vol/vol) fetal bovine serum (FBS), L-glutamine (4mM), $NaHCO_3$, (0.44M) pyridoxine-HCl, 4,500 mg/L and 1% penicillin-streptomycin solution (Mediatech, Inc., Manassas, VA). At 90%

confluence, the medium was replaced with 3 x 10^6 colony forming units/mL of *M. avium* suspended in 10 mL of DMEM containing 10% (vol/vol) FBS. After 4-6 hours of incubation, macrophages were rinsed twice with Hank's Balanced Salt Solution, then collected by gently scraping the flask with 10 mL of DMEM with 10% (vol/vol) FBS without antibiotics. Next, the cell suspension was centrifuged at 156 x g for 3 minutes (Sorvall Legend RT Plus, UK) to remove extracellular bacteria and then re-suspended with 38 mL of DMEM containing 10% (vol/vol) FBS. The cell suspension was then added in 1mL aliquots into 12 well plates at a density of 2 x 10^5 cells per well. Plates were then incubated at 37^{o}C in 5 % CO_2 for 24 hours to allow attachment of infected and uninfected J774 A.1 cells.

After 24 hours, the media was replaced with 1% (vol/vol) FBS in DMEM, containing 15 or 30 µg/mL of; free CLA, clarithromycin nanoparticles, or empty nanoparticles, along with untreated controls, and allowed to incubate at 37^{o}C in 5% CO_2. At days 0, 3 and 6, cells were lysed with 0.1% Triton X-100 and *M. avium* organisms were enumerated as colony forming units (cfu)/mL by plating serial dilutions of lysate on Middlebrook agar supplemented with 10% (vol/vol) oleate-albumin-dextrose-catalase (OADC) (Difco laboratories, Detroit, MI, USA) and 5% (vol/vol) glyercol. On day 3, the media was replaced with fresh DMEM containing 1% (vol/vol) FBS. Experiments were performed in triplicate. Statistical analysis was performed between the groups with Student's *t* tests. A "*P"* value of <0.05 was considered statistically significant for all of the experiments.

Infection and Treatment of Mice

This animal research protocol was approved by the Institutional Animal Care and Use Committee (IACUC). Female BALB/c mice, purchased from Charles River, were housed in an Animal Biosafety Level 2 facility with food and water *ad libitum.* At 13 weeks of age, 19 mice weighing approximately 25 grams, were infected intraperitoneally (IP) with 200 µL of $6x10^6$ cfu/mL of *M. avium* ATCC 49601. One week post infection, 3 groups of mice, containing 5 mice per group, were treated IP with 250 µL of a 10 mg/mL solution (100 mg/kg) of free CLA, clarithromycin nanoparticle or copolymer thrice weekly for 2 weeks. As a positive control, 2 infected mice were treated with 250 µL of sterile de-ionized water IP. As a negative control, two uninfected mice were treated with 250 µL of sterile de-ionized water IP.

Determination of M. avium counts in spleen and liver

Four days after the last treatment, mice were sacrificed humanely to quantify the colony forming units per organ from liver and spleen. The organs were removed aseptically from each mouse and placed separately into 50 mL tubes containing 2 mL of Middlebrook broth 7H9 supplemented with 10% (vol/vol) ADC enrichment. The organs were homogenized for 1-2 minutes using a Tissuemiser homogenizer (Fisher Scientific, USA). Next, aliquots of each organ homogenate were serially diluted in Middlebrook broth to a maximum of 10^5 dilutions, plated on Middlebrook 7H10 agar plates supplemented with 10% (vol/vol) OADC

enrichment and incubated for 7-14 days at 37°C. The number of colonies per dilution were counted and reported as CFUs/organ. An unpaired, two tailed student's *t* test was performed and a "P" value of < 0.05 was considered statistically significant.

Histopathology

Kidneys from each mouse were collected, fixed in 10% neutral buffered formalin, trimmed, routinely processed and embedded in paraffin blocks. Five (5) micron sections were cut with a microtome, fixed on a glass slide and stained with hematoxylin and eosin. In a blinded study, two veterinary pathologists independently examined the kidney samples and scored changes (degeneration/necrosis, inflammation, hemorrhage, edema) using a scale from 0 to 4. The degree of pathological change was recorded as; (0) = unremarkable, (1) = minimal, (2) = mild, (3) = moderate, and (4) = marked.

Hematology Analysis

Blood was obtained from each mouse via the retro orbital plexus while under general anesthesia (1.5% isofluran and 1.5 L/min of oxygen), just before euthanasia. Blood was collected into a micro hematocrit tube to determine Total Protein (TP) and Packed Cell Volume (PCV), which accesses hydration and volume percentage of red blood cells present in whole blood.

Results

Physico-chemical Characterization of Clarithromycin Nanoparticles

Dynamic Light Scattering (*DLS)*

Several physico-chemical properties were measured by DLS (Table 4.1). The relative size or intensity-average diameter of the clarithromycin-loaded nanoparticle was found to be 174 nm (±2). The zeta potential or surface, charge was slightly anionic at -4.4 mV (± 0.6). Lastly, the polydispersity index (PDI) which measures the variance of size of the nanoparticle was 0.188 (± 0.012). The physicochemical parameters of the block co-polymer alone were as follows; 122 nm (±5) for the average intensity diameter, -2.8 mV (±0.3) for the zeta potential and 0.180 (±0.014) for the PDI.

Measurement of Clarithromycin Content by HPLC and Bioassay of Clarithromycin Loaded Nanoparticles

The encapsulation efficiency of the CLA NP was calculated to be greater than 98%. The MIC of the clarithromycin-loaded nanoparticles using *M. luteus* as an indicator organism was 0.12 µg/mL. The MIC of free CLA was 0.015 µg/mL. The pH of a 10 mg/mL solution of CLA-NP was measured at 8.3, the free CLA at 8.4 and the empty nanoparticle or copolymer at 6.0 (Table 4.2).

Storage Studies via bioassay with M. luteus.

The stability of the nanoparticles was measured as a function of the ability of the nanoparticles to inhibit growth of *M. luteus* during MIC analysis (Table 4.3). Results show that after 10 days of incubation under varying environmental

conditions the biologic activity for both the free CLA and CLA NP remained. After 22 days of incubation under varying environmental conditions an increase in the MIC was apparent in both groups (N=3).

Macrophage Viability Assay

The cyto-toxicity of CLA NP in J774A.1 cells was measured using the MTS assay and statistically analyzed using a Student's *t* test. Results showed cell viability remained above 90% at varying concentrations up to 60 µg/mL and no statistical difference in the means (Figure 4.4). The experiment was repeated three times and each group had a sample size of 6.

The cyto-toxicity of free CLA in J774A.1 cells was also analyzed using the MTS assay. The assay evaluates cytotoxicity as a function of cellular viability by measuring the amount of formazan produced by the cell's mitochondrial enzymes. At a dose of 15 µg/mL, free CLA is non-toxic in J774A.1 cells. However, at 30 µg/mL, cell viability drops to 70% and at 60 µg/mL cell viability further drops to 30%. The percent cell viability of macrophages treated with co-polymer remained above 90% (results not shown). Each experiment was repeated three times and each group had a sample size of 6.

In Vitro Efficacy Study in Macrophages

The efficacy of CLA NP against *M. avium* infected J774A.1 cells at a dose of 15 µg/mL was performed. After 6 days of incubation, cells were harvested and

revealed that both the free CLA and CLA NP reduced *M. avium* in macrophages by about 1 log (Figure 4.6). The experiments were performed in triplicate with an N of 3).

The efficacy of CLA NP against *M. avium* infected J774A.1 cells at a dose of 30 µg/mL was also performed (Figure 4.7). At 6 days the CLA NP reduced the intracellular growth of *M. avium* by a log. The free CLA at the equivalent dose reduced intracellular *M. avium* growth by 2.2 log however the standard deviation is large, (N=3).

In Vivo Efficacy Study in Mice

Figure 4.8 Treatment with CLA NP in BALB/c mice was done. Mice were treated three times weekly at a dose of 100 mg/kg body weight for 2 weeks. Organs were harvested and the bacterial load assessed via serial dilution. In the spleen, the CLA NPs reduced the bacterial load by 0.8 log. In the liver the CLA NP reduced the bacterial load by 0.9 log, but it was not statistically significant when compared to untreated controls using a Student's *t* test (Figure 4.8). The free clarithromycin reduced the bacterial load by 1.9 log in the spleen and 1.6 log in the liver (Figure 4.8).

Histopathology

Both kidneys from mice infected with *M. avium* and treated with free CLA, CLA NP, or co-polymer at a dose of 100mg/kg body weight was submitted for

histopathological analysis. A group remained infected but was not treated with drugs or nanoparticles. Two pathologists separately examined the kidney samples for lesions and scored the tissue using a scale of: 0 - normal; 1 - minimal inflammation; 2 - mild inflammation; 3 - moderate inflammation; 4 - marked inflammation. Results showed no inflammatory changes in either the CLA NP or the free CLA at the dose of 100 mg/kg per mouse. Results also showed minimal inflammation in the peri-renal area of samples of infected mice left untreated and mice treated with the copolymer alone. However, inflammation localized to the peri-renal area common findings in histopathological evaluation of kidneys.

Hematology Analysis

The packed cell volume and total protein of mice treated with clarithromycin loaded nanoparticle, free CLA, co-polymer and untreated infected mice were done at the conclusion of the two week *in vivo* study. Results of the PCV and TP for all groups were within normal range (Table 4.5). In mice range of the PCV is 39-49% and for TP it is 3.5-6.5 g/dL.

Discussion

The CLA NP has several physicochemical properties that promotes cellular uptake and thus increases its suitability as an ideal carrier for drug delivery of antimicrobials. One important physicochemical property that can enhance cellular uptake is size. As seen in Table 4.1, the CLA NP has an optimal size

because nanoparticles near the size range of 200 nm follow the same engulfment process as intracellular pathogens when given intravenously (31). This would be an ideal situation to have CLA NPs introduced into the intracellular environment, where microbes like *M. avium* hide. Further evaluation of this likelihood would require flow cytometry and confocal microscopy studies.

The zeta potential or overall surface charge of a nanoparticle within the range of +/- 30 mV will enhance particle stabilization and facilitation of cellular uptake (33). The CLA NP was within this range and slightly negative. Bhattacharjee et al. investigated the role of surface charge and cellular uptake and found that polymeric anionic nanoparticles 100nm or less are more efficiently engulfed than polymeric cationic particles of the same size range (33). Additionally, neutral particles have the slowest rate of macrophage engulfment. The polydispersity index (PDI), which measures the variance of size of the clarithromycin nanoparticle was below 0.2 indicating relative size uniformity in the sample of the nanoparticle solution.

Recent research has shown that shape also affects cellular uptake. It is speculated that the shape of the clarithromycin nanoparticle is spherical due to its amphiphilic composition that forms micelles in solution (24). Doshi and Mitragotri (32) noted that spherical or rod shaped particles are engulfed more readily than other shapes when comparing particles within the same size range of our current CLA NP.

From the DLS analysis, there is a size difference noted in nm between the larger clarithromycin loaded nanoparticle and the empty co-polymer. The discrepancy could be accounted for by the amount of drug loaded in the nanoparticle. The clarithromycin nanoparticle has been shown to have a high drug load (34) and it is possible that the drug molecules are physically making the nanoparticle slightly bigger since clarithromycin interacts directly with the caprolactone side chains through hydrophobic interactions (35).

HPLC and MIC analysis of the CLA NP indicate high encapsulation efficiency. Also, the MIC values of the CLA NP and free CLA indicated biologically activity after 24 hours of incubation. It was noted that the values of the MIC of the free CLA and CLA NP were dissimilar by two fold dilutions. This minor discrepancy may indicate the drug release pattern of the nanoparticle is slow to compare accurately within twenty-four hours or that the amount of drug load determined by HPLC may be slightly less than calculated. A drug release study would be a valuable next test. When *M. luteus* was used as the indicator organism in MIC storage stability analysis, an increase in the MIC values was seen indicating that the nanoparticles and free drug were less biologically active after 3 weeks at 4º C, 25º C and 37º C.

The CLA NP's are non- toxic in murine macrophages as determined by the MTS assay at the doses used. In comparison, when free CLA was assayed, cell

viability was above 90% at a dose of 15 µg/mL. However, when free CLA was assayed at 30 µg/mL, cell viability drops below 90 % to 70% indicating toxicity of free drug to macrophages. This is an interesting finding because perhaps the CLA NP has a sustained drug release pattern that enables it to avoid cellular toxicity in J774A.1 cells. This would be beneficial to treat *M. avium* infections because the CLA NP could deliver a high drug load to the site of infection, while also having a sustained release pattern that is both non-toxic to host cells and bactericidal. Drug release studies would yield valuable information of the CLA NP. In the absence of drug release studies, in vitro efficacy studies could help decipher the nanoparticle's drug release profile.

In the treatment of *M. avium* infected J774A.1 murine macrophages, a dose of 15 µg/mL of both the CLA NP and free CLA reduced the bacterial load by 1 log as compared to untreated controls on day 6 (Figure 4.6). At 30 µg/mL the CLA NP reduced *M. avium* by a log while free CLA reduced the bacterial load by 2.2 log (Figure 4.7). Although both results are statistically significant, the free CLA group had a large standard deviation indicating variance within the treatment group. Although speculative, it is possible the large standard deviation could be the result of macrophage detachment and loss from the high free CLA concentrations used. A Trypan Blue assay would help enlighten these findings. However, if the macrophages are sensitive to high concentrations of free CLA as indicated by MTS assay, detached *M. avium* infected macrophages will be washed away during processing resulting in a falsely low cfu/mL. Additionally,

daily monitoring of the macrophage culture plate revealed signs of cellular death. Macrophages began to appear rounder, smaller and detach from the plate bottom 2-3 days after addition of free CLA at 30µg/mL. In contrast, macrophages treated with CLA NP at the equivalent dose, were not observed microscopically to have cell detachment or loss. Although CLA is considered a relatively safe drug, some toxicity has been reported when doses above 15 ug/ml are used. In a study done by Karabulut et al., embryonic toxicity was observed in rats at a dose of 30µg/mL. (36).

In mice, CLA NP were able to successfully reduce viable *M. avium* organisms in the spleen by 0.8 log and in the liver by 0.9 log (although not statistically significant) as compared to untreated controls. Free CLA reduced the bacterial load by 1.9 log in the spleen and 1.6 log in the liver. The difference in efficacy between the two drug groups could be attributed to the length of the experiment and drug release pattern of the nanoparticle. Even though the clarithromycin nanoparticle has an extremely high drug load, the drug release pattern of this nanoparticle is unknown. It has been previously documented that nanoparticles containing polycaprolactone have a slow drug release pattern (37). It would have been advantageous to extend the length of the experiment to investigate if a difference would have occurred in the means suggesting a slow drug release pattern *in vivo*.

Histopathology of the kidneys revealed no signs of toxicity (Table 4.4) in any of the groups of mice treated with free CLA, encapsulated clarithromycin or copolymer alone. This indicates a dose of 100mg/kg given IP thrice weekly for 2 weeks is non-toxic in BALB/c mice.

Other parameters investigated were Packed Cell Volume (PCV) which measures the percent of red blood cells in blood and Total Protein (TP) (Table 4.5) which can aid in assessing dehydration or biochemical imbalances. Mice treated with encapsulated clarithromycin nanoparticle, free CLA, copolymer and controls had PCV and TP values within normal range, showing no signs of pathology. Clinically, none of the mice showed any abnormal signs of illness such as lethargy, rough hair coat or weight loss.

Conclusion

An improved treatment modality to treat *M. avium* infections was investigated. CLA NP were fabricated then analyzed for size, shape and charge before being tested for toxicity and efficacy in both cell culture and mouse studies. Results reveal the clarithromycin nanoparticle was non-toxic in cell and mouse experiments at the respective dose used. In cell culture studies, the clarithromycin nanoparticle was as effective in reducing viable *M. avium* as the free CLA at 15 µg/mL. In mouse studies, the clarithromycin nanoparticle was effective at reducing bacterial counts in spleen but not the liver as compared to untreated controls. Future studies would include drug release studies of the

nanoparticle so that adjustments could be made for continued release of CLA and increasing the duration of the mouse experiment may be needed to really discern the effectiveness of CLA NP.

References

1. Falkinham III J. O. (1996). “Epidemiology of Infection by Nontuberculous Mycobacteria” Clinical Microbiology Reviews Apr **9**(2):177-215.
2. Thoen, C. O. (1994). "*Mycobacterium avium* infections in animals" Res Microbiol **145**(3): 173-7.
3. Inderlied C. B., Kemper C. A., Bermudez L. E. (1993). “The *Mycobacterium avium* complex” Clinical Microbiology Reviews July **6**(3):266-310.
4. Nightingale S. D., Saletan S. L., Swenson C. E., Lawrence A. J., Watson D. A., Pilkiewicz F. G., Silverman E. G., Cal S. X. (1993). “Liposome-encapsulated gentamicin treatment of *Mycobacterium avium-Mycobacterium intracellulare* complex bacteremia in AIDS patients” Antimicrob Agents Chemother. September **37**(9): 1869–1872.
5. Chatterjee D. (1997). “The mycobacterial cell wall: structure, biosynthesis drug action and sites of drug action.” Curr Opin Chem Biol. Dec; **1**(4):579-88.
6. Rastogi, N., David H. L. (1981). *“*Growth and Cell Division of *Mycobacterium avium.”* Journal of General Microbiology **126**:77-84.
7. Heifets, L. (1996). “Clarithromycin against *Mycobacterium avium* complex infections” Tuber Lung Dis Feb **77**(1):19-26.
8. Furney S. K., Skinner P. S., Farrer J., Orme I. M. (1995) “Activities of Rifabutin, Clarithromycin and Ethambutol in a Mouse Model” Antimicrobial Agents and Chemotherapy Mar;**39**(3):786-789.

9. Klemens S. P., DeStefano M. S., Cynamon M. H. (1992). “Activity of clarithromycin against *Mycobacterium avium* complex in beige mice” Antimicrobial Agents and Chemotherapy Nov **36**(11):2413-2417.
10. Fernandes P. B., Hardy D. J., McDaniel D., Hanson C. W., Swanson R. N. (1989). “*In vitro* and *in vivo* activities of clarithromycin against *Mycobacterium avium”* Antimicrobial Agents and Chemotherapy Sept **33**(9):1531-1534.
11. Mor N., Vanderkolk J., Mezo N., Heifets L. (1994). “Effects of Clarithromycin and Rifabutin Alone and in Combination on Intracellular and Extracellular Replication of *Mycobacterium avium*” Antimicrobial Agents and Chemotherapy Dec **38**(12):2738-2742.
12. Mor, N., Vanderkolk J., Heifets L. (1994). “Accumulation of Clarithromycin in macrophages infected with *Mycobacterium avium*” Phamacotherapy **14**(1):100-104.
13. Chu S. Y., Sennello L. T., Bunnell S. T,. Varga L. L., Wilson D. S., Sonders R. C. (1992). “Pharmacokinetics of Clarithromycin, a New Macrolide, after Single Ascending Oral Doses.” Antimicrobial Agents and Chemotherapy. Nov; **36**(11): 2447-2453.
14. Pandey R., Khuller G. K. (2007). “Nanoparticle based oral drug delivery system for an injectable antibiotic-streptomycin. Evaluation in a murine tuberculosis model.” Chemotherapy **53**:437-441.

15. Pawar K. R., Babu R. J. (2010). :Polymeric and lipid based materials for topical nanoparticle delivery systems." Crit. Rev. Ther. Drug Carrier Syst. 27(**5**)419-59.
16. Nagarwal R. C., Kant S., Singh P. N., Maiti P., Pandit J. K. (2009). " Polymeric nanoparticulate system: A potential approach for ocular drug delivery." Journal of Controlled Release. **136:** 2-13.
17. Davis M. E., Chen Z. G., Shin D. M. (2008). "Nanoparticle therapeutics: an emerging treatment modality for cancer." Nature Reviews Drug Discovery **7** 771-782.
18. Panyam, J., Labhasetwar V. (2003). "Biodegradable nanoparticles for drug and gene delivery to cells and tissue." Advanced Drug Delivery Reviews **55**:329-347.
19. Kakizawa Y., and Kataoka K. (2002) "Block copolymer micelles for delivery of gene and related compounds." Advanced Drug Delivery Reviews **54**: 203-222.
20. Caruthers S. D., Wickline Lanza G. M. (2007) "Nanotechnology applications in medicine." Current Opinion in Biotechnology **18**: 26-30.
21. Yokoyama M., Okano T., Sakurai Y., Fukushima S., Okamoto K., Kataoka K. (1999). "Selective delivery of adriamycin to a solid tumor using a polymeric micelle carrier system." J Drug Target **7**:171–86.
22. Ge H. X., Hu Y., Jiang X. Q., Cheng D. M., Yuan Y. Y., Bi H., Yang C. Z. (2002). "Preparation, characterization and drug release behaviors of drug nimodipine-loaded poly (e-caprolactone)–poly (ethylene oxide)–poly (e-

caprolactone) amphiphilic triblock copolymer micelles." J. Pharm Sci **91:**1463–73.

23. Zhang Y., Zhuo Ren-xi. (2005). "Synthesis and in vitro drug release behavior of amphiphilic triblock copolymer nanoparticles based on poly (ethylene glycol)
and polycaprolactone." Biomaterials **26**:6736–6742.
24. Ha J. C., So Yeon Kim S. Y., Lee Y. M. (1999) "Poly(ethylene oxide)-poly(propylene oxide)-poly(ethylene oxide) (Pluronic)/poly(epsilon-caprolactone) (PCL) amphiphilic block copolymeric nanospheres. I. Preparation and characterization" Journal of Controlled Release Dec **62**(3): 381–392.
25. Heifets, L. (1996). "Susceptibility of *Mycobacterium avium* complex Isolates" Antimicrobial Agents and Chemotherapy **40**(8):1759-1767.
26. Mor N. and Heifets L. (1993). "MIC and MBC's of Clarithromycin against *Mycobacterium avium* within Human Macrophages "Antimicrobial Agents and Chemotherapy Jan **37**(1):111-114.
27. Telles, M.A.S., Yates M. D. (1994). "Single and double drug susceptibility testing of *Mycobacterium avium complex* and mycobacteria other than tubercle (MOTT) bacilli by a micro-dilution broth minimum inhibitory concentration (MIC) method." Tubercule and Lung Disease **75:** 286-290.
28. Ranjan A., N. Pothayee, T. P. Vadala, M. N. Seleem, E. Restis, N. Sriranganathan, J. S. Riffle and R. Kasimanickam. (2010). "Efficacy of Amphiphillic Core Shell Nanostructures Encapsulating Gentamicin in an *In*

Vitro Salmonella and *Listeria* Intracellular Infection Model." Antimicrob. Agents Chemother. Aug **54**(8):3524-6.

29. Wright E.L., Quenelle D.C., Suling W.J., Barrow W.W. (1996) "Use of Mono Mac 5 Human Monocytic cell line and J774 Murine Macrophage cell line in parallel antimycobacterial drug studies" Antimicrobial Agents and Chemotherapy Sept; **40** (9):2206-2208.

30. Barrow E.L.W., Barrow W.W. (2007) "Efficacy of Rifabutin loaded microspheres for treatment of *Mycobacterium avium* infected macrophages and mice" Drug Delivery **14:** 119-127.

31. Gelpernia S., Kisich K., Iseman M. D., Heifets L. (2005). "The Potential Advantages of Nanoparticle Drug Delivery Systems in Chemotherapy of Tuberculosis" Am J Respir Crit Care Med **172:**1487–1490.

32. Doshi N., Mitragotri S. (2010). "Macrophages Recognize Size and Shape of Their Targets." PLoS One. **5**(4): e10051.

33. Bhattacharjee S., Ershov D., Fytianos K., van der Gucht J., Alink G. M., Rietjens I. M., Marcelis A. T., Zuilhof H. (2012). "Cytotoxicity and cellular uptake of tri-block copolymer nanoparticles with different size and surface characteristics." Part Fibre Toxicol. Apr ;**9**(11):1-19.

34. Mohammadi G., Nokhodchi A., Barzegar-Jalali M., Lotfipour F., Adibkia K, Ehyaei N., Valizadeh H. (2011). "Physicochemical and anti-bacterial performance characterization of clarithromycin nanoparticles as colloidal drug delivery system." Colloids Surf B Biointerfaces. Nov ;**88**(1):39-44.

35. Zhang Y., Zhuo R. (2005). “Synthesis and in vitro drug release behavior of amphiphilic triblock copolymer nanoparticles based on poly (ethylene glycol) and polycaprolactone.” Biomaterials. **26**(33):6736-6742.
36. Karabulut, A. K., Uysal, I. I., Acar, H. and Fazliogullari, Z. (2008). “Investigation of Developmental Toxicity and Teratogenicity of Macrolide Antibiotics in Cultured Rat Embryos” Anatomia, Histologia, Embryologia **37**:369–375.
37. Sahoo R., Sahoo S., Nayak P., Sahoo S., Nayak P. (2011). “Controlled Release of the Drug Cefadroxil from Polycaprolactone-Polylactic Acid Nanocomposites” European Journal of Scientific Research **53** (2):154-162.

Tables and Figures

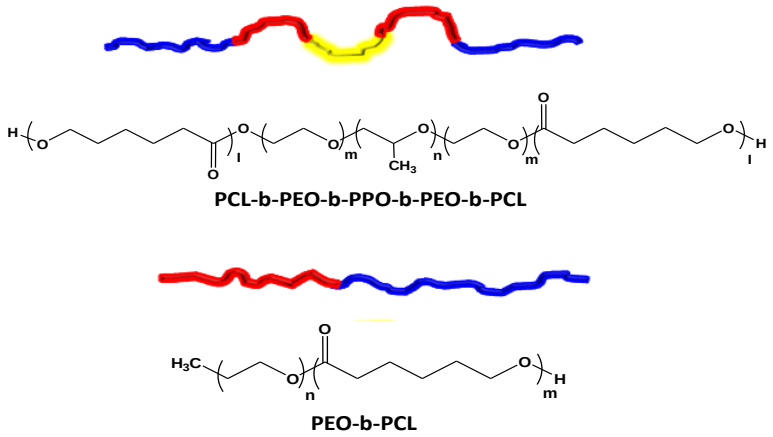

Figure 4.1 Structure of clarithromycin-loaded polymeric nanoparticle

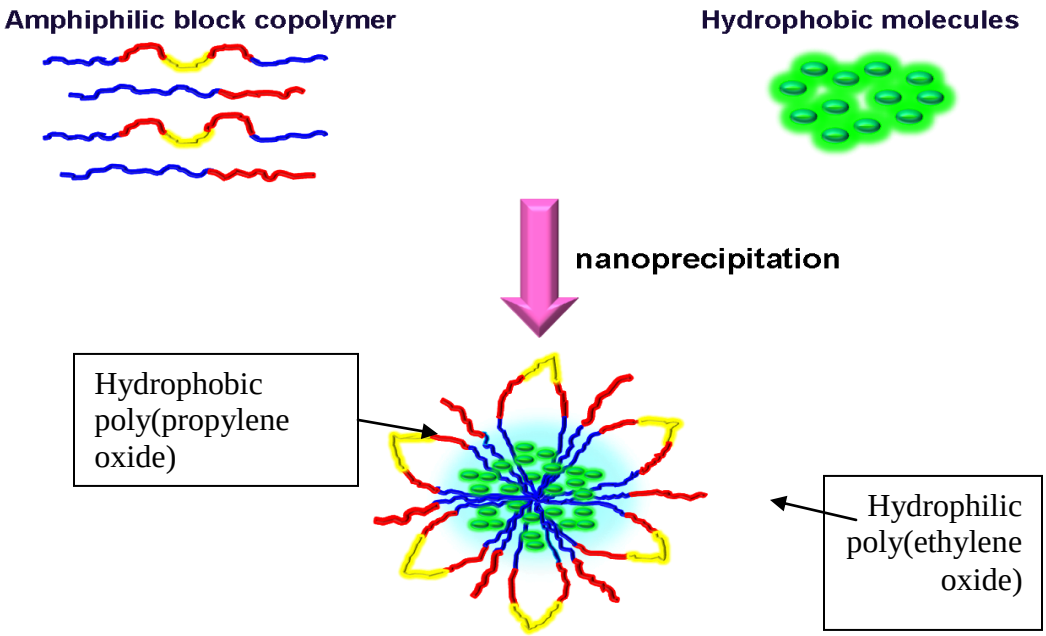

Figure 4.2 Self-assembly process to form clarithromycin-loaded polymeric nanoparticles by the nano-precipitation method.

Name	Intensity Diameter (nm) ± SD	Zeta Potential (mV) ± SD	PDI ± SD
CLA NP	174 ± 2	-4.4 ± 0.6	0.188 ± 0.012
Copolymer	122 ± 5	-2.8 ± 0.3	0.180 ±0.014

SD = Standard deviation

Table 4.1 Physico- chemical characterization of clarithromycin loaded polymeric nanoparticles by DLS.

CLA NP	Free CLA	Copolymer
8.3	8.4	6.0

Table 4.2 pH of solutions at 10 mg/mL for injection in mice used during *in vivo* studies.

MIC of CLA NP in µg/mL			
	4^0C	25^0C	37^0C
Day 5	0.03	0.03	0.03
Day 10	0.03	0.06	0.12
Day 22	1.95	0.975	1.95

MIC of Free CLA in µg/mL			
	4^0C	25^0C	37^0C
Day 5	0.015	0.015	0.015
Day 10	0.03	0.03	0.03
Day 22	0.03	0.12	0.06

Table 4.3 Storage Studies via bioassay with *M. luteus.* Results show that after 10 days of incubation under varying environmental conditions the biologic activity for both the free drug and clarithromycin nanoparticle remained (N=3). After 22

days of incubation under varying environmental conditions a more pronounced increase in the MIC was apparent in both groups (N=3).

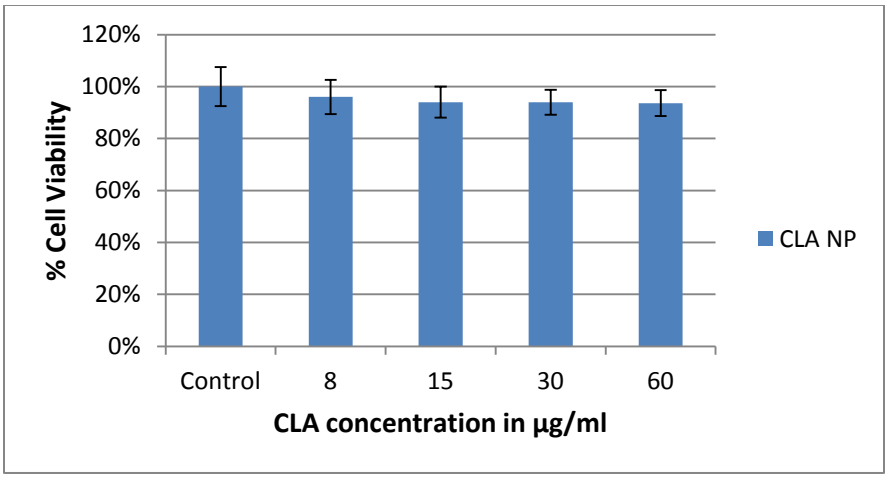

Figure 4.4 Cyto-toxicity of clarithromycin-loaded nanoparticles (CLA NP) in J774A.1 cells using the MTS assay. Cell viability remains above 90% at varying concentrations up to 60 µg/mL. Results show no statistical difference in the means. Experiments were done in triplicate, (N=6).

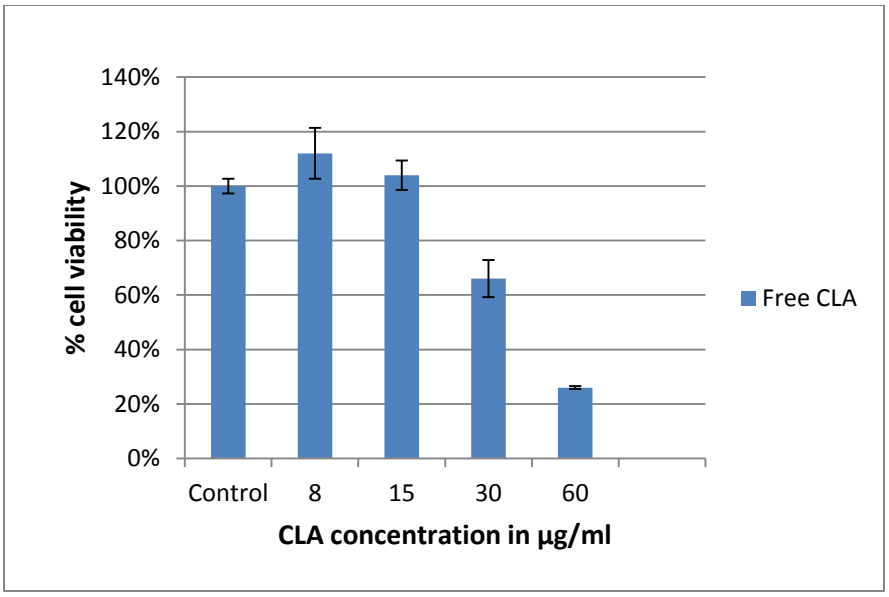

Figure 4.5 Cyto-toxicity of free clarithromycin in J774A.1 cells via the MTS assay. Cell viability is above 90% at a dose of 15 µg/mL. At 30 µg/mL, cell viability drops to 70%, indicating macrophage toxicity. Percent cell viability of macrophages treated with co-polymer remained above 90% (results not shown), (N=6).

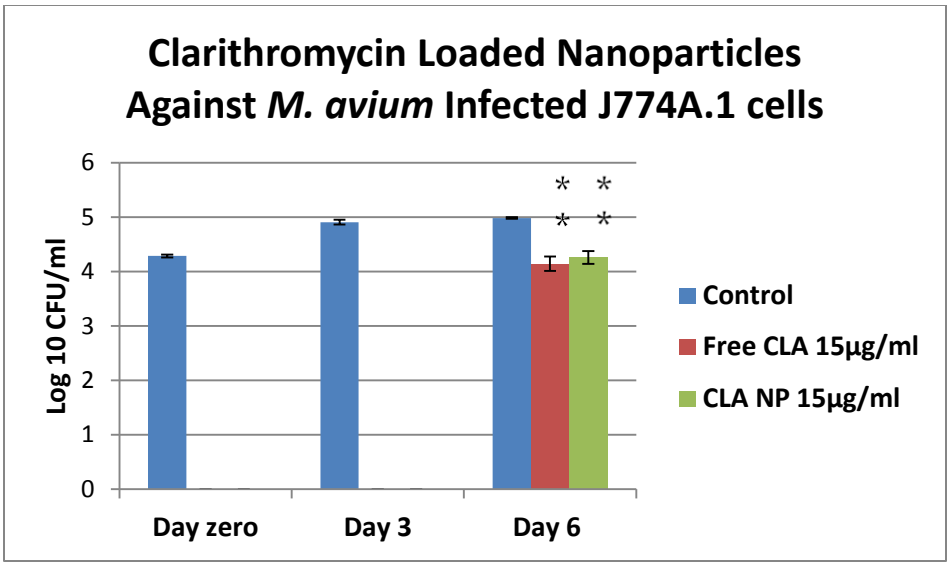

Figure 4.6 Clarithromycin-loaded nanoparticles (CLA NP) against *M. avium* infected J774A.1 cells at 15 µg/mL. On day 6, both free drug and CLA NP reduced *M. avium* in macrophages by about 1 log, (N=3). P value .< .001, results were done in triplicate.

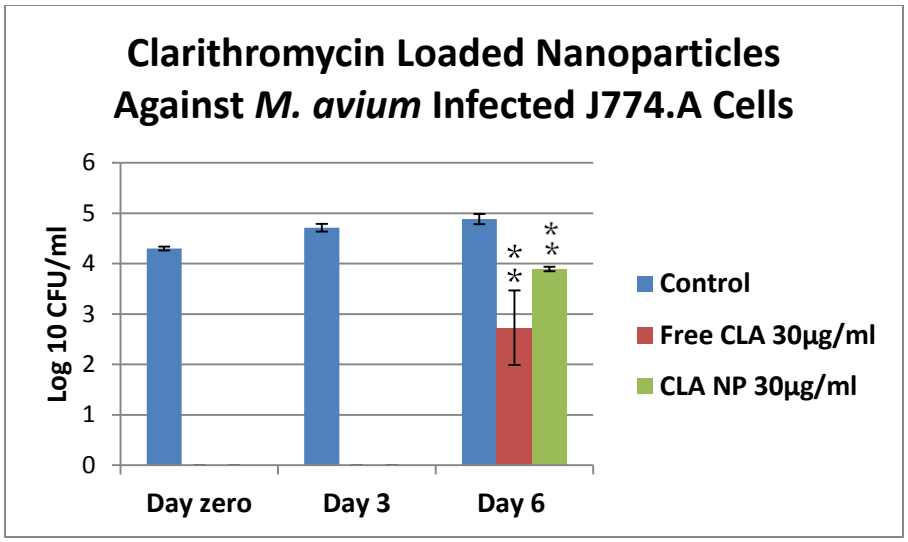

Figure 4.7 Clarithromycin-loaded nanoparticles (CLA NP) against *M. avium* infected J774A.1 cells at 30 µg/mL. On day 6, CLA NP reduces *M. avium* by a log (P value 0.001) while free clarithromycin reduced *M. avium* by 2.2 log, however the standard deviation is large, (N=3).

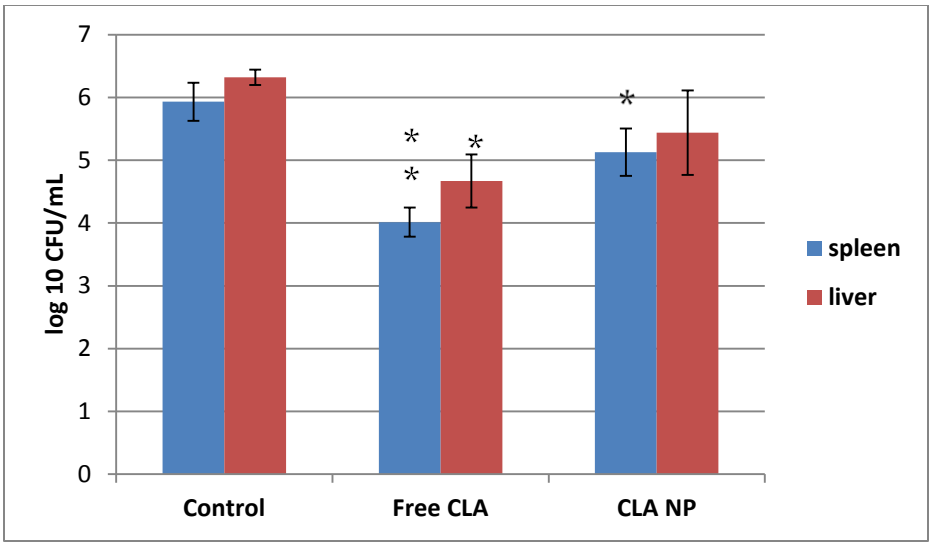

Figure 4.8 Treatment with clarithromycin-loaded nanoparticles (CLA NP) in BALB/c mice. Mice were treated thrice weekly at a dose of 100 mg/kg body weight for 2 weeks.

CLA NP reduced the bacterial load in the spleen by 0.8 log but was ineffective in reducing the bacterial load in the liver * = $P < 0.05$, ** = $P < 0.001$.

Kidney no	Kidney score CLA NP		Kidney score Free CLA		Kidney score Empty CLA NP		Kidney score Positive Control	
	1st Path-ologists	2nd Path-ologists	1st Path-ologists	2nd Path-ologists	1st Path-ologists	2nd Path-ologists	1st Path-ologists	2nd Path-ologists
1	0	0	1*	1*	0	0	1*	1*
2	0	0	1	0	0	0	0	0
3	0	0	0	0	0	1	0	0
4	0	0	0	0	0	0	1*	0
5	0	0	0	0	1*	1*	-	-
6	0	0	0	0	0	0	-	-
7	0	0	0	0	0	0	-	-
8	0	0	0	0	0	0	-	-
9	0	0	0	0	0	0	-	-
10	0	0	0	0	0	0	-	-

* indicates aggregates of leukocytes in the peri-renal fat

Table 4.4 Kidney scores by individual pathologist of *M. avium* infected kidneys. Mice were treated at a dose of 100 mg/kg with; free clarithromycin, clarithromycin loaded nanoparticles or co-polymer. One group remained infected but was not treated with drugs or nanoparticles. Kidney scores: 0 - normal; 1 - minimal inflammation; 2 - mild inflammation; 3 - moderate inflammation; 4 - marked inflammation.).

Category	Mean Pack Cell Volume (PCV) in % ± SD	Mean Total Protein (T.P.) in g/dL ± SD
CLA NP Group N=5	45.5 ± 3.0	5.9 ± 0.21
CLA Group N=5	44.2 ± 4.5	5.9 ± 0.61
Empty CLA NP Group N=5	48.2 ± 4.3	5.8 ± 0.13
Negative control N=2	49 ± 4.2	5.7± 0.35
Positive control N=2	51 ± 1.4	5.4± 0.70

SD= Standard Deviation

Table 4.5 Packed Cell Volume and Total Protein of mice treated with clarithromycin loaded nanoparticle, free clarithromycin, co-polymer and controls.

Note: Normal range of PCV in mice is 39-49% and TP is 3.5-6.5.

Chapter Five

Efficacy of Rifampicin, Clarithromycin, and Ethambutol Aerogel Nanoparticles in *Mycobacterium avium* Infected Mice

Abstract

Mycobacterium tuberculosis is an intracellular pathogen that currently infects more than 3 billion people worldwide, making it the number one cause of death due to a bacetrial infection in the world. Treatment with antimicrobials are curative but many people fail to finish the prescibed 6-9 month course of therapy because of cost, inconvenience, lengthy treatment schedule or toxic side effects from the drugs. A new approach to treat tuberculosis is urgently needed. The goal of this project was to develop a novel drug delivery system that utilizes biocompatible silica based nanoparticles called aerogel as an antimicrobial carrier. Commercially obtained aerogel was incubated with a solution containing 250 mg of clarithromycin, 13 mg of rifampicin, and 155 mg of ethambutol dissolved in 10 mL of dimethyl sulfoxide (DMSO) for three days. Physico-chemical parameters including Dynamic Light Scattering (DLS), Scanning Electron Microscopy (SEM) and HPLC of the antibiotic aerogel nanoparticle were measured. DLS of the aerogel nanoparticle was 593 nm (+/- 65 nm), SEM was 292 nm – 420 nm and HPLC results revealed a drug load of 6% by weight of nanoparticle. Cytotoxicity assays showed the the antibiotic loaded aerogel nanoparticles were non-toxic in J774A.1 cells at 50 µg/mL. *In vivo* efficacy

studies were done in BALB/c mice infected with $2x10^6$ cfu/mL of *M. avium* strain ATCC 46901 and treated orally, thrice weekly with either; antibiotic aerogel nanoparticles containing clarithromycin, rifampicin and ethambutol or the free drug combination of clarithromycin, rifampicin and ethambutol with appropriate controls for two weeks. Results showed that the antibiotic loaded aerogel nanoparticles did not reduce the bacterial load in the liver or spleen as compared to controls. Histopathology of both kidneys revealed the aerogel nanoparticles were non-toxic at the dose given.

Keywords

Mycobacterium, Aerogel, Nanoparticles

Introduction

Mycobacterium tuberculosis is an intracellular pathogen that currently infects more than 3 billion people worldwide, making it the number one cause of death due to a bacetrial infection in the world (1). *M. tuberculosis* is transmitted via aerosolized respiratory secretions typically by coughing or sneezing, causing primarily pulmonary disease although other areas of the body can be affected (2). This successful human pathogen has the ability to cause overt disease in a host or adjust its cellular machinery to a lower energy state to evade detection by the host's immune system (3, 4). When an opportunity arises, like an event that causes immuno-suppression in the host, *M. tuberculosis* can return to a dynamic

state, replicate in macrophages and other immune cells, and cause an active infection (4).

Fortunately, there are successful tuberculosis treatments that when correctly followed have a 95% cure rate (5). However, treatment is expensive and involves taking multiple drugs for long periods of time (6). Also, first line tuberculocidal drugs such as; rifampicin, ethambutol, and isoniazid, can have many toxic side effects ranging from mild nausea and gastrointestinal distress to severe liver and kidney damage (7). For these reasons, some patients do not finish the prescribed 6-9 month course of therapy. Not completing the full treatment protocol is a key factor in the development of drug-resistant bacteria, contributing to the infection of others, and increasing the chance of re-emergence of active disease (1).

Addressing poor patient compliance is essential in the control and treatment of *M. tuberculosis* (6). One way to improve patient compliance is to reduce the amount and frequency of dosing that is required to treat mycobacterial infections. This can be done by finding an appropriate drug carrier that has the capacity to yield a high drug load of multiple antimicrobials simultaneously while providing a sustained drug release profile that is non-toxic to patients. In order to investigate this drug delivery approach, commercially available aerogel particles were combined with three frontline tuberculocidal drugs; clarithromycin, rifampicin and ethambutol, to test the hypothesis that antimicrobials adsorbed to aerogel

nanoparticles will be more effective in treating mycobacteriosis caused by *M. avium* in a mouse model compared to rifampicin, clarithromycin and ethambutol given as free drugs.

Aerogel is a low-density solid state material that has a fine open pore structure (8). Aerogels are extremely light and comprised of 96% air (9). This biocompatible material can be synthesized from silica oxide or other materials such as titanium oxide, aluminum oxide and carbon, among others. Silica aerogels are synthesized by hydrolysis and condensation reactions (10). The condensation process produces a gel-like structure that is further processed by a supercritical drying step. This extraction phase removes fluid slowly from the gel-like structure without disrupting the matrix leaving only air and thus producing aerogel (11).

Aerogels are interesting drug delivery agents to investigate because of their high porosity and large surface area. Many hydrophilic or hydrophobic drugs may be adsorbed onto the aerogel matrix depending on the charge and solubility of the drug (10, 12). In addition, chemical modifications such as polymer coatings can be performed to the aerogel structure to enhance suitability as a drug delivery carrier (8, 12, 13). Furthermore, aerogels are considered chemically inert and therefore not harmful to the human body (8).

Materials and methods

Method of production of rifampicin, clarithromycin and ethambutol aerogel nanoparticles

Aerogel nanoparticles are commercially available and were obtained by the Material Science and Engineering Department. Briefly, aerogel particles were incubated at room temperature with a pre-made antibiotic solution for 72 hours to allow for optimum antibiotic adsorption and drying. The antibiotic solution consisted of 250 mg of clarithromycin, 13 mg of rifampicin, and 155 mg of ethambutol dissolved in 10 mL of dimethyl sulfoxide (DMSO). This amount was calculated as the total amount of drug required for the treatment of infected mice for the duration of the experiment. For a 25 g mouse, the dose for each drug was as follows; clarithromycin 200 mg/kg, rifampicin 10 mg/kg and ethambutol 125 mg/kg. The antimicrobial doses were chosen based on previously published reports of experimentally induced *M. avium* infection in mice (14, 15, 16).

Following the adsorption and drying process, the antibiotic aerogel particles were finely ground with a mortar and pestle, sealed in a glass test tube, and refrigerated until use. The “empty” aerogel powder was also milled with a mortar and pestle and sealed in a glass tube and refrigerated until use. A sterility check was performed on the antibiotic aerogel and “empty” aerogel nanoparticles by reconstituting 10 mg of powder in 10 mL of sterile water and plating 100 µl aliquots on TSA plates in triplicate.

To prepare the antibiotic aerogel nanoparticles *in vivo studies*, 210 mg of the powder was reconstituted in 1.75 mL of molecular grade, de-ionized, distilled water. To prepare the free drug combination, 35 mg of clarithromycin, 1.75 mg of rifampicin, and 21 mg of ethambutol was dissolved in 1.75 mL of DMSO. Prior to administration by oral gavage, each solution was sonicated for 10 minutes to aid in dispersion.

Physico-chemical characterization of antibiotic aerogel nanoparticles

Dynamic Light Scattering (DLS)

The solute size and surface charge of the aerogel antibiotic nanoparticles and the empty aerogel particles were characterized by DLS using the Zetasizer Nano ZS at 25 ± 0.1 °C. Samples were diluted in Phosphate Buffered Saline, (PBS) (Sigma, St. Louis, MO) to a concentration of 1 mg/mL, sonicated in a water bath sonicator (Model 8890, Cole-Parmer, Chicago, IL) for 10 minutes and then passed through a 1 micron sized filter before analysis. The intensity-average diameter (*DI*) was recorded for each sample and averaged from three measurements.

Scanning Electron Microscopy (SEM)

In order to confirm size and shape of antibiotic aerogel nanoparticles and aerogel nanoparticles, SEM was performed. Particles were suspended in molecular grade de-ionized water at 1 mg/mL, placed in a water bath sonicator for 10 minutes then passed through a micron sized filter. For analysis, a drop of the

dispersion was deposited onto a copper tape and dried under vacuum. Observations were performed using a scanning electron microscope (LEO (Zeiss) 1550) with a voltage of 5 kV.

Measurement of Drug Content by High Performance Liquid Chromatography (HPLC) and Mass Spectrometry

The amount of rifampicin, clarithromycin, and ethambutol associated with the antibiotic aerogel nanoparticles was measured by HPLC and mass spectrometry. For analysis, 5 mg of antibiotic aerogel or “empty” aerogel was dissolved in 5 mL of methanol. The solution was sonicated for 15 minutes and then centrifuged at 6440g for 10 minutes to obtain the supernatant. Next, the supernatant was used as is or was diluted with acetonitrile for injection in the HPLC. Rifampicin was analyzed by HPLC on a reverse phase column (C18) with UV detection at 335 nm. Clarithromycin was analyzed by HPLC on a reverse phase column (C18) with UV detection at 210 nm. Ethambutol was analyzed by gas chromatography-mass spectrometry (GC-MS) with a detection limit of 1 ng.

Measurement of minimum inhibition concentration (MIC)

The procedure for the MIC was adapted from Heifets (17) and Falkinham (personal communications) with the following modifications. Briefly, 10 mg of antibiotic aerogel and 10 mg aerogel powder were added to separate tubes containing to 10 mL of sterile water and vortexed for 3 minutes. Then, 100 µl of each solution was transferred into the appropriate well of a micro titer plate and

diluted serially before inoculation with 100 µl of *M. avium* at ~1 *x* 10^6 cfu/mL. Each free drug was prepared following manufacture's recommendations to a final concentration of 1 mg/mL. Next, 33.3 µl of each of the three antibiotics was combined in one well and diluted serially. After a 7 day incubation period at 37°C, the plates were scored by eye for turbidity and recorded. The test was repeated in triplicate.

Cytotoxicity assay

Cell viability was evaluated using the MTS Cytotoxicity Assay (Promega Corporation) by incubating J774A.1 cells with antibiotic aerogel, empty aerogel and untreated controls at a dose of 50 µg/mL for 24 hours as described as by Ranjan et al. (18). Absorbance at 490 nm was measured and results were expressed as the percentage of cell viability upon incubation with various treatments compared to untreated controls. Experiments were performed in triplicate and data was analyzed using the Student's *t* test. A p value of < 0.05 was considered significant.

Mycobacterial strain

A single transparent colony of strain *Mycobacterium avium* subspecies *hominissuis* ATCC 49601, was grown in Middlebrook 7H9 Broth containing 10% (vol/vol) of albumin-dextrose-catalase (ADC) enrichment (Difco Laboratories, Detroit, MI) and 2% (vol/vol) glycerol to mid-log phase at 37°C with aeration before being frozen at minus 20ºC in aliquots containing ~5 x 10^7 cfu/mL.

Verification of colony forming units by serial dilutions was done in triplicate before each use.

Infection and Treatment of Mice

Animal experiments were performed with approval of the Virginia Tech Institutional Animal Care and Use Committee (IACUC). Nine female BALB/c mice purchased from Charles River Laboratories (Charles River, MA) were housed in an ABSL 2 facility with food and water *ad libitum.* At 20 weeks of age, weighing approximately 25 grams, mice were infected intraperitoneally (IP) with 200 µL of $2x10^6$ cfu/mL of *M. avium* ATCC 49601, 90% transparent colonies. After one week, mice were placed into three treatment groups and treated every other day orally with either 250 µl of; clarithromycin, rifampicin and ethambutol entrapped aerogel nanoparticles, or free drug combination containing clarithromycin, rifampicin and ethambutol or sterile de-ionized water for two weeks. Mice were monitored daily for signs of adverse reactions and weighed weekly.

Two days after second week of treatment, mice from Groups 1-3 were sacrificed to determine colony forming units per organ (CFU/organ) in liver and spleen. The organs were removed aseptically from each mouse and placed separately into 50 mL tubes containing 2 mL of Middlebrook broth 7H9 containing 10% (vol/vol) ADC enrichment. The organs were homogenized for 1-2 minutes using a Tissuemiser homogenizer (Fisher Scientific, USA). Next, aliquots of each

organ homogenate were serially diluted in 7H9 Middlebrook broth to a maximum of 10^5 dilutions, plated on Middlebrook 7H10 agar plates containing 10% (vol/vol) OADC enrichment with 5% (vol/vol) glycerol and incubated for 7-14 days at 37°C. The number of colonies per dilution were counted and reported in CFU/organ. An unpaired, two tailed student's *t* test was performed and a P value of < 0.05 was considered statistically significant. Kidneys from all mice were collected for histopathology.

Histopathology

Kidneys from the mice were collected, fixed in 10% neutral buffered formalin, trimmed, routinely processed and embedded in paraffin blocks. Five (5) micron sections were cut with a microtome, fixed on a glass slide and stained with hematoxylin and eosin. In a double-blinded study, two veterinary pathologists independently examined the kidney samples and scored histopathological changes (degeneration/necrosis, inflammation, hemorrhage, edema) using a scale from 0 to 4. The degree of pathological change was recorded as; (0) = unremarkable, (1) = minimal, (2) = mild, (3) = moderate, and (4) = marked.

Results

Physico-chemical characterization of antibiotic aerogel nanoparticles

Dynamic light scattering revealed that the intensity-average diameter or relative size of the aerogel nanoparticle without antibiotics was 150 nm (+/- 2 nm) (Table

5.2). Additionally, the scanning electron micrograph (SEM) depicted a size range of 132 nm to 158 nm at 1 mg/mL (Figure 5.1).

The intensity-average diameter of the antibiotic aerogel nanoparticle at 1 mg/mL in PBS was approximately 580 nm (+/- 65 nm) as seen in Table 5.2. The SEM (Figure 5.2) depicts two random measurements of 292 nm and 420 nm.

HPLC and Mass Spectrometry

Drug concentrations of antibiotic aerogel nanoparticles were determined by HPLC and Mass Spectrometry analysis. The total amount of drug load per mg of nanoparticle was found to be 6%. The amount of Rifampicin in nanoparticle was found to be 1.5 µg/mg. The amount of Clarithromycin in nanoparticle was found to be 37 µg/mg and the amount of Ethambutol in nanoparticle was 20 µg/mg (Table 5.3).

Minimum Inhibitory Concentration (MIC)

MIC analysis of free drugs and antibiotic aerogel nanoparticles were done. The average MIC of antibiotic aerogel nanoparticles was 5.3 µg/mL, n=3. The average MIC of the free drugs combination was 0.04 µg/mL, n=3. The empty aerogel did not show any inhibition of growth of *M. avium* as seen in Table 5.4.

Cytotoxicity Assay

The cytotoxicity of antibiotic aerogel and aerogel nanoparticles in J774A.1 cells was done via the MTS assay. At a concentration of 50 µg/mL, the cell viability was above 90% for the antibiotic aerogel and aerogel nanoparticles, n=6 (Figure 5.3).

In Vivo Efficacy Study

Efficacy of treatment of antibiotic aerogel nanoparticles compared to free drugs and untreated controls in the liver and spleen of BALB/c mice was determined. After 2 weeks of treatment, the results show that the antibiotic aerogel nanoparticles did not reduce the bacterial load in liver and spleen. The free drug combination of clarithromycin, rifampicin and ethambutol did reduce bacterial load by (1.4) log in both liver and spleen (Figure 5.4) *P <0.05.

Histopathology

The degree of pathological change present in kidney samples was scored by two individual pathologists after two weeks of treatment with antibiotic aerogel nanoparticles, free drugs and untreated but infected controls using the scale: (0) = unremarkable, (1) = minimal, (2) = mild, (3) = moderate and (4) = marked (Table 5.5). Results show minimal inflammation was present in each of the three groups.

Discussion

Dynamic light scattering revealed that the intensity-average diameter or relative size of the aerogel nanoparticle without antibiotics was 150 nm (+/- 2 nm) (Table 5.2). The scanning electron micrograph (SEM) was consistent with these results and depicted a size range of 132 nm to 158 nm (Figure 5.1), although some minor aggregation was present. In contrast, the intensity-average diameter of the antibiotic aerogel nanoparticle at 1 mg/mL in PBS was approximately 580 nm (+/- 65 nm) as seen in Table 5.2. The SEM (Figure 5.2) also confirms this and shows two random measurements of 292 nm and 420 nm taken of the antibiotic aerogel nanoparticles.

The apparent increase in size noted on DLS and SEM is most likely attributable to particle agglomeration, which can occur during drug loading (19, 20). There are two ways to load aerogel with drugs; one way is to add the drugs during the sol-gel process before gelation and the other is to load the drugs from a liquid or gas phase to the dried aerogel matrix (20). The latter procedure was pursued in this research effort. Aerogel nanoparticles were loaded with a rifampin, clarithromycin and ethambutol mixture in the liquid phase using DMSO as the solvent. One limitation of loading drugs by incubation is that the drugs can easily cause the pores of the aerogel matrix to collapse due to capillary pressures (20, 21). The collapse and subsequent agglomeration can be avoided by drying the aerogel slowly in a controlled manner as done in the supercritical drying process (20). Supercritical drying is the preferred way to produce drug-loaded aerogel but requires specialized equipment.

Although it is logical to assume the increase in size may be due to absorption of the drug, there is no report in the literature that a physical increase in size occurs in drug loading. In fact, Smirnova et al. noted that during loading, drugs are adsorbed onto the surface of the aerogel matrix through hydrogen bonding with the silica in a thin layer as seen by x-ray diffraction (2, 22). Additionally if the particle size of the drug grows larger than the aerogel pores via crystallization, destruction of the aerogel matrix can occur, resulting in partial collapse and shrinkage of the aerogel (8).

The estimated drug load of the antibiotic aerogel nanoparticle used in these studies was approximately 20% of drug load by weight of nanoparticle. This was calculated by the equation: total amount of drug added in mg/total amount of aerogel powder recovered in mg x 100%. Calculations for further experiments were based on this estimation while HPLC analysis was underway.

However, after the completion of all experiments, the actual amount of drug load per mg of nanoparticle was found to be 6% by HPLC analysis, which was significantly below the expected amount of drug load and consequently adversely affected the outcome of the following experiments. Although aerogels are known to have a relatively high drug load capacity due to their large surface area and porosity (10, 23), the lower than expected drug load could have been a result of the processing technique. During the drug load process, the aerogel was

incubated with the three antibiotics dissolved in DMSO. DMSO was chosen because it is non-toxic in the mouse model at the doses used and it readily dissolves rifampicin and clarithromycin, which are hydrophobic drugs. DMSO is also known for its evaporative capacity and it is possible that some portion of the drug mixture evaporated before the adsorption process could fully occur (24).

The minimum inhibitory concentration of the free drug combination containing rifampicin, clarithromycin and ethambutol was found to be 0.03 µg/mL (SD+/- 1/2 dilution), for *M. avium* strain ATCC 49601. This is in agreement with other *M. avium* strains that are susceptible to this drug combination (17, 25, 26). The MIC of antibiotic aerogel was found to be 4 µg/mL (SD+/- 1/2 dilution), which is considered mildly active against *M. avium*. However, it is difficult to draw conclusions from these results since the MIC value of the antibiotic aerogel and free drug are not based on the same initial concentration. Upon re-examination the actual MIC of the antibiotic aerogel, as calculated for clarithromycin was 0.2 µg/mL, which is effective against *M. avium*. This was found by calculating the actual amount of clarithromycin (from HPLC) in 1 mg of aerogel antibiotic powder and back calculating to find the correct MIC.

Next, the MTS assay was performed which can be used as a direct correlation to cell viability by measuring mitochondrial activity of macrophages. Results showed that the aerogel nanoparticles were non-toxic at a dose of 50 µg of aerogel antibiotic powder per mL. Toxicity is acknowledged when the percent of

cell viability drops below 90%. Since the actual amount of drug load was unknown at the time of test, a high dose was chosen. The actual amount of each drug in 50 µg of powder per mL was 30 µg/mL of clarithromycin, 1.5 µg/mL of rifampicin and 18.5 µg/mL of ethambutol. Earlier work with free rifampicin and ethambutol in cytotoxicity assays in J774A.1 cells was also found to be non-toxic at similar doses (data not shown). Interestingly, free clarithromycin at 30 µg/mL has been shown to be toxic to J774A.1 cells by MTS analysis (see Chapter 3 for details). However, when clarithromycin is combined with aerogel, toxicity was not apparent. This phenomenon was also seen when clarithromycin is combined with polymeric nanoparticles (see Chapter 3). Clarithromycin is a hydrophobic drug and readily permeates cellular membranes. Perhaps at high doses, the free form enters cells quickly causing toxicity. Conversely, when clarithromycin is released in a sustained manner from a nanoparticle, the cell might be able to adjust. Many cells have an active drug efflux system (27) and it is possible some clarithromycin is being expelled from the cell, thus reducing signs of toxicity. Another possibility that may account for the difference in toxicity or cell viability between free drug and antibiotic nanoparticle is that the drugs may be only partially released from the nanoparticle. In studies by Smirnova et al. hydrophilic aerogels have been shown to have an extremely fast or burst release pattern due to the collapse of the aerogel in aqueous media (22). In contrast, hydrophobic aerogels have been shown to have a slow or sustained release pattern and have been observed floating on top of media solution (12). Interestingly, this floating phenomenon was observed during in vitro work when the antibiotic aerogel

nanoparticles were suspended in DMEM media indicating hydrophobicity and perhaps a slow release pattern. Drug release studies would be a logical next step to confirm this theory.

In the *in vivo* experiments, the antibiotic aerogel nanoparticle failed to reduce the bacterial load in mice infected with *M. avium*. This was most likely a result of inadvertent under-dosing. A 30 mg dose of nanoparticle was given per mouse based on an estimated 20% drug load per weight of nanoparticle. This is equivalent to 6 mg of total drug given orally to each mouse. With further calculations, each individual drug load in 30 mg of powder was estimated to be; 3.6 mg of clarithromycin, 0.18 mg of rifampicin, and 2.2 mg of ethambutol, which is within therapeutic levels. However after HPLC analysis, the actual amount of total drug given to each mouse was 1.745 mg in 30 mg of antibiotic aerogel. Individual calculations for each drug was as follows; 1.1 mg of clarithromycin, 0.045 mg of rifampicin, and 0.6 mg of ethambutol in 30mg of aerogel powder which is below therapeutic concentrations and is shown by a lack of reduction of bacterial load (Figure 5.4).

Although the nanoparticle was not successful in reducing the bacterial load, it was relatively non-toxic in BALB/c mice at the dose given as seen in Table 5.5. Histopathology of kidney samples from antibiotic aerogel treated mice showed minimal inflammation. Similarly, the free drug combination and untreated infected control group also showed minimal inflammation. All three drugs are

primarily excreted via the kidneys and any renal impairment would increase the likelihood of toxicity (27, 28, 29), although histopathological evaluation of the liver would have been ideal. In retrospect, it would have been interesting to also examine the alimentary tract for any abnormalities since the route of administration was oral. Also, adding another treatment group consisting of empty aerogel would have been beneficial to compare against the other groups. Unfortunately at the time of the experiment, additional empty aerogel was not available.

Conclusion

In this experiment, antibiotic aerogel nanoparticles were fabricated by incubating commercially available aerogel with a premade antibiotic solution for three days. The particle size in nm was then estimated by DLS and SEM. HPLC results showed the amount of drug load per mg of nanoparticle to be 6%. The *in vivo* activity of the nanoparticle was hypothesized to improve efficacy, reduce toxicity and extend dosing intervals as compared to the standard treatment. Although the antibiotic aerogel nanoparticle was unable to reduce the bacterial load in the liver and the spleen when compared to controls, it was shown to be non-toxic in both *in vitro* and *in vivo* models. For future experiments, analysis of drug load should occur prior to beginning animal studies, however a lengthy delay in receiving HPLC results mandated moving forth with the animal model without knowing the true concentration per mg. Still, the information and experience

gained during this maiden experiment was invaluable and improved our future research efforts.

References

1. World Health Organization, www.who.int/tb/publications/global_report/2011/gtbr11_full.pdf.
2. Mc Donough K. A., Kress Y., Bloom B. R. (1993). “Pathogenesis of Tuberculosis: Interaction of *Mycobacterium tuberculosis* with Macrophages.” Infection and Immunity **61**(7): 2763-2773.
3. Riska P. F., Carleton S. (2002). "Latent tuberculosis: models, mechanisms, and novel prospects for eradication." Semin Pediatr Infect Dis **13**(4): 263-72.
4. Talaat A. M., Ward S. K., Wu C.W., Rondon E., Tavano C. C., Bannantine J. P., Lyons R., Johnston S. A. (2007). “Mycobacterial Bacilli Are Metabolically Active During Chronic Tuberculosis in Murine Lungs: Insights from Genome-Wide Transcriptional Profiling.” Journal of Bacteriology **189**(11) 4265–4274.
5. Cole S. T. Tuberculosis and the Tubercle Bacillius. Washington, DC: American Society for Microbiology, 2004.
6. World Health Organization, http://www.who.int/tb/dots/en/
7. Awofesoa, N. (2008). “Anti-tuberculosis medication side-effects constitute major factor for poor adherence to tuberculosis treatment.” Bulletin of the World Health Organization Mar; **86** (3):b-d.

8. Smirinova, I., Suttiruengwong S. Arlt W. (2005). “Aerogels: Tailor-made Carriers for Immediate and Prolonged Drug Release”. KONA (No.23) 86-97.

9. Patel R. P., Purohit N.S., Suthar A. M. (2009).”An Overview of Silica Aerogels.” International Journal of ChemTech Research **1**(4):1052-1057.

10. Shah C., Patel R., Mazumder R., Bhattacharya S., Mazumder A., Gupta R. N. (2009). ”Aerogels: Novel Drug Carriers” The Pharma Review 164-167.

11. Tewari P. H., Hunt A. J., Lofftus K. D. (1985). “Ambient-temperature supercritical drying of transparent silica aerogels.” Materials Letters July;**3**(9–10):363–367.

12. Giray S., Bal T., Kartal A. M., Kizilel S., Erkey C. (2012). “Controlled drug delivery through a novel PEG hydrogel encapsulated silica aerogel system.” J Biomed Mater Res A. May;**100**(5):1307-1315.

13. Barbe C., Bartlett J., Kong L., Finnie K., Lin H. Q., Larkin M., Calleja S., Bush A., Calleja G. (2004). “Silica Particles: A novel drug delivery system.” Advanced Materials **16**(21):1959-1966.

14. Pandey R., Sharma S., Khuller G. K. (2006) “Chemotherapeutic efficacy of nanoparticle encapsulated antitubercular drugs” Drug Delivery **13**: 287-294

15. Sharma A., Pandey R., Sharma S., Khuller G. K. (2004) “Chemotherapeutic efficacy of poly (DL-lactic-co-glycolide) nanoparticle

encapsulated antitubercular drugs at sub-therapeutic dose against experimental tuberculosis" Int. J. Antimicrob. Agents 24: 599-604.

16. Furney S. K., Skinner P. S., Farrer J., Orme I. M. (1995) "Activities of Rifabutin, Clarithromycin and Ethambutol in a Mouse Model." Antimicrobial Agents and Chemotherapy Mar;39(**3**):786-789.

17. Heifets L. (1996). "Susceptibility of *Mycobacterium avium* complex Isolates" Antimicrobial Agents and Chemotherapy **40**(8):1759-1767.

18. Ranjan A., Pothayee N., Vadala T. P., Seleem M. N., Restis E., Sriranganathan N., Riffle J. S., Kasimanickam R. (2010). "Efficacy of Amphiphillic Core Shell Nanostructures Encapsulating Gentamicin in an *In Vitro Salmonella* and *Listeria* Intracellular Infection Model. Antimicrob. Agents Chemother. Aug;**54**(8):3524-6.

19. Sui R., Rizkalla A. S., Charpentier P. (2004). "Synthesis and Formation of Silica Aerogel Particles By a Novel Sol-Gel Route in Supercritical Carbon Dioxide." J. Phys. Chem. B, **108**(32):11886-11892.

20. García-González C.A., Alnaief M., Smirnova I. (2011). "Polysaccharide-based aerogels-Promising biodegradable carriers for drug delivery systems". Carbohydrate Polymers **86**:1425–1438.

21. Smirnova I., Applications of aerogel in the life sciences, http://www.isasf.net/fileadmin/files/Docs/Arcachon/oraux/c51-CO63%20Smirnova%20Full_paper_applications_in_life_science_IS.pdf.

22. Smirnova I., Suttiruengwong S., Seiler M., Arlt W. (2004). “Dissolution rate enhancement by adsorption of poorly soluble drugs on hydrophilic silica aerogels.”Pharm Dev Technol. Nov;**9**(4):443-52.

23. Alnaief M., Smirnova I. (2009). “Functionalized Silica Aerogels for Advanced Drug Carrier Systems.” 9th Symposium International on Supercritical Fluids, Arcachon, France (Poster).

24. Gaylord Chemical Corporation, http://www.gaylordchemical.com/uploads/images/pdfs/literature/101B_english.pdf

25. Telles M. A. S., Yates M. D. (1994). ”Single and double drug susceptibility testing of *Mycobacterium avium complex* and mycobacteria other than tubercule (MOTT) bacilli by a microdilution broth minimum inhibitory concentration (MIC) method.” Tubercule and Lung Disease **75:** 286-290.

26. Wallace Jr. R. J., Nash D. R., Steele L. C., Steingrube V. (1986). “Susceptibility testing of slowly growing mycobacteria by a microdilution MIC method with 7H9 broth.” Journal of Clinical Microbiology **24**(6): 976-981.

27. Rodrigues L., Sampaio D., Couto I., Machado D., Kern W. V., Amaral L., Viveiros M. (2009). “The role of efflux pumps in macrolide resistance in *Mycobacterium avium* complex.” International Journal of Antimicrobial Agents **34**(6): 529-33.

28. Sharif Y, Sheikh M. A., M. Zia A., Iqbal T. (2001). “Renal Clearance and Urinary Excretion of Clarithromycin in Human Male Volunteers.” Pakistan Journal of Biological Sciences **4** (2): 201-203.

29. Singhal K. C., Rathi R., Varshney D. P., Kishore K. (1985). “Serum concentration and urinary excretion of ethambutol administered alone and in combination with isoniazid in patients of pulmonary tuberculosis.” Indian J Physiol Pharmacol. Oct-Dec;**29**(4):223-6.

30. Acocella G. (1983). “Pharmacokinetics and Metabolism of Rifampin in Humans.”

Reviews of Infectious Diseases Jul –Aug; **5**(3):S428-S432.

Tables and Figures

	Group 1 n=3	**Group 2** n=3	**Group 3** n=3
Week 0	Infect mice	Infect mice	Infect mice
Week 1	Treat with water	Treat with aerogel+AB	Treat with free drugs
Week 3	Sacrifice 3 mice	Sacrifice 3 mice	Sacrifice 3 mice

Table 5.1 Experimental design of aerogel efficacy study in mice.

Name	**Intensity Diameter**
Aerogel	150 nm +/- 2 nm SD
Antibiotic Aerogel	593 nm +/- 65 nm SD

SD= Standard deviation

Table 5.2 Average size of antibiotic aerogel nanoparticles at 1 mg/mL via dynamic light scattering.

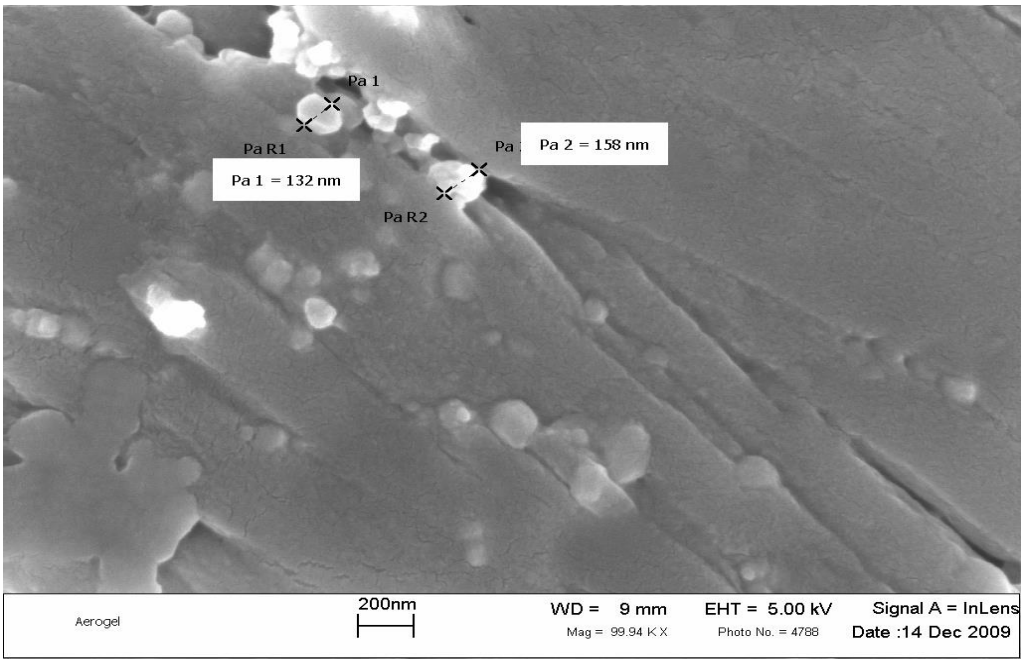

Figure 5.1 SEM of aerogel nanoparticle without antibiotics at 1 mg/mL using LEO (Zeiss) 1550 with a voltage of 5 kV.

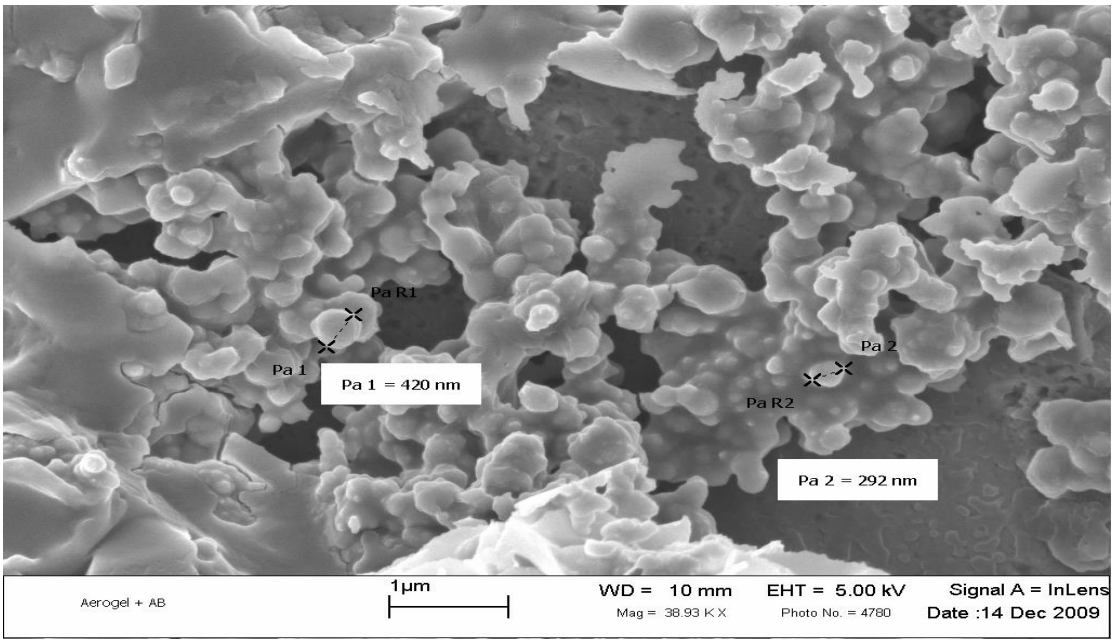

Figure 5.2 SEM of antibiotic aerogel nanoparticle at 1 mg/mL using LEO (Zeiss) 1550 with a voltage of 5 kV.

ID	Rifampicin in µg/mg of nanoparticle		Clarithromycin in µg/mg of nanoparticle		Ethambutol in µg/mg of nanoparticle
Aerogel + Antibiotics	**1.5**		**37**		**20**
Aerogel	None detected		None detected		None detected

Table 5.3 Drug concentrations of antibiotic aerogel nanoparticles were determined by HPLC and Mass Spectrometry analysis. The total amount of drug load per mg of nanoparticle was found to be 6%.

	MIC		
Type	Trial 1	Trial 2	Trial 3
Aerogel+ (Rif+Cla+Eth)	4 µg/mL	4 µg/mL	8 µg/mL
Free drugs combined (Rif+Cla+Eth)	0.061 µg/mL	0.03 µg/mL	0.03 µg/mL
Aerogel (empty)	No inhibition	No inhibition	No inhibition

Table 5.4 MIC analysis of free drugs, antibiotic aerogel nanoparticles and empty aerogel particles after a 7 day incubation period at 37°C with *M. avium*. The plates were scored by eye for turbidity.

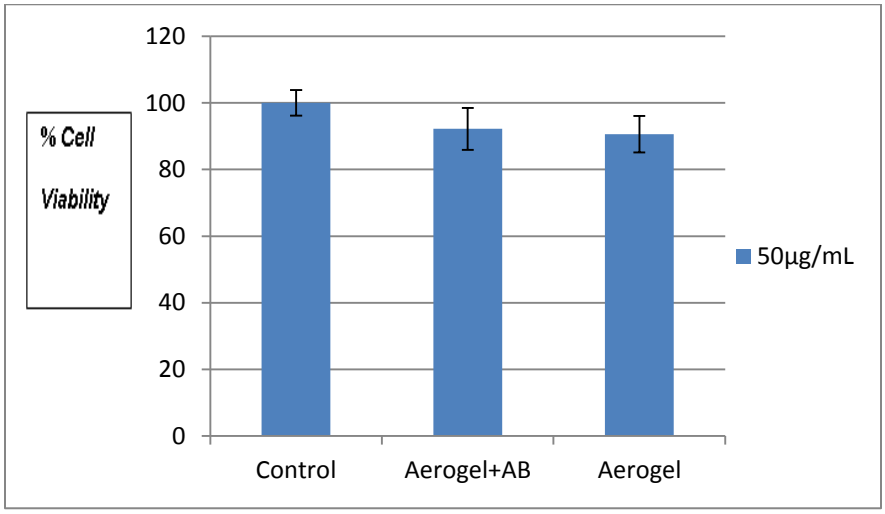

Figure 5.3 Cytotoxicity of antibiotic aerogel and aerogel nanoparticles in J774A.1 cells at 50 µg/mL for 24 hours. Cell viability remains above 90%, n=6, results were done in triplicate.

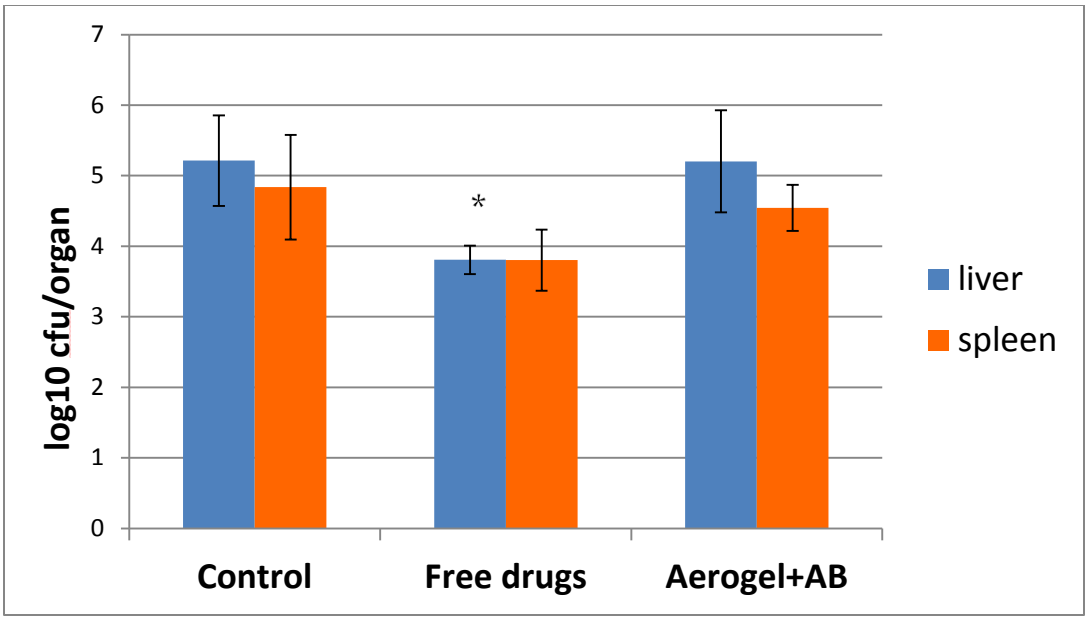

Figure 5.4 Efficacy of treatment of antibiotic aerogel nanoparticles compared to free drugs and untreated controls in liver and spleen in BALB/c mice. After 2 weeks of treatment, results show that the antibiotic aerogel nanoparticles were unsuccessful at reducing the bacterial load in liver and spleen. The free drug did reduce bacterial load by (1.4) log in both liver and spleen. *P <0.05

Kidney no	Kidney score Aerogel NP		Kidney score Free Antibiotics		Kidney score Untreated	
	1st pathologist	2nd pathologist	1st pathologist	2nd pathologist	1st pathologist	2nd pathologist
1	**1**	**0**	**0**	**1**	**0**	**1**
2	**0**	**4***	**1**	**0**	**1**	**0**
3	**0**	**2**	**1**	**0**	**0**	**0**
4	**0**	**1**	**0**	**1**	**1**	**0**
5	**1**	**1**	**0**	**1**	**1**	**0**
6	**1**	**4***	**1**	**0**	**0**	**0**

***autolysis/poor fixation is present

Table 5.5 Degree of pathological change present in kidney samples, scored by two individual pathologists after two weeks of treatment: (0) = unremarkable, (1) = minimal, (2) = mild, (3) = moderate and (4) = marked.

Chapter Six

CONCLUSION and FUTURE RESEARCH

In this dissertation, an improved treatment modality to treat mycobacterial infections was investigated. In chapter 3 amikacin polymeric nanoparticles were explored with success showing that encapsulation of antimicrobials with nanoparticles can reduce the bacterial load in liver and spleen of mice using a prolonged treatment interval of three treatments per week without toxic side effects. In chapter 4, Clarithromycin loaded nanoparticles were investigated as a drug delivery model in both cell culture and mouse studies. Results showed that clarithromycin nanoparticles were non-toxic in cells and mouse experiments at the respective dose used. In cell culture studies, the clarithromycin nanoparticle was as effective in reducing viable *M. avium* as the free clarithromycin at 15 µg/mL. In mouse studies, the clarithromycin nanoparticle was effective at reducing bacterial counts in spleen but not the liver as compared to untreated controls. In chapter 5, antibiotic aerogel nanoparticles were fabricated by incubating commercially available aerogel with a premade antibiotic solution for three days. The *in vivo* activity of the nanoparticle was hypothesized to improve efficacy, reduce toxicity and extend dosing intervals as compared to the standard treatment. Although the antibiotic aerogel nanoparticle was unable to reduce the bacterial load in the liver and the spleen when compared to controls, it was shown to be non-toxic in both *in vitro* and *in vivo* models. In general, encapsulation of antimicrobials in nanoparticles to treat mycobacterial infections

could improve efficacy, lessen toxic side effects prolong treatment intervals all resulting in an improved patient compliance.

Additional research is definitely warranted in this growing area of science. Future research efforts should focus on determining the amount of drug load and drug release kinetics of the nanoparticle both in vitro and in vivo before developing animal models. Additionally, determining how the nanoparticles enter the cell and what path is taken, in real time with some visualization (i.e., electron or confocal microscopy) would be beneficial. It would also be enlightening to monitor the disease process and its effect on treatment in the mouse. By using a *M. avium* strain that expresses fluorescence and a nanoparticle that is tagged with a chemical agent/dye that is detectable with *in vivo* imaging systems, the progression and treatment of disease can be followed in the same animal. Alternatively, encapsulation of amikacin with another anti-mycobacterial drug would be a great endeavor to improve efficacy in treatment. In final conclusion, there are many avenues yet to be explored in Nanomedicine and the possibilities are as limitless as one's imagination.